DISSERTATION

Compression Pressurized Direct Fuel Injection to Reduce Emissions from Existing Small Two-Stroke Transports

Submitted by

Horizon Walker Gitano-Briggs

Department of Mechanical Engineering

In partial fulfillment of the requirements

for the Degree of Doctor of Philosophy

Colorado State University

Fort Collins, Colorado

Summer 2004

COLORADO STATE UNIVERSITY

April 19, 2004

WE HEREBY RECOMMEND THAT THE DISSERTATION PREPARED UNDER OUR SUPERVISION BY HORIZON WALKER GITANO-BRIGGS ENTITLED *COMPRESSION PRESSURIZED DIRECT FUEL INJECTION TO REDUCE EMISSIONS FROM EXISTING SMALL TWO-STROKE TRANSPORTS* BE ACCEPTED AS FULFILLING IN PART REQUIREMENTS FOR THE DEGREE OF DOCTOR OF PHILOSOPHY OF MECHANICAL ENGINEERING.

Committee on Graduate Work

Dr. Nancy E. Levinger

Dr. Charles E. Mitchell

Adviser Dr. Bryan Willson

Department Head Dr. Allan Kirkpatrick

ABSTRACT OF THE DISSERTATION
COMPRESSION PRESSURIZED DIRECT FUEL INJECTION TO REDUCE EMISSIONS FROM EXISTING SMALL TWO-STROKE TRANSPORTS

The two-stroke engines commonly used in transports in developing countries suffer from exceedingly high emissions of hydrocarbons (HC) and carbon monoxide (CO). The problem of emissions from two-stroke engines will be largely addressed via emissions regulations on new vehicles typically resulting in their replacement with four-stroke engines. The existing fleet of two-stroke vehicles, however, is liable to be a major source of air pollution for the next few decades. Technologies, such as direct fuel injection (DI) and catalytic after-treatments, exist which are capable of being retrofitted to existing two-stroke engines to resolve their emissions problems. However, they are generally prohibitively expensive for applications in developing countries. A review of existing technologies indicates that direct fuel injection is the most promising and mature technology readily applicable to existing two-stroke machines. A cost reduced design modification using compression pressurization of an Air Blast DI (ABDI) system is proposed and modeled. A compression pressurized DI engine retrofit is designed and fabricated. Finally, emissions and power output measurements are taken on the compression pressurized direct fuel injection system showing similar power production to the carbureted engine, an 86% reduction in HC emissions, and an 83% reduction in CO at a cost of approximately two thirds of the ABDI system.

Horizon Walker Gitano-Briggs
Department of Mechanical Engineering
Colorado State University
Fort Collins, CO 80523
Summer 2004

ACKNOWLEDGMENTS

I would like to thank Dr. Rudolf Stanglmaier for his wisdom and guidance in this area and Tim Bauer and Nathan Lorenz for their helpful input.

DEDICATION

This work is dedicated to all those who fight for economic, ecological, ideological and political freedom against the formidable powers of a corrupt and irresponsible government that actively supports an atmosphere of rabid consumerism which contributes to an overly rapid destruction of natural resources, mass discontent, competitiveness, greed, materialism and ultimately the economic enslavement and domination of the masses by the hyper-wealthy that control the government.

It may be human nature to be short sighted, covetous, and easily distracted by the glimmer of new things. This is, however, not generally in the best interest of the individual or society. Human values can easily be usurped by clever images which promise fulfillment if we would just spend a little more money. We find ourselves manipulated, discontent with what we have, spending our selves into debt to "keep up", impress and compete, becoming wage slaves, impotent cogs in a monstrous economic machine controlled by a corporate board of directors and other major campaign contributors.

It is the duty of government to have the well being of the masses in mind. This includes the obvious things like access to education and healthcare. A just government would also attempt to encourage the populace to avoid the pitfalls of humanity and instead foster conservation of scarce resources and cooperation, using education, logical reasoning and perhaps even economic incentives.

Instead what we have in the US is a government which uses emotional arguments and scare tactics to justify foreign wars with dubious economic objectives, exceedingly

expensive superfluous "missile defense" systems, provides tax breaks to the rich for the purchase of wasteful luxury vehicles, a soaring federal deficit, insufficient funds for education and virtually no social health care system.

There is no lack of important work to which our government could be dedicating it energies. Our judicial system is in desperate need of an overhaul, we are burdened with a massive trade deficit, we have more people in prisons than any society ever, and we kill each other at a greater rate than almost anywhere else in the world.

There is, however, a glimmer of hope. Victor Papanek blazed a trail with his book *Design for the Real World* and E. F. Schumacher noted that we are meant for something more than "high mass consumption" in his book *Small is Beautiful*.

It is with the hope of changing the shamefully negligent governmental situation that I continue to work, and teach, and dedicate the rest of my life. I hope that some day our children may be able to live in freedom and equity, and realize that enough is enough rather than having boundless desire for more, and consuming needlessly.

TABLE OF CONTENTS

LIST OF ABBREVIATIONS

ABDI	Air Blast Direct Injection
ATDC	After Top Dead Center
BTDC	Before Top Dead Center
BVC	Blast Valve Closed
CNC	Computer Numeric Control
CSU	Colorado State University
CO	Carbon Monoxide
CO_2	Carbon Dioxide
CPDI	Compression Pressurized Direct Injection
CPDI-1	CPDI – Single Blast Valve Actuation
CPDI-2	CPDI - Doubly Actuated Blast Valve
DCA	Degrees Crank Angle
DI	Direct Fuel Injection
DVC	Disk Valve Closed
DVO	Disk Valve Open
ECU	Electronic Control Unit
EECL	Engines and Energy Conversion Laboratory
EFI	Electronic Port Fuel Injection
EOB	End Of Blast
EOR	End Of Recharge
EPC	Exhaust Port Closed
EPO	Exhaust Port Open
FSSI	Foundation for a Sustainable Society Inc.
FTIR	Fourier Transform Inferred Spectroscopy
GDI	Gasoline Direct Fuel Injection
HC	Hydrocarbons
NO_x	Oxides of Nitrogen (NO and NO_2)
PID	Proportional, Integral, and Differential Control
SMD	Sauter Mean Diameter
SOB	Start Of Blast
SOR	Start Of Recharge
TDC	Top Dead Center
UNEP	United Nations Environmental Program
VOC	Volatile Organic Compounds
WOT	Wide Open Throttle
XPC	Transfer Port Closed
XPO	Transfer Port Open

CHAPTER 1 MOTIVATION FOR THE WORK

AIR POLLUTION IS A GLOBAL CONCERN

The flowering of mankind's domination of technology over the last several hundred years has yielded many obvious benefits including greater productivity and mobility, improved health, and more leisure time. With this cornucopia of improvements there has also been an increase in the less obvious dangers including environmental contamination and air pollution. Air pollution often results in highly localized problems, such as particulate matter in the exhaust of diesel buses, which may cause significant contamination of the urban centers which they serve. There is, however, an increasing focus on the global effects of air pollution. Many pollutants can degrade the ozone layer in the upper atmosphere, resulting in increased solar infiltration and potentially contributing to global warming thereby affecting everyone on the planet.

Environmental degradation due to air pollution is being substantially addressed in developing countries via emissions standards for mobile and stationary sources. Due to economic constraints, however, developing countries are only now beginning to address the issues of emissions standards. The lack of emissions controls coupled with the rapid rate of population growth has resulted in exceptionally poor air quality in many

developing countries. In South East Asian cities it has been estimated that air pollution causes nearly 100,000 premature deaths per year (World Bank 1997).

Transportation is responsible for much of the overall air pollution problem. It has been estimated that transportation accounts for from 21% (Gorham 2002) to 25% (UNEP Website) of carbon dioxide emissions globally. In developing countries transportation may account for a much higher fraction on the overall air pollution. In New Delhi, for example, vehicle emissions account for 90% of the carbon monoxide and 85% of the volatile organic compound emissions (Gorham 2002).

Apart from a few electric vehicles, almost all surface transportation is powered by either two-stroke cycle internal combustion engines, or four-stroke cycle engines. Details of these engines may be found in Appendix A and B respectively. Due to their relatively low cost and high power to weight ratio, carbureted crankcase scavenged two-stroke engines are the most popular for transport power plants in developing countries. In India, 78% of the motorcycles and 85% of the three-wheelers are powered by two-stroke engines (Iyer 2000) and virtually all of these are crankcase scavenged and carbureted.

As a result of their popularity and poor emissions characteristics two-stroke transports account for a disproportionately large fraction of the overall air pollution in developing countries. In India for example up to 70% of all hydrocarbon (HC) emissions and 48% of carbon monoxide emissions are believed to come from two-stroke transports (Pundir et al. 1994). It is therefore believed that the largest reduction in atmospheric pollution can be gained by focusing on reducing emissions from two-stroke transport engines in developing countries.

Figure 1.1 Small two-stroke powered vehicles make up a large part of the overall transportation sector in developing countries. Photo by Dr. Bryan Willson

THE EXISTING TWO-STROKE FLEET: A POLLUTING LEGACY

While recent emissions limits on new vehicles introduced in many developing countries will help improve the air quality in the future, this will most likely be at the expense of removing two-strokes from the market altogether. In general, the legislation does little to address the problem of the existing fleet of two-stroke vehicles. These older vehicles cannot meet up-to-date emissions requirements, and an outright ban of these vehicles would cause significant political problems as they may compromise up to 65% of the total vehicle population in some areas. While projections typically assume a 10-year vehicle life expectancy, in developing countries vehicles are more often used for 20 years, and it is not uncommon to see many 30+ year old vehicles plying the roads on a daily basis. Even if another two-stroke vehicle were never produced again, there would still be two-stroke vehicles on the roads of developing countries for years to come.

EMISSIONS PROBLEMS OF TWO-STROKE ENGINES

There are several factors that contribute to the poor emissions from carbureted, crankcase scavenged, two-stroke engines including:

- Fuel Short-Circuiting
- Rich Tuning
- Lubricant Loss

FUEL SHORT-CIRCUITING

Short-circuiting of fuel is a consequence of two-stroke engine design. After a combustion event, the piston descends in the cylinder, opening first the exhaust port, then the transfer ports. The combustion products exit via the exhaust port and are purged, or scavenged, by the fresh air-fuel mixture entering the cylinder through the transfer ports. As the piston begins the compression stroke the transfer ports are closed, and later the exhaust port is closed. The exhaust port is therefore open during the entire scavenging process, and is still partly open even after the transfer ports are closed. As a result approximately 20% to 40% of the air-fuel mixture entering the combustion chamber exits the cylinder through open exhaust port without ever participating in the combustion process. This, referred to as fuel short-circuiting, is the major cause of poor emissions from small two-stroke engines.

RICH TUNING OF TWO-STROKE ENGINES

Carbureted two-stroke engines are generally tuned rich for a number of reasons. First, they produce more power when running slightly rich. Furthermore, there will always be some amount of exhaust products remaining in the cylinder even after scavenging. The presence of these exhaust products may interfere with ignition making it more difficult to start combustion, and running a richer mixture helps improve ignition. Additionally, when the throttle is rapidly opened the airflow increases more quickly than the fuel flow. This results in a lean mixture, which is more difficult to ignite, and may result in misfiring. In carbureted four-stroke engines a transient enrichment technique or accelerator pump is generally used to combat this; however, due to the increased carburetor-to-combustion chamber distance with crankcase scavenging it is generally not as effective in two-stroke engines. Instead, the overall mixture is generally run rich enough to avoid misfiring during acceleration. Finally, the additional fuel provided by a rich mixture helps keep the cylinder temperatures lower, reducing the potential for seizing.

TWO-STROKE ENGINE LUBRICATION

The total mass of air consumed by crankcase scavenged two-stroke engines passes through the crankcase. If they were to be lubricated via the "sump and pump"

system, as most four-stroke engines are, an unacceptably high amount of oil would be lost to the air, resulting in rapid depletion of the oil supply. Historically, the most popular way of supplying lubricating oil was simply to mix it with the fuel prior to admission to the carburetor. The oil/fuel mixture would then pass through the crankcase where special bearing design (for example slots or holes through the connecting rod ends) allowed greater wetting of the bearing surfaces by the oil/fuel mixture. The gasoline and lighter components of the mixture tended to volatilize, and be removed along with the airflow, while the heavier lubricating oils tended to stay and lubricate the surface. As there is no recirculation of the oil, this type of system us referred to as a "total loss" lubrication system. The fuel to oil ratio was historically on the order of 20:1, occasionally going as low as 6:1 (Caines 1996), but in more recent years has been improved to between 50 to 100:1. This contrasts very poorly with typical four-stroke engine oil consumption rates of 10,000:1 (Bortz 1993).

There are two fundamental reasons why two-stroke engines consume dramatically more lubricating oil than four-stroke engines. First, as the oil in a two-stroke engine is transported in droplet form by the scavenging air a significant amount of the oil may remain suspended in the air, never becoming deposited on a surface of the engine. This oil eventually reaches the combustion chamber and is either burnt, or exhausted in the short-circuited air. Approximately 95% of the particulate emissions from two-stroke engines are raw, or partially combusted oil droplets (Kataoka,, et al 1994).

Additionally once the oil has found a surface to lubricate, it must continually contend with being washed off by the fuel present in the circulating air. This makes it especially difficult to maintain an adequate oil film on parts of the piston and the rings.

Japanese motorcycle manufacturers pioneered the modern two-stroke oil delivery system by separating the oil from the fuel supply. In this system lubricating oil is either gravity fed, or mechanically pumped to a metering valve controlled by the throttle. As the throttle is opened, more oil is allowed to flow to the engine. Typically the oil is simply allowed to mix with the incoming air being transported in a manner similar to the fuel-oil premixed systems, but it may also be sprayed directly at critical components.

A more complete discussion of two-stroke engine oils may be found in Appendix C.

DIRECT INJECTION: THE TWO-STROKE SOLUTION

The fundamental emissions problem with carbureted two-stroke engines is the loss of raw fuel out the tail pipe during "short-circuiting" of the scavenging air. The most obvious solution to this problem is to inject the fuel directly into the cylinder only after the exhaust port is closed. When direct fuel injection (DI) is applied to two-stroke engines, scavenging air is still lost via short-circuiting but it no longer contains large amounts of unburned fuel. Two-stroke engines with direct fuel injection may reduce their lubricant oil flows to as low as 200:1 as fuel washing is no longer an issue (Wilson 1997), and the use of an electronically controlled fueling system eliminates the need to run the engine rich full time. Converting a carbureted two-stroke engine to DI may reduce the emissions of unburnt hydrocarbons by approximately 85% (Willson et al. 2002). Finally, converting a two-stroke engine to direct injection may allow the use of a catalytic

converter to remove most of the rest of the remaining HCs and CO, and, in general, reducing the emissions to below that of an equivalent four-stroke engine.

One drawback of DI in two-stroke engines is that the NO_x emissions tend to increase slightly as combustion temperatures increase. However, due to the large amounts of retained combustion products from incomplete scavenging, the NO_x emissions levels from DI two-stroke engines tend to be much lower than equivalent four-stroke engines.

ADDITIONAL CONSTRAINTS

While the DI technology for two-stroke engines is fairly mature, it is also still prohibitively expensive (approximately $200 to $400 per vehicle) for use on small transports in developing countries, which may cost as little as $1000 new. Any attempt to solve the emissions problems of existing two-stroke vehicles must consider several aspects:

- What is an acceptable budget per vehicle?
- What is the emissions reduction target?
- How long is an acceptable vehicle conversion time?
- Is the new system maintainable?
- How reliable is the new system?
- Are there any cultural barriers to implementation?

EMISSIONS REDUCTION COST-BENEFIT ANALYSIS

One way of deciding the value of an emissions reduction project is to analyze the project's cost-benefit curve. In many cost-benefit analyses there is a characteristic "S" curve indicating that there are modest gains to be made for modest investments. For greater levels of investment, the relative benefit increases up to a point beyond which the incremental benefit from additional investment drops off, and the system is essentially saturated. The optimum point of return on investment lies near the steep part of the curve, where small incremental investments yield the largest possible gains in benefits. Cost-benefit data for several possible two-stroke engine conversions (adapted from Willson et al. 2002) is presented in the table and graph of figure 1.2. The first stage, "tuning" refers to simply adjusting and maintaining the existing carbureted system. The second stage is electronic port fuel injection (EFI) where an electronic controller measures various engine parameters (such as air flow, engine temperature and engine speed, etc.) and controls a port type fuel injector spraying fuel directly into the transfer port passage. This system is similar to the fueling system used on most modern four-stroke automobiles. The next stage is direct fuel injection, and the final stage is direct fuel injection plus use of an oxidation catalyst in the exhaust path.

		% Reduction HC	
Conversion	**Cost $**	**Min**	**Max**
Tune Carburetor	5	5	10
Port EFI	200	15	30
Direct Injection	240	75	85
DI + Catalyst	340	95	99

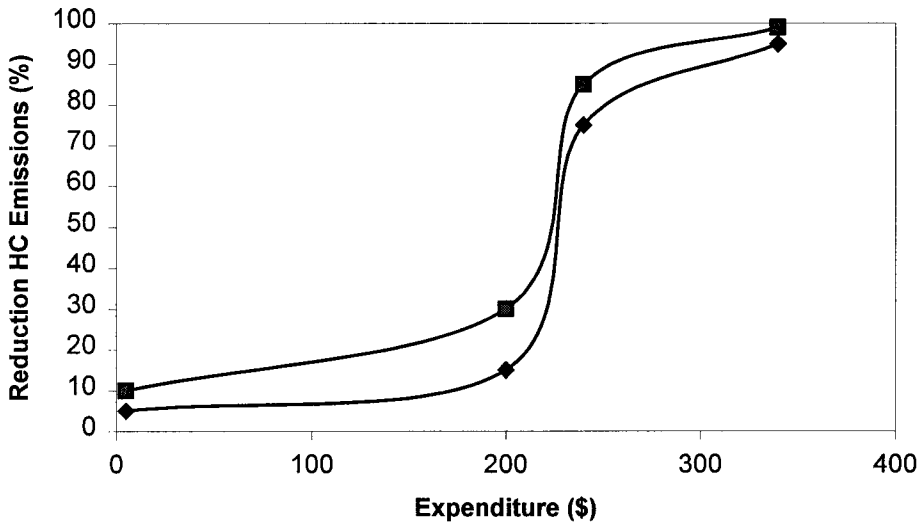

Figure 1.2 Cost Benefit analysis based on Colorado State University's Snowmobile Project.

These data show a distinct "S" curve, with the greatest incremental gain in emissions occurring with the conversion to direct fuel injection. Simply tuning and maintaining the existing carbureted system may achieve relatively minor gains at very low cost. Port fuel injection makes additional improvements in emissions, however, at a much higher incremental cost. For a slightly greater investment the DI system can

remove approximately 80% of the HC emissions. The addition of the catalytic exhaust after treatment has a much smaller incremental gain in emission reduction for the incremental cost.

We have therefore decided to focus our efforts on developing and demonstrating a less-expensive direct fuel injection technique for retrofit application to small two-stroke engines.

CHAPTER 2 CHOOSING THE APPROPRIATE TECHNOLOGY

TWO-STROKE DIRECT INJECTION TECHNIQUES

There are many possible options for direct fuel injection of small two-stroke engines. Many different configurations and technologies have been developed to overcome the fundamental problem of direct fuel injection systems: air – fuel mixing and vaporization. In carbureted and port fuel injected engines, relatively low-pressure fuel is introduced into the airflow before it enters the combustion chamber. Even if the fuel is poorly atomized initially, it tends to atomize finely as it passes the throttle valve (on carbureted engines at low loads) or as it is drawn into the cylinder through the intake valve or port. Fine atomization is necessary as there is a limited amount of time before combustion occurs. If large drops of liquid fuel are present, they may not have sufficient time to evaporate and burn. This results in poor emissions and may cause spark plug fouling. The relationship between fuel droplet diameter and evaporation time depends on many parameters including the fuel volatility, air temperature and chamber temperature and relative air-fuel velocity. For a quiescent atmosphere the relationship is of the form:

$$t_0 = d_0^2 / k \qquad (2.1)$$

where $\mathbf{t_o}$ is the time to vaporize a droplet of diameter $\mathbf{d_o}$. The constant **k** is a lumped parameter containing the effects of fuel characteristics and engine and air parameters (Turns 2000). Taking an air temperature of 330 K, and n-octane as our fuel, a value of **k** = 2.7E-7 m^2/s will result. The resulting relationship between droplet size and evaporation time is shown in the graph of figure 2.1.

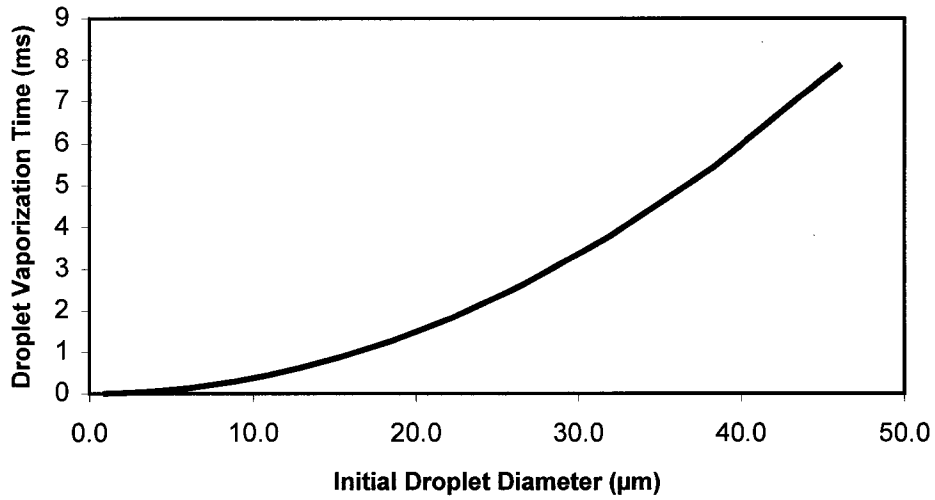

Figure 2.1 The relationship between fuel droplet size and evaporation time for typical engine temperatures in quiescent air.

For a two-stroke engine operating at 6000 rpm, there may be as little as 2 ms from the time the exhaust port is closed to the start of ignition. Figure 2.1 shows that this corresponds to a droplet size of approximately 23 μm, i.e. the maximum size droplet capable of evaporating completely in this time is 23 μm. As this represents the largest

droplet capable of fully evaporating in time, we would like an average droplet diameter significantly smaller then 23 μm.

When fuel is injected into a gaseous environment it atomizes into a spectrum of droplet sizes. In engine applications it is common to refer to the Sauter Mean Diameter or SMD (the diameter of a droplet such that the droplet surface area to diameter ratio is equivalent to the surface area to diameter ratio of the total volume of liquid) of a spray as a useful metric of the droplet sizes. While this is not the only important metric of a fuel spray, it is sufficient for our purposes and any further reference to droplet size will be in terms of SMD. It is generally accepted that DI systems should have a mean droplet size of no bigger then approximately 15 μm (Zhao 2002). To achieve such fine atomization "single fluid" DI systems (those that inject liquid fuel alone into the cylinder) require large fuel pressures of typically 5 MPa to 10 MPa. Mean droplet diameter is related to the injection pressure by the following equation:

$$\mathbf{d} = \mathbf{C} / \mathbf{P}^{1/2} \qquad (2.2)$$

where **d** is the mean droplet diameter, **P** is the differential pressure between the injected fuel and the air into which it is being injected and **C** is a lumped constant containing effects of the injector design and others. Figure 2.2 shows the relationship for equation 2.2 using a value of $\mathbf{C} = .05\ \text{mPa}^{1/2}$ and several data points from experimental DI systems.

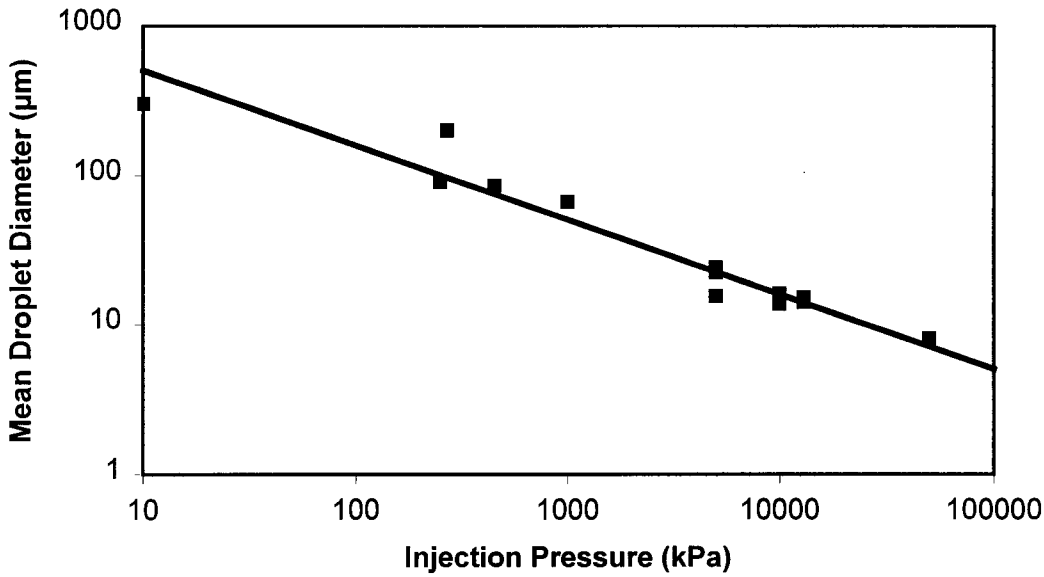

Figure 2.2 The logarithmic relationship between injection pressure and average droplet diameter (SMD) for gasoline. Straight line is a curve of the form of equation 2.2 with **C** = .05. Square points are data taken from various studies (Zhao 2002).

From figure 2.2 we can see that achieving an acceptable mean droplet SMD of 15 µm requires an injection pressure of approximately 8 MPa.

HIGH PRESSURE DI

The most obvious direct injection technique simply involves use of a large mechanical fuel pump to generate the high fuel pressure (typically 5 to 10 MPa) required to adequately atomize the fuel. As with Diesel engines, the pump is generally run via a linkage to the crankshaft as shown in figure 2.3 (Sogawa and Kato, 2001). This technique

was first used to directly inject gasoline by Mercedes in the 1950s and has more recently been commercialized by Mitsubishi in their gasoline direct injection (GDI) four-stroke automobile engines. Apart from being rather heavy and requiring invasive changes to the host vehicle for retrofit implementation, these pumps also are rather expensive as fine tolerances are required to generate such high pressures. For this reason engineers have developed several alternate methods of attaining fine atomization, the most common of which will now be discussed.

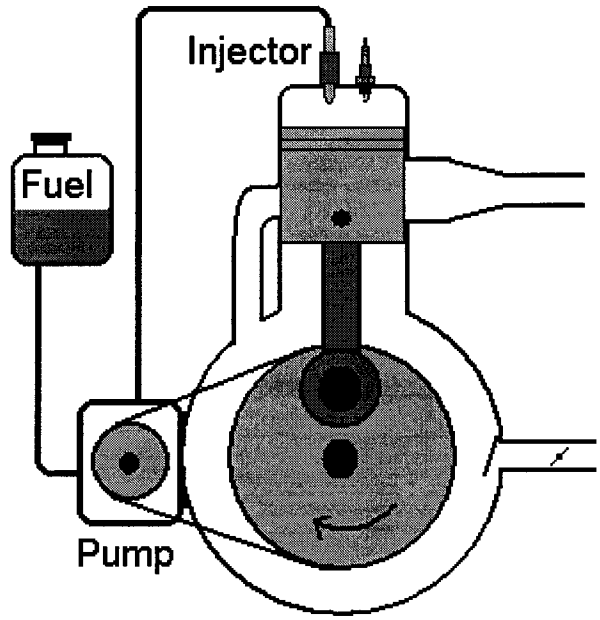

Figure 2.3 Schematic of a high-pressure direct injection two-stroke engine

SOLENOID PUMPED DI

With the solenoid pumped DI system relatively low-pressure fuel (approximately 300 kPa) is supplied to an outwardly opening injector with a very large solenoid, as in figure 2.4 (Heimberg 1993). When the injector is activated, the large solenoid's force pushes the fuel through the injector nozzle with peak pressures of up to approximately 2

MPa. While the fuel pump may be smaller than the high pressure-type DI pump, the injector is correspondingly larger, and requires more electrical power to operate. This technique, developed by the Ficht Company, was used in a number of marine engines with poor results due to low injection pressures and resulted in deposit buildup and spark plug fouling (Ajootian 1999). The deposits were formed as a result of incomplete combustion of large fuel droplets which were injected at lower pressures at either the beginning or end of the solenoid's stroke.

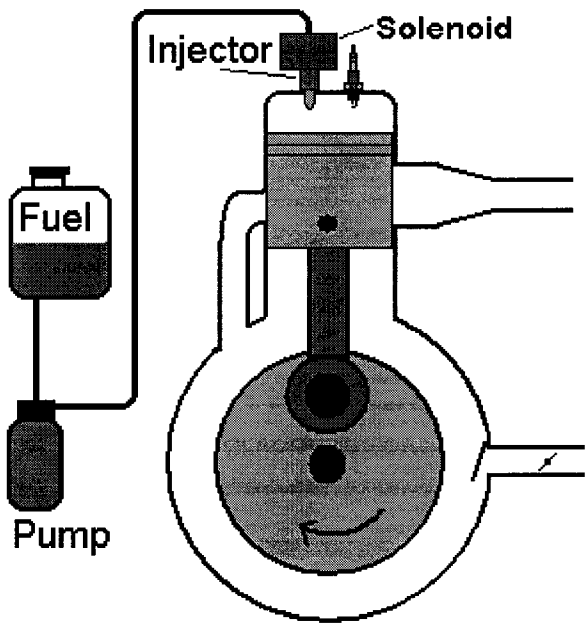

Figure 2.4 Schematic of a solenoid pumped direct injection two-stroke engine

HYDRAULIC RAM DI

The hydraulic ram or "water hammer" effect may also be used to raise the pressure of the fuel for injection as in figure 2.5. In this technique a relatively low-pressure (approximately 300 kPa) fuel pump maintains a continuous flow of fuel through a fuel rail connected to the injector (Bartolini et al. 2001).

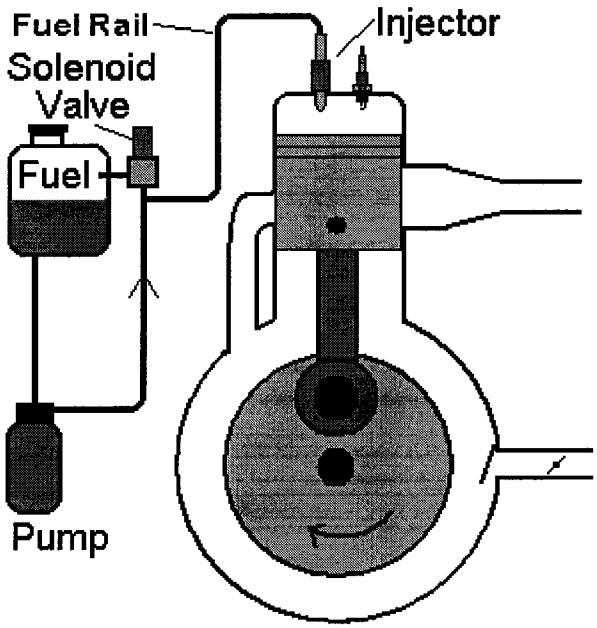

Figure 2.5 Schematic of a hydraulic ram direct injection two-stroke engine.

Shortly before injection is to take place, a solenoid valve in the fuel line down-stream of the injector is closed, causing rapid deceleration of the fuel in the line, and a corresponding rise in fuel rail pressure in the form of a high pressure wave. This high pressure wave travels back through the fuel line and through the fuel rail towards the injector. If the injector is opened when the high-pressure wave is present, the resulting fuel will receive the benefit of the high fuel rail pressure and achieve fine atomization as it enters the combustion chamber.

An alternative version of this same method has a mechanically resonating fuel circuit consisting of the low-pressure pump, a long section of stout pipe called the "acceleration tube" and a low-pressure check valve in the fuel return path replacing the solenoid valve. As fuel surges forward through the check valve it closes, creating the same high-pressure reflection wave. When the high-pressure wave reaches the fuel pump

entrance (or an expansion section in the circuit) it is again reflected but as a low-pressure wave. When this reaches the in-line check valve it opens again, re-establishing the fuel flow, and eventually repeating the cycle as fuel flow once again increases.

Instead of passing directly to the injector, the high pressure reflected wave in the acceleration tube is fed through a check valve into a high-pressure fuel cavity, which feeds the injector. The injector is then operated as in the high pressure DI technique.

While this system is not currently in use on any commercial systems, it is being investigated extensively in Italy for application to small displacement two-stroke motorcycles.

AIR BLAST DI

The Air Blast Direct Injection (ABDI) technique takes a slightly different approach to fuel atomization. Moderate pressure fuel (approximately 750 kPa) is injected into a cavity in an air rail mounted on top of a gaseous injector, called the blast valve. Air is continuously supplied from an air pump at a slightly lower pressure (approximately 650 kPa) to the same cavity (Huston 1998).

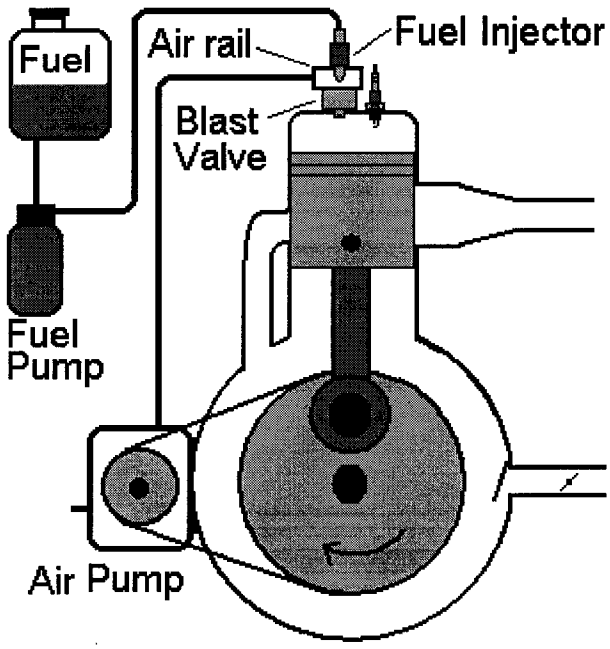

Figure 2.6 Schematic of an air blast direct injection two-stroke engine.

The blast valve allows the mixture from the cavity into the combustion chamber when opened. As the mixture passes through the valve into the chamber the high shear rates between the carrier fluid (the injected air) and the cylinder air cause fine atomization of the fuel.

This technique, pioneered by the Orbital Engine Company, has been applied extensively to two-stroke and four-stroke engines, and applied successfully as a retrofit to two-stroke engines in snowmobiles in the United States, and on three-wheeled transports in India (Willson et al. 2002).

COMPRESSION PRESSURIZED DI

A Compression Pressurized Direct Injection (CPDI) system is similar to the ABDI except for the source of pressurization. In a CPDI system fuel is injected to an intermediate mixing cavity containing a pressurized carrier gas. Once the exhaust port has closed a solenoid valve is opened between the mixing cavity and the combustion chamber and the mixture is blast into the combustion chamber. Again, the high shear rates between the injected fluids and the combustion chamber gases finely atomizes the fuel as it enters the combustion chamber.

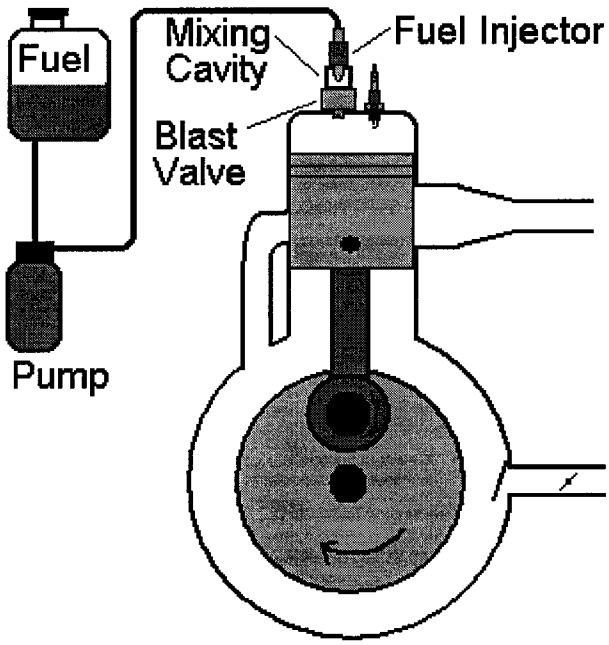

Figure 2.7 Schematic of a compression pressurized DI two-stroke engine

The difference between air blast DI and compression pressurized DI is in the source of the carrier gas pressurizing the mixing cavity. As the mixing cavity has a relatively small

volume, the pressure in the cavity drops rapidly as the contents are blast into the combustion chamber. As the piston rises, compressing the air/fuel mixture in the combustion chamber, the combustion chamber pressure will rise higher than that of the mixing cavity. If the blast valve is opened at this time, gases from the combustion chamber will flow back into the mixing cavity, raising the pressure of the mixing cavity. Through careful timing of the blast valve, enough pressure may be maintained in the mixing cavity for the direct injection of the fuel on the subsequent cycle. Initial work on this technique was performed by AVL of Austria on four stroke engines, however, it has never been exploited commercially (Fraidl 1996).

COMPRESSION WAVE DI

This method has an additional port in the combustion chamber connected to a sealed "wave tube". The new "injection port" is located at approximately the same height as the exhaust port (Cobb 2001). As the piston uncovers this port a compression wave from the chamber travels into the wave tube entraining fuel from an injector as in figure 2.8. The wave carries the fuel towards the closed end of the tube, significantly evaporating the fuel as the combustion chamber gases are hot.

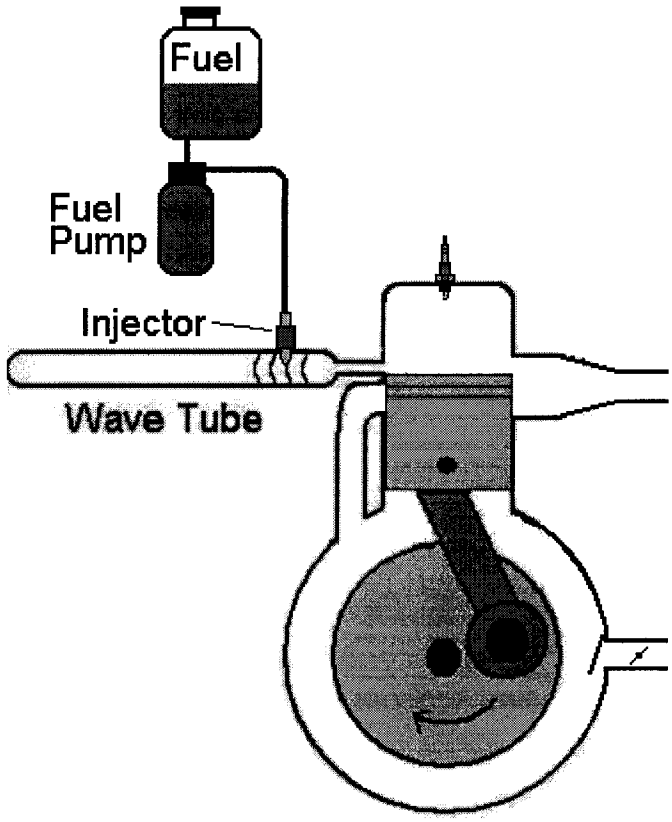

Figure 2.8 Compression wave is propagating to left past injector in wave tube.

The tube is sized such that the reflected compression wave re-enters the cylinder after the majority of the scavenging has taken place, i.e. slightly before the injection port is closed, thereby reducing significantly the amount of short-circuited fuel lost out the exhaust port. Obviously the port entry position and angle will have major effects on its overall effectiveness.

The compression wave technique was pioneered by John Deere and is probably most applicable to single speed operations, such as chain saws and "weed eaters".

GASEOUS FUEL SYSTEM

Another alternative method of direct injection is to use a gaseous fuel, such as Compressed Natural Gas (CNG is comprised mostly of methane) or propane, as shown in figure 2.9. These fuels have the advantage of having significant vapor pressure at ambient temperatures which eliminates the need for a pump to pressurize the fuel for injection. A system of this type would use an injector, similar to the "blast" injector of the previously discussed air blast system, to admit the gaseous fuel directly into the combustion chamber once the exhaust port is closed.

This technique is very common on large two-stroke engines used for power generation, pumps and compressors.

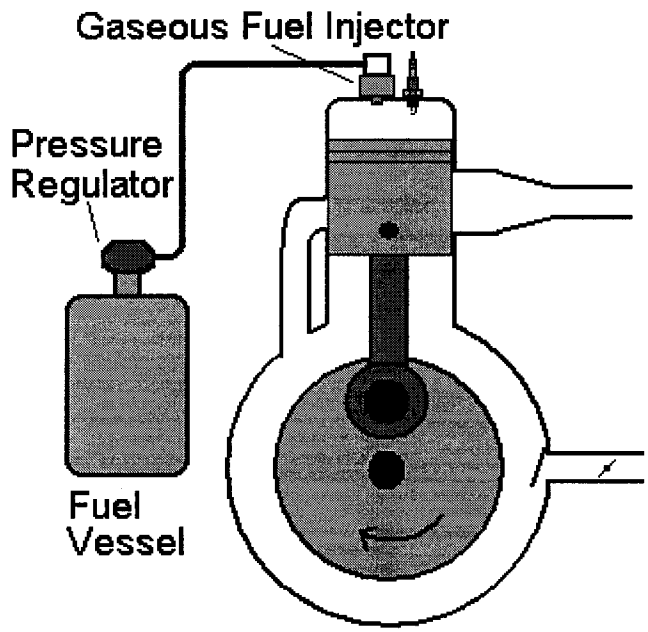

Figure 2.9 Gaseous direct fuel injection two-stroke engine.

COMPARISON OF THE VARIOUS DI TECHNIQUES

Each technique presented here has a unique set of advantages and disadvantages for our intended application. Figure 2.10 is a table listing the additional parts necessary for each technique and their approximate cost (some data from Little, 2001). While the numbers are only approximate, it is apparent that all of the various techniques are significantly more expensive than the original carbureted engine.

TECHNIQUE

Item	Carb.	High Press.	Solenoid Pumped	Hydro-Ram	Air Blast	Comp. Blast	Comp. Wave	Gaseous Fuel
Head	10	12	12	12	15	15	30[2]	12
Fuel Pump Press. (100 kPa)	0 Grav.	200 50	40 3.0	40 3.0	50 7.5	50 7.50	50 7.5	0
Carburetor	30	0	0	0	0	0	0	0
Fuel Injector	0	30	30	30	15	15	15	0
Regulator Fuel	0	5	3	0	3	3	3	0
Air Pump	0	0	0	0	30*	0	0	0
Gaseous Injector	0	0	0	0	15	15	0	15
Regulator Gas	0	0	0	0	5	5	0	5
Solenoid Valve	0	0	0	10	0	0	0	0
Additional Stator and modification	0	0	20[1]	0	0	0	0	0
Electronic Cntl. Unit	0	100	100	100	100	100	100	100
Sensors	0	35	35	35	35	35	35	35
Wiring & Misc.	0	10	10	10	10	10	10	10
Total	40	392	250	237	278	248	243	177

1 Denotes a price which includes significant required changes to the base motor
2 Price given for Cylinder in Compression wave technique, not head

Figure 2.10 Approximate price breakdown (in US$) of each technique (our estimates).

According to this analysis, the gaseous fuel injection system is the least expensive option. Among the liquid fuel (gasoline) systems the hydraulic ram technique will likely be the least expensive due to the low number of components. The air blast and high-pressure injection techniques will likely be the more expensive options, due to a larger number of components and modifications to the engine to incorporate the air pump or fuel pump respectively. Additionally, among the lower cost gasoline injection techniques (solenoid pumped, hydraulic ram, compression pressurized blast and compression wave) there is relatively little difference in cost. Finally, it is apparent that the Electronic Control Unit (ECU) is one of the most expensive components in all of the electronically controlled injection techniques.

Beyond the simple bottom line of cost, there are a number of other considerations that can greatly influence the ultimate success of implementing such a project on a large scale. Obviously, any modification made to improve emissions must maintain similar reliability to the original system. Carbureted two-stroke engines are inherently quite reliable due, in part, to the relatively small number of moving parts. While carburetors may wear and require some adjustment, they rarely fail catastrophically and result in an inoperable vehicle. These engines are, however, subject to spark plug fouling from excessive amounts of unburned hydrocarbons, including lubricating oil, which continually pass through the combustion chamber.

As vehicle operators often rely on their vehicle as a source of income either as a taxi or delivery vehicle, the time required for conversion may be a significant factor: the operator simply can not afford to have the vehicle laid up for too long during the

conversion. Both the reliability and conversion time will be strongly influenced by the invasiveness of the conversion, i.e. the fewer changes to be made to the basic engine, the less there is to go wrong, and the faster the conversion.

As the purpose of the conversion is to reduce the amount of engine emissions, one of the important considerations is how effective the conversion is at reducing emissions. This will be related to the ultimate fuel droplet size present in the chamber, combustion stability, and how much fuel escapes via short-circuiting.

Finally, one issue frequently overlooked is cultural barriers which may exist to inhibit the acceptance of the conversion. While, in general, there will be a high degree of acceptance of the technologies involved (especially as it should generally be transparent to the end user), there may be strong resistance to changing habitual patterns of behavior. This point may count strongly against the acceptance of gaseous fuels: operators are simply not accustomed to "filling up" on propane or natural gas, and the infrastructure may not exist as universally as it does for the gasoline fuel techniques, which require no habitual changes.

Figure 2.11 is a table comparing the various techniques in each of these areas. Again as these comparisons are by nature qualitative, the most significant issues are highlighted in **bold** and discussed below.

	TECHNIQUE						
Item	**High Press.**	**Solenoid Pumped**	**Hydro Ram**	**Air Blast**	**Comp. Blast**	**Compress. Wave**	**Gaseous Fuel**
Conversion (days required)	2	1	1	2	1	1	2
Reliability Rank:	Proven *3*	Problem *1*	Exptl. *2*	Proven *3*	Exptl. *2*	Exptl. *2*	Proven *3*
Cultural Barriers Rank:	None *3*	None *3*	None *3*	None *3*	None *3*	None *3*	Change of fuel *1*
Invasiveness of Mechanics Rank:	Head pump *1*	Head Gen. *1*	Head *2*	Head pump *1*	Head *2*	Cylinder *2*	Head Tank *2*
Emissions Rank:	15% *3*	15% *3*	15% *3*	15% *3*	15% *3*	30% *2*	15% *3*
Cost Rank:	292 *1*	260 *2*	237 *2*	278 *1*	248 *2*	243 *2*	177 *2*
SCORE (Average of Ranks)	2.2	2	2.4	2.2	2.4	2.2	2.2

Figure 2.11 Approximate ranking of the various techniques for several criteria. A higher rank indicates more acceptable (i.e. *3* = Good, *2* = Intermediate, *1* = Low). Conversion time has not been explicitly ranked as it depends on too many external factors to be reliably predicted.

Emissions are compared in terms of the expected emissions as a percentage of that exhausted by the original carbureted engine. For the truly direct injection techniques a decrease of approximately 85% in HC and CO emissions is expected. As the compression wave may allow some fuel short-circuiting, especially at off-design engine speeds, the emissions are expected to be some what higher.

Both high pressure DI and air blast DI require pumps driven directly from the crankshaft, greatly increasing the invasiveness of the conversion and increasing the time required for conversion. The solenoid pumped injection will also require a more

substantial generator to be installed, possibly requiring a new rotor and stator. As discussed earlier gaseous fuels will have a significant cultural barrier to their acceptance because of the need to change fueling habits.

Finally the reliability is based in part on the maturity of the technique, and partially on field experience. Several of the techniques (solenoid pumped, high pressure, air blast and gaseous DI) have been used on large numbers of engines, generally increasing the confidence in their viability. The solenoid pumped method has had significant problems in the field, related with poor atomization due to the relatively low pressure (2 MPa) upon injection, lowering its attractiveness as a possibility for our purposes. Additionally both the hydraulic ram and compression pressurized DI techniques have been demonstrated in bench tests, but have yet to be used in the field on a large scale.

If each of the five categories of cost, emissions, invasiveness, cultural biases, and reliability is given an equal weight, and we take the some-what arbitrary rankings as listed in figure 10, the average rank of each method may be then compared as a basis for choosing which method is most likely to succeed. Scores for each technique are listed in the bottom row of figure 10 indicating that the hydraulic ram and compression pressurized techniques are the most promising. While there is not a large spread among the ultimate scores of the various techniques arrived at by this technique, it does generally agree with the observation that these two techniques have no major strikes against them based on the previous analysis.

Choosing between the hydraulic ram and compression pressurized technique is more difficult, and may be considered arbitrary: both have a reasonable chance of

success, and they have similar costs. One deciding factor may be the consideration of leveraging existing technology: the compression pressurized gas technique shares a lot in common with the air blast DI system, which has proven its self in numerous field trials. For this reason we will be focusing our efforts on further development of the compression pressurized direct injection technique.

CHAPTER 3 NUMERICAL SIMULATION OF THE ENGINES

MOTOR SELECTION

Having chosen the compression pressurized direct injection technique for fuel delivery, we must now decide on a specific vehicle for our modification. There are a wide variety of two-stroke powered vehicles in use in developing countries. Perhaps the largest user of two-stroke powered vehicles is India, where individually owned motorcycles and purpose built three-wheeled *Bajaj* taxis are common. As China develops, the number of two-stroke engines there is also increasing in the form of two, three and four-wheeled vehicles of all kinds. Thailand also has a large individual motorcycle ownership, in addition to three-wheeled *Tuk-tuk* taxis, and motorcycle taxis (where passengers ride on the back of the motorcycle, women often riding side-saddle!). In the Philippines small motorcycles are fitted with a custom-made sidecar, and used as taxis called *tricycles*. India and Thailand have both been investigating ways to improve two-stroke vehicular emissions. There is currently a project in India to implement an air-blast direct injection system on the Bajaj taxis, and Thailand has been using gaseous fuels in their Tuk-tuks in Bangkok for some years, albeit through a gaseous carburetor rather than direct injection.

The Engines and Energy Conversion Laboratory (EECL) of Colorado State University had recently received a request for help in reducing the emissions of the two-stroke tricycles. As no other two-stroke conversion projects are currently underway in the Philippines despite a population of approximately 1.3 million two-stroke vehicles, it appears to be an excellent choice for our study. Based on a survey of tricycle taxis in the metro Manila area, the Kawasaki HD-III is clearly the most common single model motorcycle in use in Manila (see figure 3.1).

Model	Capacity (cc)	Stroke (2/4)	Qty (#/64)	Popularity (% of pop.)
Kawasaki HDIII	125	2	28	44%
Suzuki X-4	125	2	11	17%
Honda	155	4	4	6%
Suzuki	123	2	3	5%
Yamaha RS	100	2	3	5%
Suzuki X-3	100	2	2	3%
Kawasaki CDI	125	2	1	2%
Skygo	125	4	1	2%
Kawasaki HD 140	140	2	1	2%
Yamaha RXT	135	2	1	2%

Figure 3.1 Relative Popularity of various motorcycles for use as "tricycle" taxis in Manila based on a survey of 64 vehicles by the author, summer 2003.

Through the generous support of the Foundation for a Sustainable Society Incorporated of the Philippines (FSSI) we acquired our own copy of this vehicle, shown in figure 3.2, thus our engine modification is based on the Kawasaki HD-III engine. The stock HD-III engine is an ideal test engine for our modifications being a 125 cc, carbureted, crankcase scavenged two-stroke in relative abundance on the roads today.

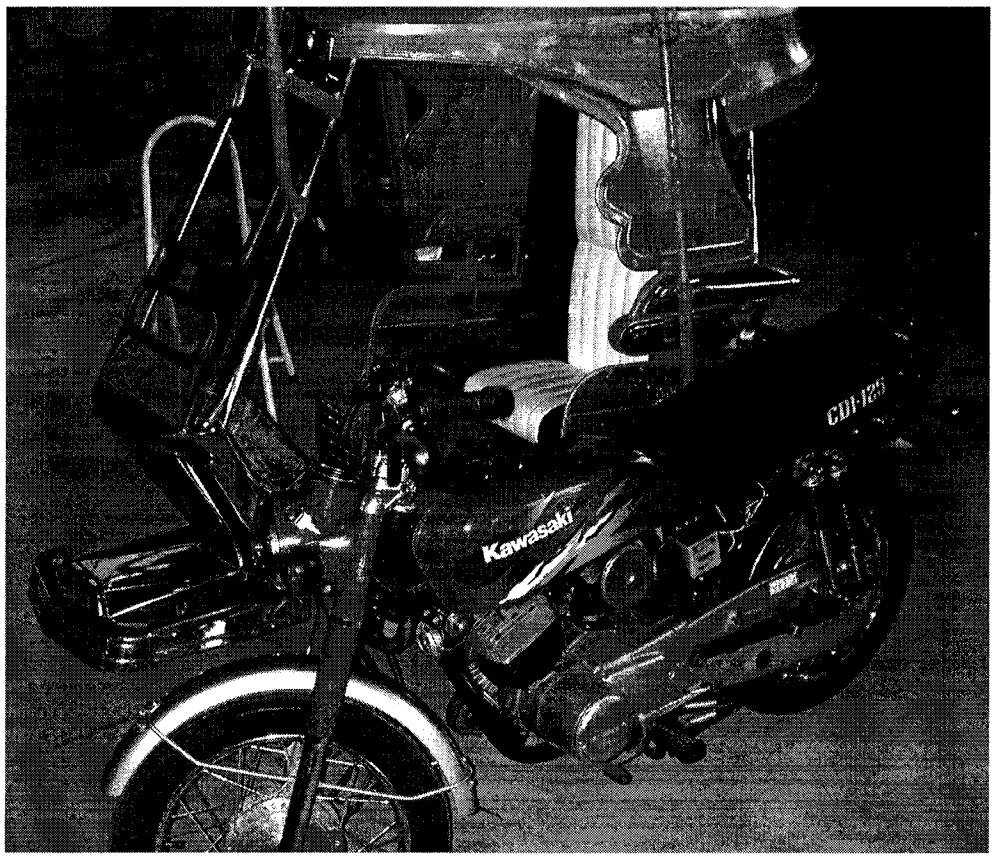

Figure 3.2 The Kawasaki HD-III Tricycle at the EECL.

MODELING

To aid in the design of our CPDI system, we would like to be able to predict the effect of changing mixing cavity volume and blast valve timings on mixing cavity pressure, combustion chamber air/fuel ratio and engine performance. Fortunately there

are several good engine simulation software packages available. Currently at CSU the most common engine simulation software is Ricardo's WAVE dynamic engine simulation program.

WAVE is a one-dimensional fluid dynamic engine simulation program with combustion heat release and heat transfer modeling (Ricardo 2001). In the model of the engine all gaseous passageways are modeled as ducts of the appropriate length, curvature and cross-sectional area. Momentum of intersecting flows is taken into consideration and special attention is paid to flow or discharge coefficients of flow discontinuities, ports and valves. Given the appropriate input parameters, WAVE has been successfully used to predict engine power production, fuel consumption, exhaust emissions for hydrocarbons, carbon monoxide and carbon dioxide, as well as cylinder pressures and the influence of exhaust tuning (Gitano-Briggs 2003).

The engine's air passages were carefully measured. Special attention was given to measurements of the carburetor, disk valve, crankcase, transfer ports, combustion chamber, exhaust port and exhaust system. Some of the most significant parameters are shown in figure 3.4

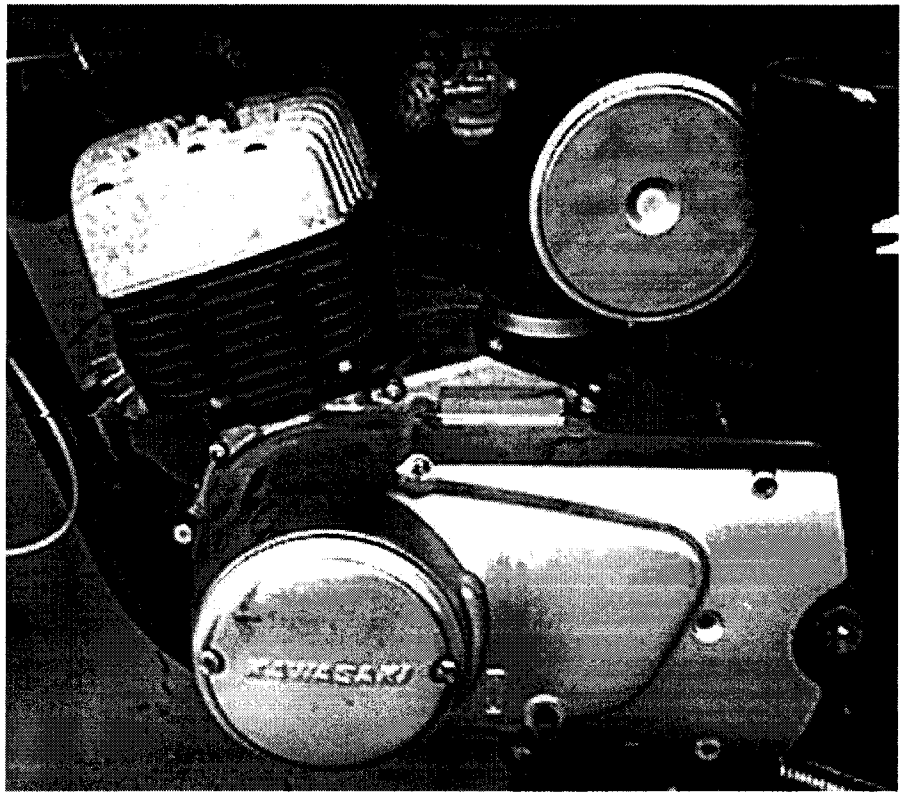

Figure 3.3 Kawasaki HD-III 125cc carbureted two-stroke engine. The carburetor is hidden inside the engine housing on the far side of the block.

Bore	54.9mm	**EPO**	105deg
Stroke	52.5mm	**XPO**	127deg
Connecting Rod	115.0mm	**DVO**	-110deg
Dead Volume	15.8cc	**DVC**	48deg
Displacement	124.2cc	**Ignition**	-17deg
Compression Ratio	8.9		
Crankcase CR	1.3		

Figure 3.4 Basic Parameters of the Kawasaki HD-III Engine. EPO is Exhaust Port Open, XPO is Transfer Port Open and DVO/DVC is Disk Valve Open/Close.

Additionally ignition timing and cylinder pressure were measured to determine the appropriate combustion parameters for the model. Figure 3.5 is a comparison of measured cylinder pressure versus time, and the modeled curve of the same using a Wiebe function where the function parameters were determined from fit to the data.

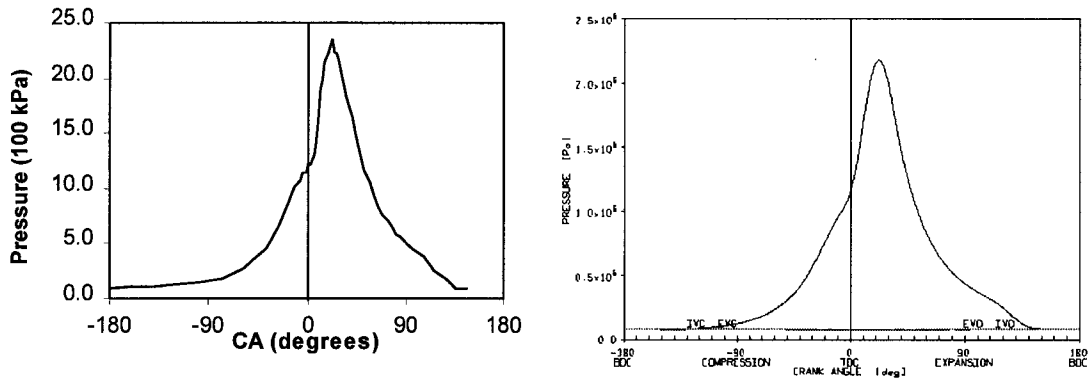

Figure 3.5 Combustion pressure measured (left) and modeled (right) based on Wiebe function exponent of 2, burn duration of 24 degrees, and 50% burn at 15 degrees ATDC.

CARBURETED MODEL

As WAVE models pressure waves and their reflections from discontinuities in the flow path, each segment of the flow path must be carefully measured to properly model the flow in the actual engine. The flow passages of the HD-III engine were broken down into 27 separate segments, excluding the combustion chamber. The measured diameter, length and effective bend angle of each segment is shown in figure 3.6, along with a brief explanatory label.

Pipe	Diameter	Length	Angle	Temp	Comment
1	3.09	5.6	0	308	Intake
2	11.6	6	90	308	Can
3	0.1	1	0	308	Filter (n=1000)
4	6.7	5.7	90	308	Inside Filter
5	6.7	0.905	0	308	Boot
6	6.6	3	0	330.5	Black flange
7	8.8	11.4	90	353	Rear block
8	4	2.5	0	353	Entry to side case
9	15	20	180	353	Side path to carburetor
10	2.7	1	0	353	Carburetor ram
11	2.215	0.52	0	353	Taper
12	2.215	1.4	0	353	pre-throttle
13	0.25	1.5	0	353	THROTTLE 0.1 to 2.17 Diameter
14	2.225	1.1	0	353	post-throttle
15	2.311	6.3	0	353	Feed to Disk Valve
16			90	353	CRANK CASE
17	2.55	1.8	0	393	XP1 and XP2
18	1.6	1.5	0	393	XP1 and XP2
19	2.2	1	45	393	XP1 and XP2
20	2.15	3.2	0	393	XP3
21	1.7	1.02	45	393	XP3
22	3.6	4.8	25	393	Exhaust Port
23	3.6	40.6	160	413	Exhaust Pipe curve
24	6.35	27.9	0	413	Expansion
25	1.25	53.3	0	413	Muffler (n=4)
26	2.8	3.8	0	413	Compression
27	2.8	1.27	0	413	Tip

Figure 3.6 Gaseous passages of the HD-III engine (lengths in cm, angles in degrees and temperatures in K). Grey numbers indicates parts of the carburetor.

With these gaseous passages, or ducts, entered in to the WAVE software, along with the crankcase, combustion chamber and atmospheric boundary conditions we have the schematic model of figure 3.7.

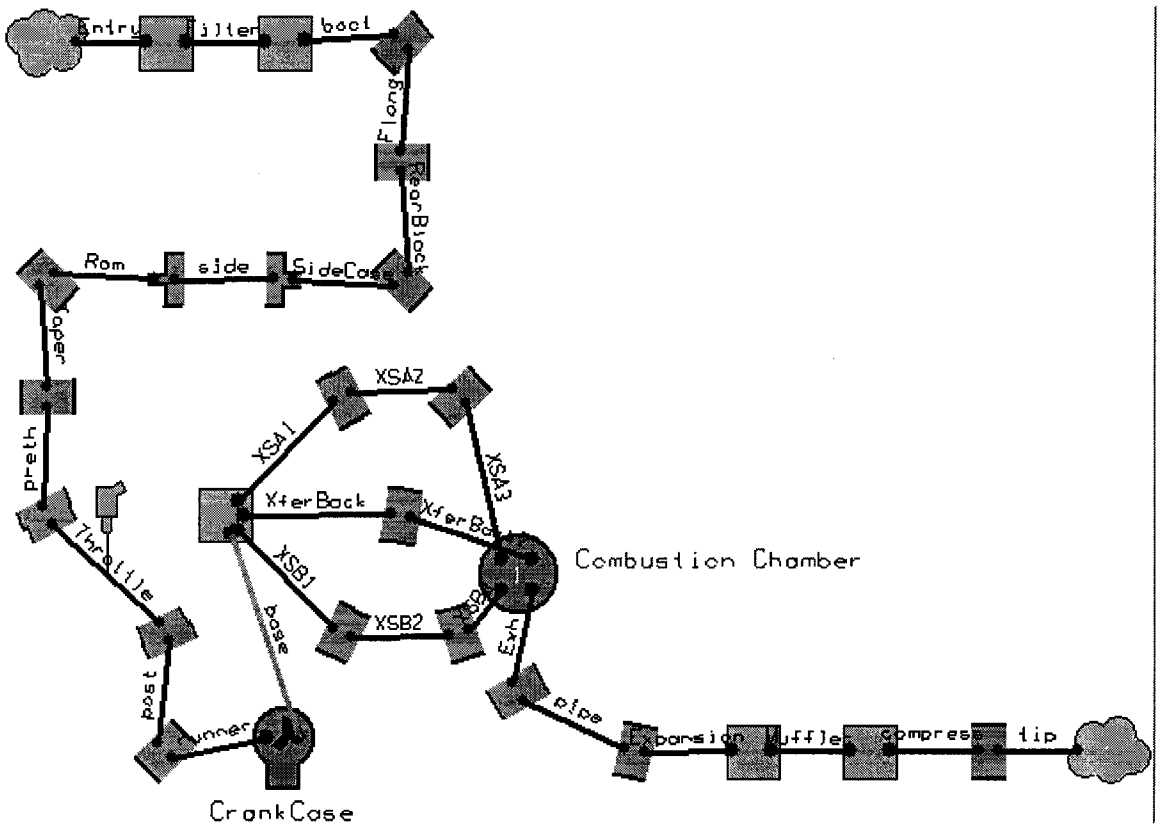

Figure 3.7 Schematic of the carbureted Kawasaki HD-III model

Each duct is represented by a black line in the graphic schematic. Junctions between different sections are shown as rectangular segments joining two or more ducts. Atmospheric boundary conditions are represents by the cloud-shaped icons at the upper left (intake to air cleaner) and lower right (end of exhaust pipe). The crankcase is graphically represented by the skeleton keyhole shaped icon in the lower left, and the combustion chamber is represented by the large round icon. Notice that the combustion chamber has 3 ducts entering from the left representing the three transfer ports, and a single duct exiting from the lower right, representing the exhaust port. Additionally there is a fuel injector icon attached to a duct on the left labeled as the Throttle. The diameter of this duct is variable, allowing simulation of the various throttle settings. The

introduction of fuel into the airflow through the carburetor is accomplished in the model by a proportional injection of fuel into the air stream at the location of the injector icon, in this case in the middle of the throttle section where the needle jet of the carburetor is. Once the air/fuel ratio is set, any air passing through the duct with the injector is given a proportional amount of fuel, most of which will eventually become trapped in the combustion chamber and participate in a combustion reaction.

Appropriate data must be entered for the combustion chamber (i.e. bore, stroke, compression ratio, temperature, surface area, ignition timing, scavenging model parameters), crankcase (compression ratio, temperature, surface area), atmospheric boundary conditions (pressure and temperature), and fuel properties. A partial list of the model's input variables can be seen in figure 3.8 which is generated by the model at the beginning of execution. For our model we used the properties of Indolene for the fuel. In addition friction may be modeled via the Chen-Flynn friction correlation model.

```
-------------------------------------------------------------------------------------------
   RICARDO SOFTWARE    ---   WAVE SIMULATION CODE   ---   VERSION 5.0p3
-------------------------------------------------------------------------------------------

BAS:CONSTANTS ======================================================================
vc = .5
rpm = 6000
BVO = -85
BVd = 5.3
FO = 0
FD = 1.16
Thr = 2
ta = 308
tb = 353
tc = 393
te = 413
BAS:GENERAL PARAMETERS =============================================================
20 0.8 1.0 SI                        ! TIMT/NCYC,CFL,DDEGMX,UNITS
N N N Y                         ! RESTART,DUMPCKP,SKIPINIT,AUTOCONVERGE
INDOLENE                              ! FUELFILE
BAS:OUTPUT & PLOTTING ==============================================================
0 0 0 0 0 0 0 0 0 0                    ! IOUT1 THROUGH IOUT10
N -30. 70. auto                     ! ZOOM,TZOOM(1,2),INCPL
Postscript DRAFT
ALL NULL CASE                       ! SUMMARY,FIXSTEP,SUMFREQ
N N n N                                ! ANIMATE, SOUNDTRACE
case 25                             ! WARNFREQ, MAX_WARNINGS
BAS:SUMMARY_TABLE ==================================================================
none y y
vc rpm Thr BVD FD BPOWKW BSFCSI PHITRAP
COMBSTRT BSHC PMAXSI #
BAS:TIME PLOTS =====================================================================
```

Figure 3.8 Partial set of model input data as output by the simulation software.

Many of these input parameters, for example valve timing, and engine displacement, may be measured directly, and are crucial to the accurate modeling of the engine. Other parameters, such as piston temperature, may be more difficult to measure and a reasonable assumption must be made. Still other parameters, such as the temperature of the tip of the exhaust pipe, have relatively little effect on any of the desired results.

Many of the results of the simulation are cycle average numbers (such as engine speed), time average numbers (power output) or break-power specific numbers (i.e. hydrocarbon emissions, fuel consumption). In addition, we can request many intermediate results of the simulation, such as pressure or flow, amount of air, fuel, or exhaust products, or temperature in a duct or chamber of the engine. These intermediate results are given as a function of crank angle, such as the pressure of the combustion chamber in figure 3.5, right side.

Once all the appropriate parameters have been measured or assumed, some of the model outputs must be compared with actual data from the engine. By comparing specific results we may be able to improve our assumptions, and make the model reflect the actual engine more faithfully. The "tuning in process" should only be used to adjust parameters we cannot directly measure, and then only within reasonable bounds. Also once the final values of the input parameters have been settled on it is important not to change them in any of the subsequent models, to avoid confounding the results.

ABDI MODEL

Once the carbureted model was finalized, only relatively minor changes were required to create an air-blast direct injected model of the same engine. All the existing ducting remains, but the fuel injector was removed from the throttle and placed instead in a mixing cavity connected to the combustion chamber by a blast valve. A pressurized air source is also connected to the mixing chamber via an air rail, as shown in figure 3.9. This pressurized air source is, of course, provided by an air pump in the physical ABDI engine.

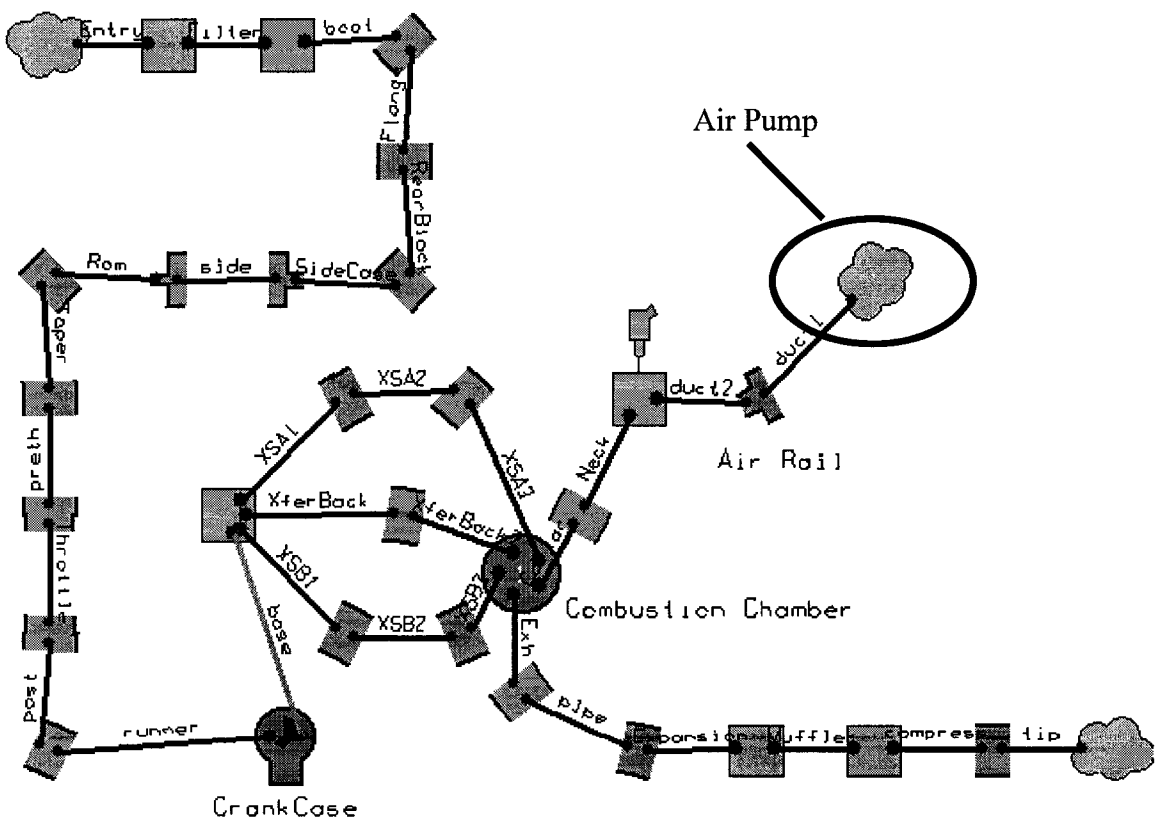

Figure 3.9 Air blast direct injected HD-III engine model

To ensure proper modeling of the actual injectors we must know their flow rates. We measured the volumetric flow rate of the air blast injector, with the results shown in figure 3.10. The fuel injector was also measured and had a flow rate of 3.8 g/sec under normal operating conditions.

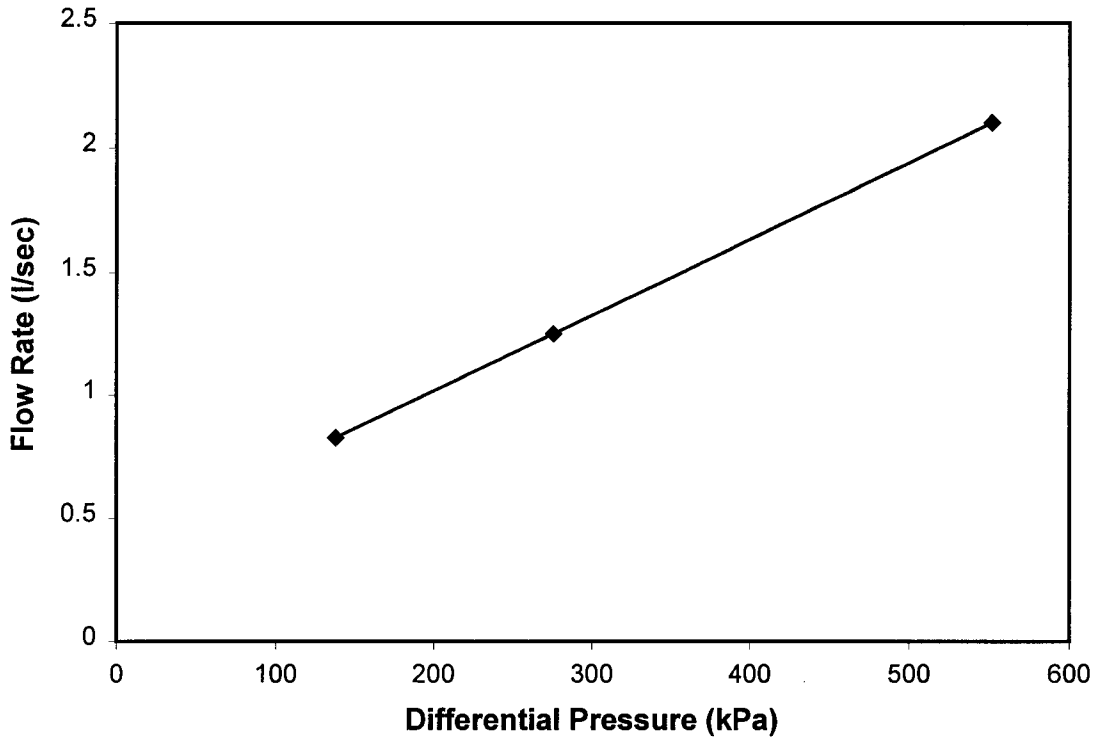

Figure 3.10 Air blast flow rates as a function of differential pressure

The air blast valve was designed to open just at Exhaust Port Close (EPC) to avoid any short-circuiting of fuel, and close as early as possible to ensure effective injection the fuel charge deposited in the mixing cavity. For WAVE to calculate the combustion reaction the air blast valve must be closed before ignition. Fuel injector duration will directly influence the equivalence ratio trapped in the combustion chamber. The fuel injector was chosen to open rather arbitrarily at TDC, depositing its charge in

the mixing chamber, behind the closed blast valve. The fuel injector was made to close at a time such that the deposited fuel was sufficient to give a trapped equivalence ratio of 1 (i.e. a stoichiometric air/fuel mixture) in the combustion chamber. Thus the duration of fuel injector opening is a function of engine speed and throttle, both of which affect the amount of air trapped in the combustion chamber. Port areas, air blast valve area are shown in figure 3.11. The fuel injector area is also shown, but with an arbitrary scale factor. Notice that the air blast injector is only opened after the exhaust port is closed, and the fuel injector is opened after the air blast valve is closed. Port timings are fixed, but injector and blast valve timings will change as a function of engine speed and throttle setting. To ensure that the blast valve duration is sufficient, the fuel fraction of the mixing chamber may be investigated.

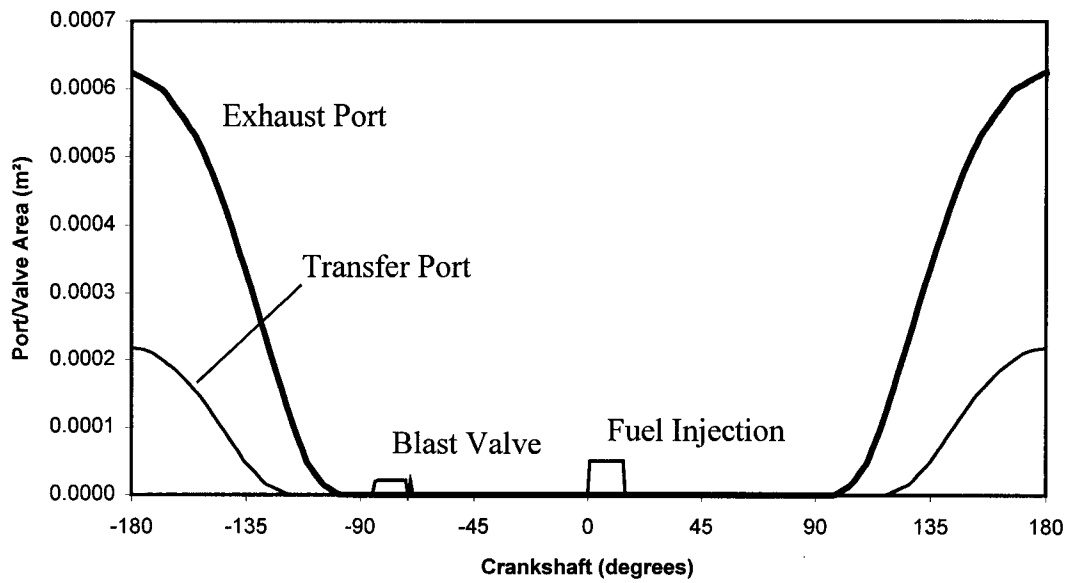

Figure 3.11 Port and air blast area open to combustion chamber. Fuel injector is open to mixing chamber only, and is shown for reference only. Data shown is for the ABDI model of HD-III at 6000 rpm, Wide Open Throttle (WOT).

The mixing chamber initially contains only air, but at TDC the fuel injector opens, rapidly injecting fuel into the mixing chamber, raising the fuel fraction. Once the blast valve is opened the contents of the mixing chamber are purged into the combustion chamber, transferring both air and reducing the fuel fraction. This sequence is shown in the modeled result of figure 3.12. Notice that there is significant fuel "hang up" in the mixing chamber (i.e. the fuel fraction does not drop to 0 after Blast Valve Closed (BVC) and before opening of the fuel injector at TDC) as the fuel is being deposited behind the blast valve and is incompletely purged with pure air.

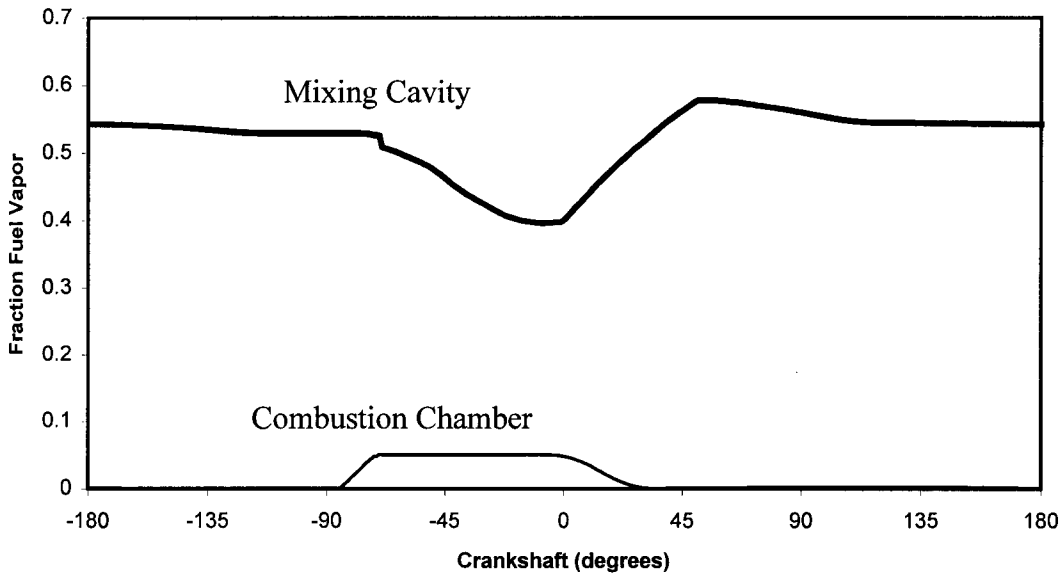

Figure 3.12 Fuel fraction in the mixing cavity and the combustion chamber of the ABDI HD-III model at 6000 rpm, Wide Open Throttle (WOT).

It can also be seen that the fuel fraction in the combustion chamber is zero until the blast valve is opened at about 85° BTDC. The fuel fraction in the chamber steadily increases as

the amount of fuel in the chamber is increased, but holds steady once the blast valve is closed. Ignition is started at approximately 20° BTDC, but it takes until about TDC to begin burning significant amounts of fuel. The combustion of the fuel is essentially complete by approximately 32° ATDC due to the particular Wiebe parameters chosen, reducing the fuel fraction in the combustion chamber to zero.

CPDI MODEL

The compression pressurized direct injected model of the HD-III engine, shown in figure 3.13 is very similar to the ABDI model but now the pressurized air source has been removed, and mixing cavity pressure is now a function of blast valve closing timing.

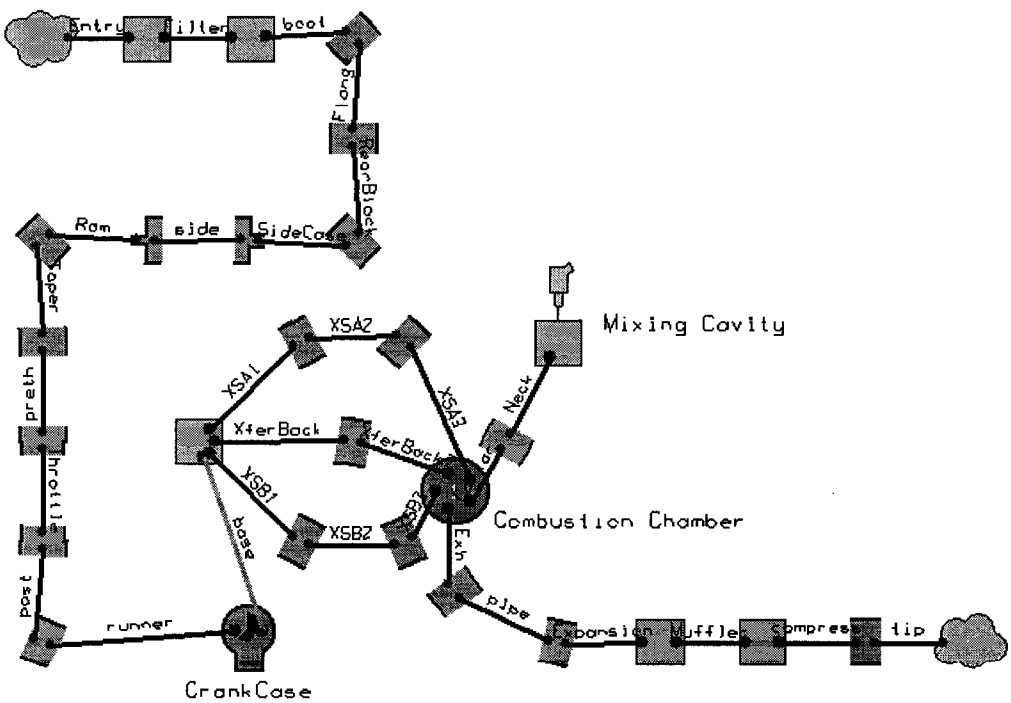

Figure 3.13 Compression Pressurized Direct Injected model of the HD-III engine. Notice the lack of air pump at the mixing cavity.

Similar to the ABDI model, fuel is injected into the mixing cavity at TDC, and the fuel injector is closed at such a time as to ensure an eventual trapped equivalence ratio of 1 in the combustion chamber. The blast valve is opened at EPC and closed at such a time as to allow the mixing cavity to re-pressurize to 500 kPa. As this will depend on the amount of air trapped in the combustion chamber, BVC will be a strong function of throttle and engine speed, as seen in figure 3.14.

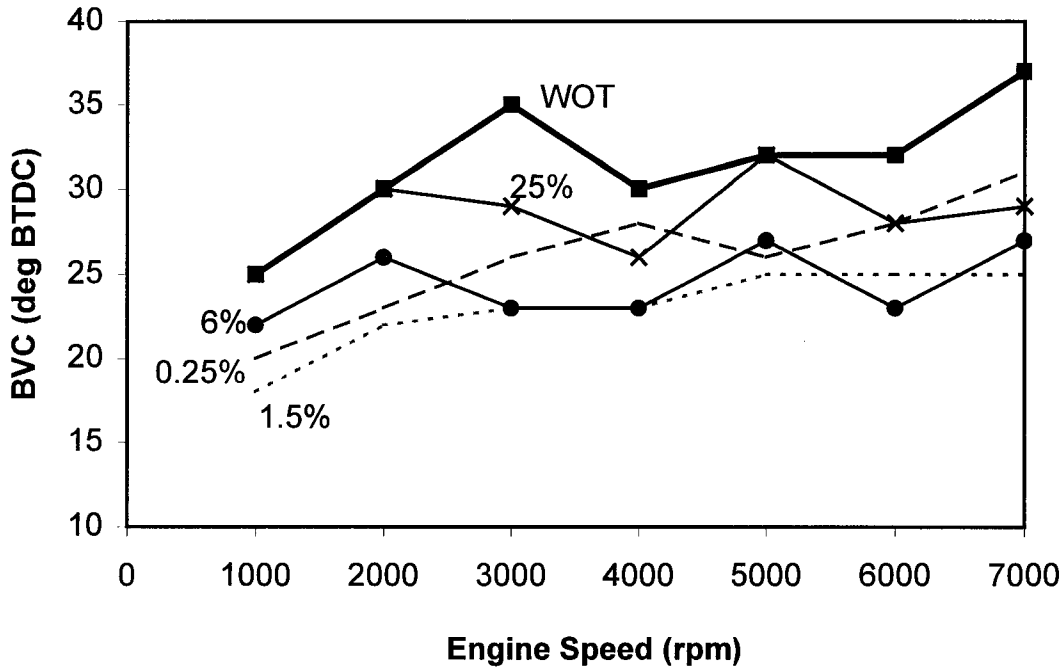

Figure 3.14 Blast Valve Closed (BVC) timing as a function of throttle and engine speed for the CPDI model of the HD-III.

The somewhat chaotic behavior of the curves is a result of the Helmholtz "ringing" of pressure waves in the cavity (discussed below), i.e. the BVC timing varies

depending on the direction of the traveling pressure wave in the neck connecting the mixing cavity to the combustion chamber. In general BVC is closer to TDC for partial throttle settings. This is due to the "rarification" effect of having the throttle closed: the tighter the throttle is closed, the lower the pressure in the intake manifold, and thus the longer the blast valve must remain open to fully re-charge the mixing cavity.

Additionally BVC is closer to TDC at low speeds, and further at high speeds. This is counterintuitive based on volumetric efficiency which results in less air in the combustion chamber at higher speeds, and would result BVC timings closer to TDC. The solution to this mystery is related to the fact that at low speeds the hot, compressed gases have greater time to transfer heat to the relatively cooler combustion chamber walls, which were modeled to have a temperature of 450K to 480K. According to the model, the gases in the combustion chamber had a temperature of approximately 800K shortly before ignition. This relatively high temperature is a result of heat transfer from the relatively warmer walls of the intake system as the gases are drawn into the engine, compression of the gases in the crank case and combustion chamber and mixing with the hot combustion products from the previous cycle during scavenging. At lower speeds the greater time allowed for heat transfer effectively lowers the cylinder pressure, and therefore requires a delay of the closing of the blast valve to achieve sufficient mixing cavity pressure.

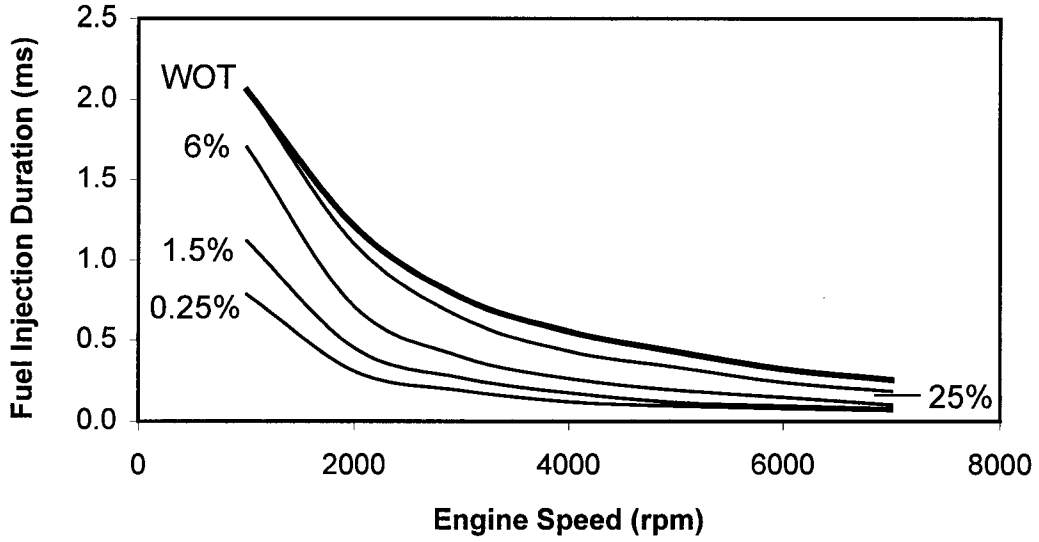

Figure 3.15 Fuel injector duration versus engine speed as a function of throttle position.

The amount of fuel injected is essentially proportional to the time the injector is held open. From figure 3.15 we can see that larger throttle settings will require larger amounts of fuel. This is expected as more air is admitted through the throttle plate at larger throttle settings. Also the amount of fuel required, per revolution of the engine, for a given throttle setting drops off with engine speed. This is due to the fact that the volumetric efficiency of the engine (the amount of air actually drawn into the engine divided by the swept volume of the engine) decreases as the engine speed increases. At high air speeds there is greater resistance to the air entering the engine, thus for a given swept volume, less air will be drawn in at higher speeds. This data is essentially the fuel map required by the Electronic Control Unit (ECU).

Modeling results for power output from the three fuel delivery designs (carbureted, air blast DI and compression pressurized DI) are shown in figure 3.16. From this figure it appears that the ABDI model will have a higher power than the carbureted version by approximately 14%. This is due to the fact that we are essentially "supercharging" the cylinder in the ABDI case with the high-pressure air from the blast charge. While this will raise the power output of the engine, it will be largely offset by the mechanical losses of running the air compressor, which has not been accounted for in this model.

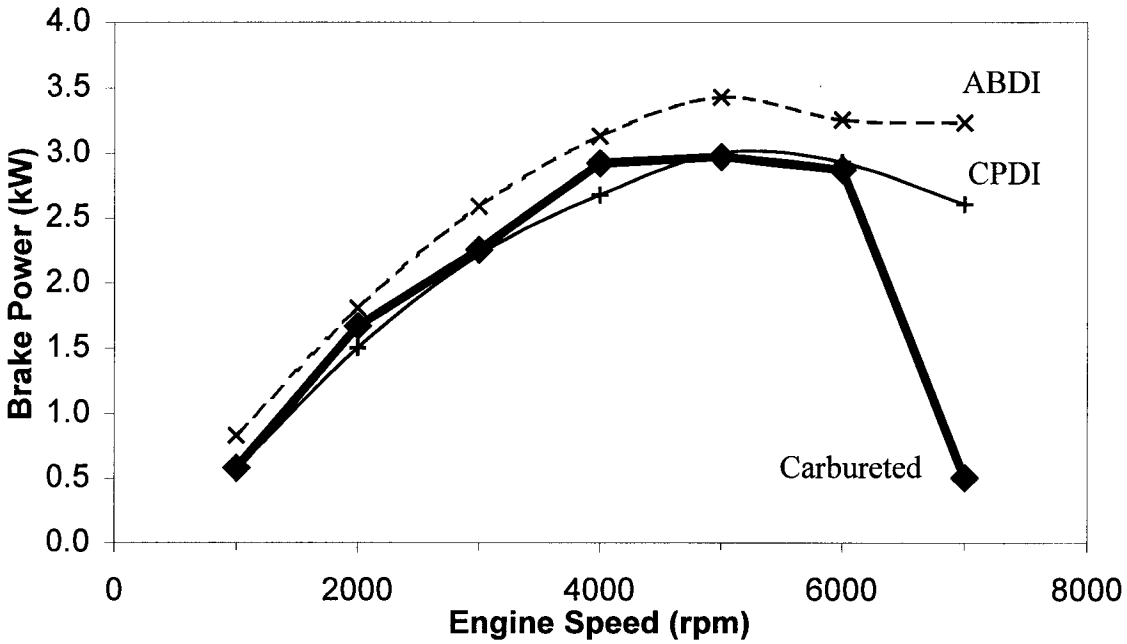

Figure 3.16 Comparison of break power as a function of engine speed for the three models at WOT.

The "pumping losses" have already been accounted for in the CPDI model, and its power curve compares quite well with the carbureted versions curve. At 7000 rpm,

however, both of the DI techniques show significant improvement over the carbureted version. This is partially due to an effect known as fuel displacement.

In the carbureted system fuel is mixed with the air as it passes through the throttle and enters the engine. In the DI techniques only air enters the engine, and the fuel is injected later. In the carbureted system some of the volume which could be occupied by air is taken up by the fuel, reducing the effective air volume trapped in the combustion chamber. This fuel displacement effect reduces the overall power available from the carbureted engine as compared with a DI engine. Finally, the carbureted model suffered from an acoustic resonance near 7000 rpm which reduced the trapped charge, resulting in less power than the DI systems which did not suffer from the resonance.

Emissions modeling results of the three techniques are shown in figure 3.17.

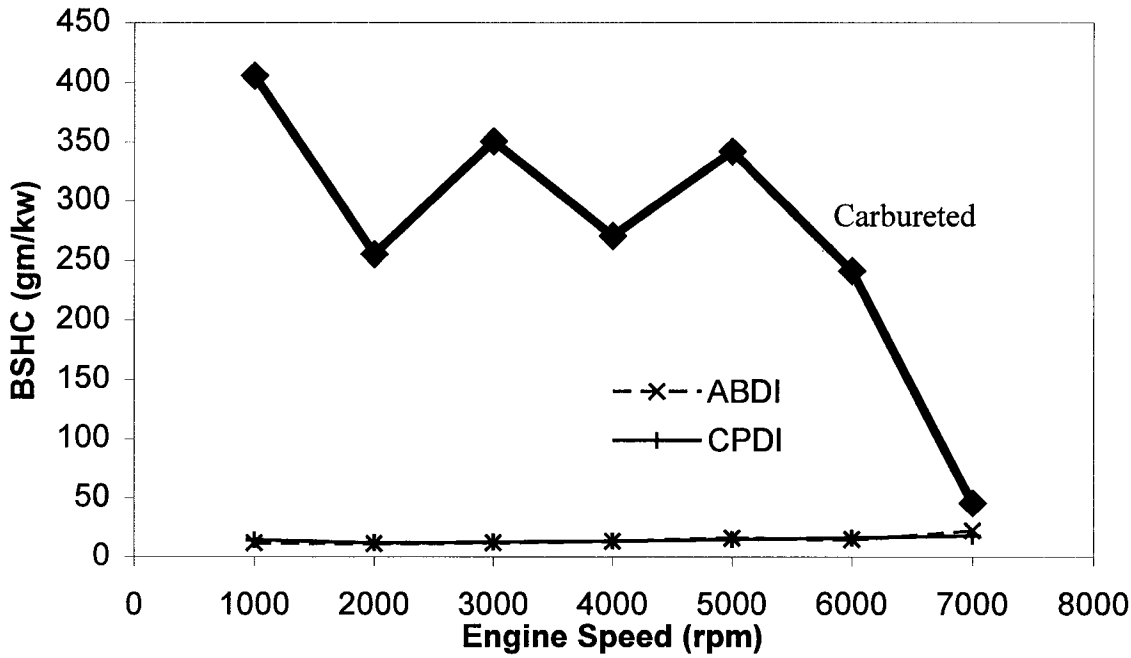

Figure 3.17 Comparison of Brake Specific Hydrocarbon (BSHC) production as a function of engine speed for the three models at WOT.

The oscillatory nature of the carbureted data in figure 3.17 and, to some extent, the strong dip in power of the carbureted power curve at 7000 rpm of figure 3.16 is related with a gas resonance in the combustion chamber and ports. As all air passages in the model are modeled as cylindrical pipes, they are much more prone to "acoustic wave resonances" than the actual engine. At certain operating frequencies acoustic resonance of gases in the combustion chamber and open ports leads to poor scavenging, and in the case of the carbureted version, greater charge loss, resulting in slightly lower power, and greater HC emissions.

Both of the DI techniques appear to have very similar HC emissions, while the carbureted emissions are more than an order of magnitude larger over the range of 1000 to 6000 rpm. This is, of course, due to the elimination of short-circuiting of fuel with the DI techniques. According to the model, at 6000 rpm the DI techniques should reduce hydrocarbon emissions by over 90%.

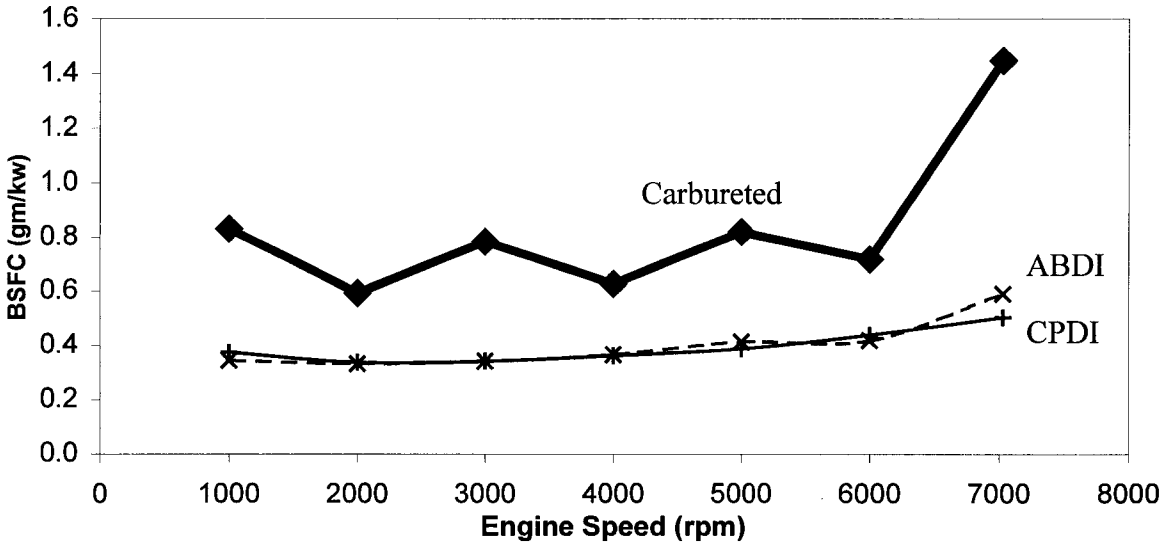

Figure 3.18 Comparison of Brake Specific Fuel Consumption as a function of engine speed for the three models at WOT.

The elimination of short-circuited fuel also shows up in results for the fuel consumption, seen in figure 3.18. Again the DI techniques are very similar, exhibiting a great improvement in fuel consumption (approximately 33% at 6000 rpm) when compared to the carbureted version. The difference in fuel consumption is, in this model, essentially all due to fuel short-circuiting, however, in a real engine there will be issues of fuel enrichment in the carbureted version (i.e. running the engine fuel rich to improve combustion), and combustion stability, which is not considered in this model.

Based on the model results we expect the DI systems to have a 33% reduction in fuel consumption and approximately a 90% reduction in HC compared to the carbureted version.

The data of the carbureted engine at 7000 rpm was dominated by an acoustic resonance, resulting in incomplete scavenging, low power production and abnormally low (for the carbureted engine) emissions numbers.

CHAPTER 4 IMPLEMENTATION OF THE ABDI SYSTEM

One of the first steps in the progression towards a working compression pressurized direct injection engine was the implementation of the air blast direct injection system on the test engine. This was done during the fall of 2003 by Tim Bauer and Nathan Lorenz, both of whom are veterans of previous two-stroke ABDI conversions on snowmobiles (Willson 2002). Most of the components for the ABDI system came from an Aprilia "Scarabeo" motor scooter which was purchased and dismantled. Custom fuel injection code was provided for the project by Orbital Engine Corporation, and replacement injection parts were acquired from Synerject.

The major modifications to the HD-III engine consisted of replacement of the head with a custom manufactured head and modification of the left side engine case to incorporate a 12V generator with magnetic position encoder wheel and air pump. Other minor modifications included mounting of the ABDI components (see figure 4.1) such as a new fuel and oil pumps, ignition coil, ECU, the throttle body (which replaced the carburetor), and machining an access hole to allow coupling of a dynamometer directly to the engine. The fuel stopcock was modified to incorporate a return line as required by the electrically driven fuel pump. Additionally several instruments were added to the display cluster.

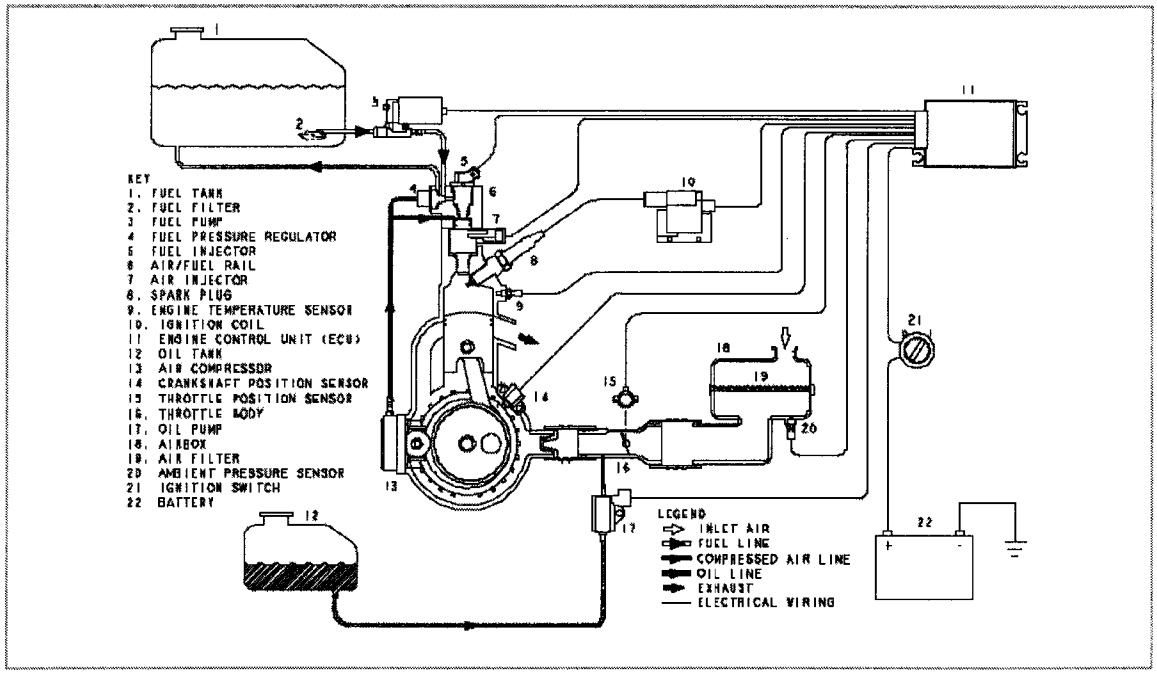

Figure 4.1 Components of the ABDI system

The head was designed by Nathan Lorenz based on a combustion chamber specified by Orbital for a similar displacement engine. It was milled out of a solid block of aluminum on a CNC (Computer Numeric Control) milling machine in the CSU Mechanical Engineering shop. Several separate stages of milling were necessary to incorporate all the features required on the head. The head is show in figure 4.2. The air blast valve can be seen mounted in a cavity on the top the head. Below that, the spark plug below can be seen to protrude and a temperature sensor is visible on the left-hand side of the head.

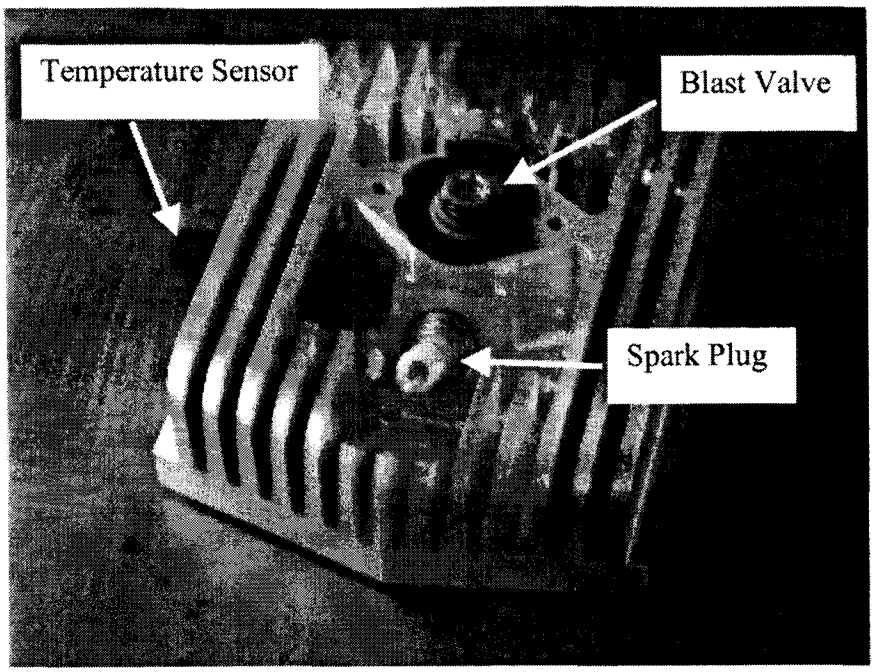

Figure 4.2 The ABDI head manufactured at CSU.

The head was designed so that the Aprilia's plastic fuel rail (figure 4.3) fits on top of the head and air blast injector. The fuel rail houses the fuel injector and incorporates a fuel pressure regulator which maintains a constant fuel-to-air pressure bias.

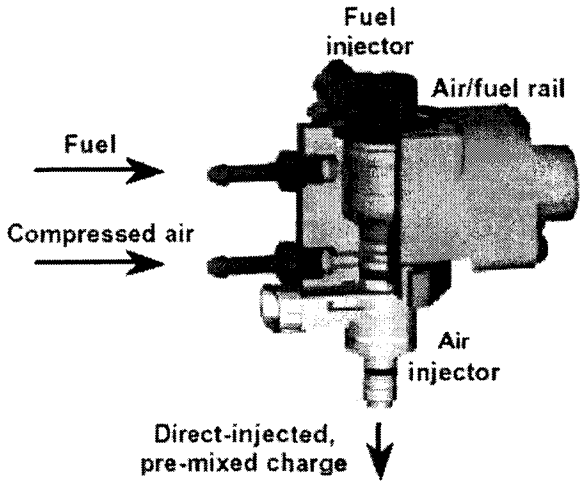

Figure 4.3 The ABDI fuel rail with the air blast valve (bottom) and the fuel injector.

While machining of the new head was an involved process, the actual replacement of the original head with the ABDI head is rather simple, only requiring removal of 4 nuts. For mass implementation of the ABDI retrofit the heads would likely be cast parts, requiring much less actual machining. Modifications to the left side of the engine case, shown in figure 4.4, were also quite significant.

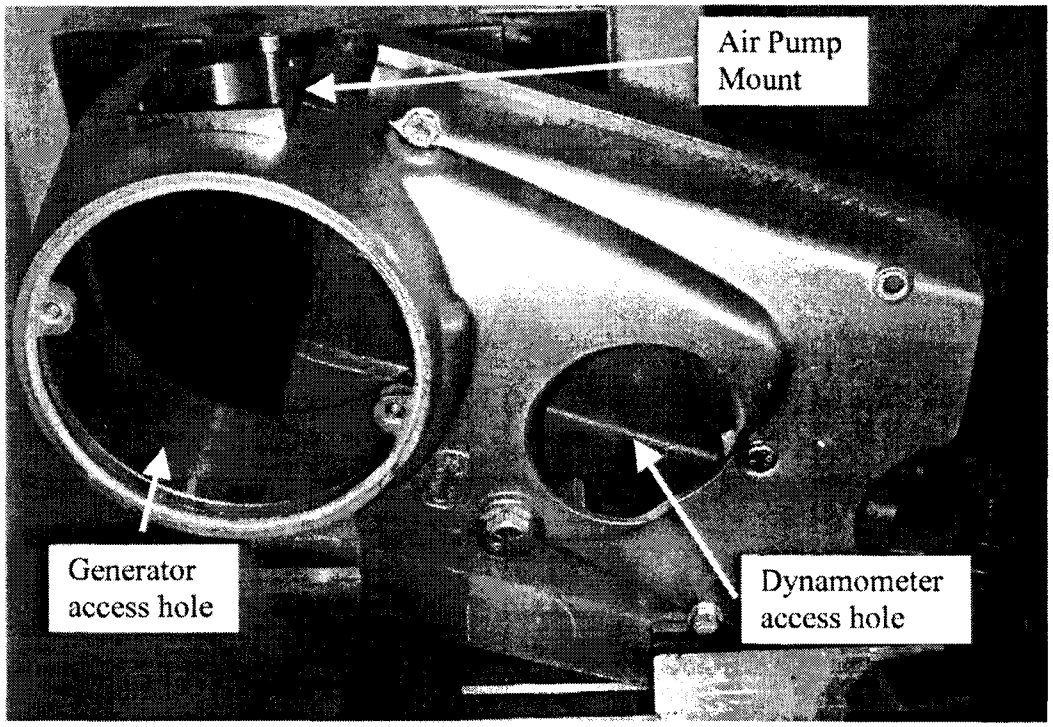

Figure 4.4 Left side of engine case showing modifications for ABDI

The smaller hole in the case just right of center is where the dynamometer will couple to the output shaft of the transmission. The large hole on the left is the generator access hole. Inside this, a custom steel sleeve has been fitted, to which the air pump mount (square with large hole protruding from the top) has been welded. The air pump is

actuated by a cam, in this case an eccentric circle, mounted to the outside of the generator, as seen in figure 4.5.

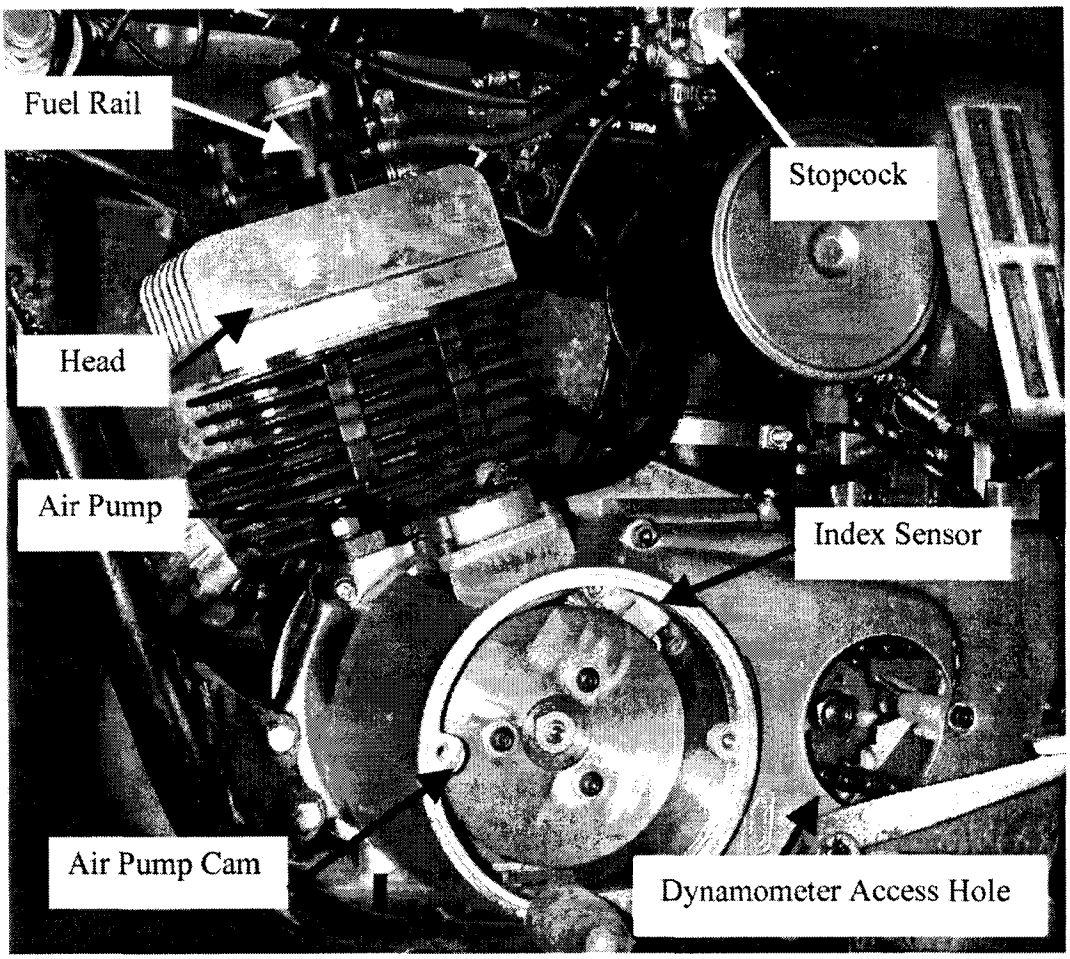

Figure 4.5 Left side of motorcycle with ABDI kit installed

Rough tuning of the system was performed initially based on vehicle drivability, audible perception of the consistency of combustion and visual perception of exhaust smoke. Fine-tuning was later performed on the dynamometer stand, measuring engine power, exhaust emissions using a gas analyzer, and combustion stability using a pressure transducer mounted in the head.

CHAPTER 5 DESIGN OF THE CPDI SYSTEM

COMPRESSION PRESSURIZED DIRECT INJECTION: ANALYSIS OF PERTINENT FACTORS

In order to successfully model such a complex system there are a number of important factors which require close investigation. We will now, therefore, describe some of the details of the CPDI system in greater detail.

In compression pressurized direct injection a poppet type solenoid valve separates a small mixing cavity from the combustion chamber, as in figure 5.1. As the piston rises during the compression stroke the valve is held open allowing cylinder pressure of perhaps 500 kPa to enter the mixing cavity. Notice also that some fuel from the combustion chamber may be present in the air entering the cavity.

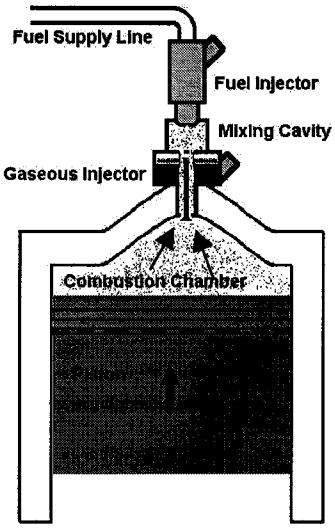

Figure 5.1 Compression pressure is admitted into the mixing cavity.

During ignition and expansion the solenoid valve is held closed, and relative low-pressure (600 kPa) liquid fuel is injected into the mixing cavity as in figure 5.2. Some of the fuel will atomize, but some of the fuel may remain as liquid droplets in the cavity.

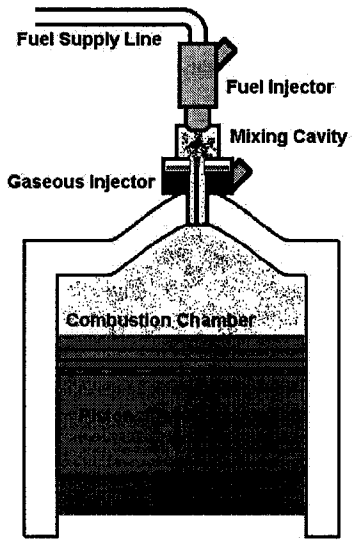

Figure 5.2 Fuel is injected into the mixing cavity while blast valve is held closed.

After exhausting the combustion products and scavenging the cylinder with fresh air, the exhaust port closes. The poppet valve to the mixing chamber is opened again, and because the combustion chamber pressure is now lower, around 150 kPa, the mixing chamber contents (at approximately 500 kPa) are blast into the combustion chamber atomizing the remaining liquid fuel as in Figure 5.3.

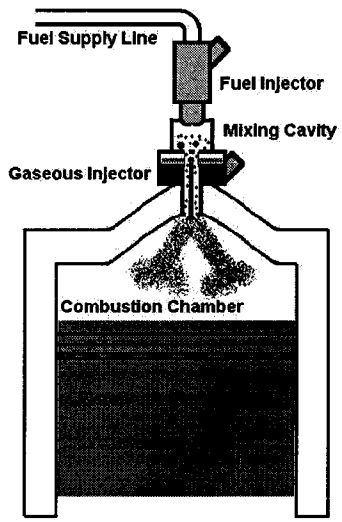

Figure 5.3 Mixture is blast into the combustion chamber.

While this is somewhat similar to the ABDI technique, where pressurized air for the conveyance of the fuel into the combustion chamber is supplied by a separate air pump, the differences have several important ramifications. First, the air pressure supplied in the air blast DI technique is essentially constant, generally being supplied by a positive displacement pump and regulator set up, and the volume of air supplied is sufficient to transport nearly all the fuel into the combustion chamber. With the compression pressurized DI technique the mixing chamber pressure drops as the mixture is injected

into the combustion chamber, as in figure 5.4. This lower pressure differential will potentially interfere with atomization quality especially as it drops to zero, which will result in "dribbling" in of larger droplets of liquid fuel from the film on the walls of the blast valve into the combustion chamber (Allen 1999). Additionally there is greater possibility of "fuel hang-up" with the CPDI system where some of the fuel is stranded in the mixing chamber. At steady state operating conditions the residual fuel in the mixing chamber will tend to balance out such that the amount of fuel injected into the mixing chamber is equal to the amount injected into the combustion chamber.

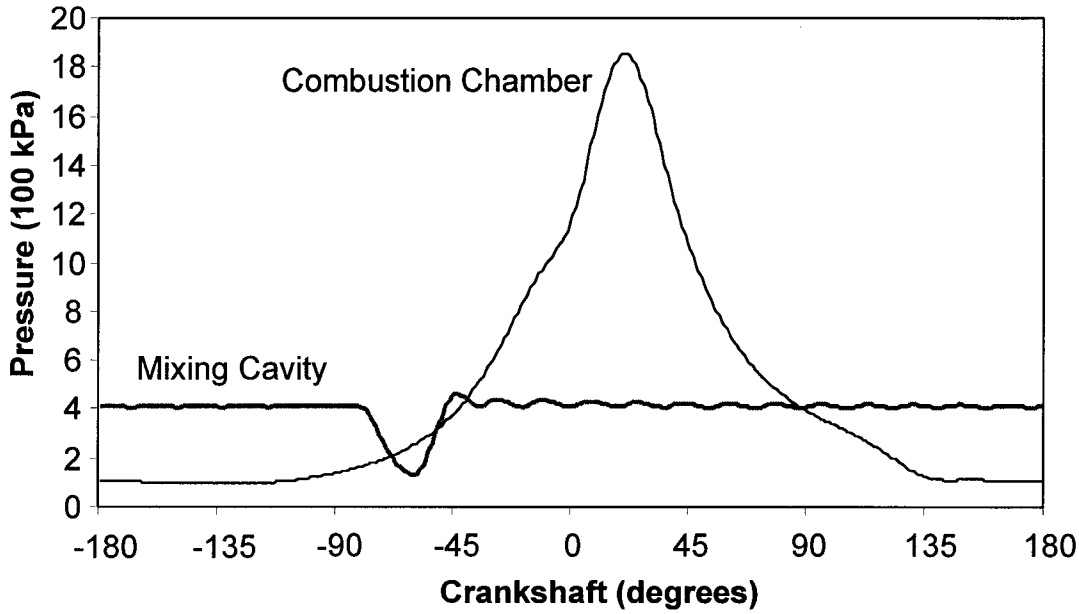

Figure 5.4 CPDI modeled mixing cavity and combustion chamber pressure versus crank angle at 6000 rpm, WOT. The blast injector opens at EPC (85° BTDC) injecting the mixture into combustion chamber and is re-pressurized as cylinder pressure rises. The injector is closed again at 39° BTDC, well before ignition.

During rapid transitions however, fuel hang-up could lead to inappropriate amounts of fuel entering the combustion chamber. This may result in higher emissions for rich deviations, or cause difficulties with ignition for lean deviations. To reduce fuel hang-up it is important to deposit the fuel as close to the blast valve as possible, and have a mixing cavity volume sufficiently large to allow the purging of most of the fuel to the combustion chamber. From the stand point of pressure differential we would like to have as large a mixing cavity as possible; the larger the mixing cavity, the smaller the drop in pressure during blast injection. As the size of the mixing cavity is increased, however, we will eventually run into problems pressurizing the mixing cavity quickly during engine start up. As the only source of pressure for the mixing cavity is the compression from the combustion chamber, a smaller volume pressurizes more quickly. Additionally, assuming homogenous distribution of fuel in the mixing cavity, the larger the mixing cavity volume, the greater the potential discrepancy in the amount of fuel delivered to the cylinder during engine transients due to fuel hang-up. For example, if we have a large mixing cavity and are running at a WOT condition, we can expect there will be a large amount of fuel in the mixing cavity. If the throttle is suddenly closed, we will inject a proportionally smaller amount of fuel into the mixing cavity, however, the amount of fuel hang up will be related to the size of the mixing cavity and the previous throttle setting, and it may take several revolutions of the engine before the mixing cavity is leaned out to the new operating point. The amount of time required to reach the new equilibrium will be proportional to the size of the mixing cavity.

Finally, there is a limit below which reducing the mixing cavity volume will have very little effect due to the dead volume of the blast valve itself. The blast valve has a

dead volume (volume within the valve itself exposed to the mixing cavity side of the valve) of approximately 0.4 cc. We have selected a mixing cavity volume of 0.5 cc for our design. This represents the minimum manufacturable mixing cavity volume. All modeling results presented in this thesis for the CPDI system are using a total mixing cavity volume (i.e. the mixing cavity proper plus the dead volume of the blast valve) of 0.9 cc.

DEPOSIT CONCERNS

The gases from the combustion chamber which pressurize the mixing cavity may contain unburned fuel and oil and/or hot combustion products as well as air. While this elevated temperature may be helpful in atomizing the fuel droplets, it may also overheat the injection valve. Additionally the combustion products may result in deposit formation in the blast valve/mixing cavity area. Combustion in the mixing cavity will not be an issue as the valve area is small enough to inhibit flame propagation, and the blast valve is generally closed prior to ignition.

To combat deposit formation it is favorable to use a good quality two-stroke oil with detergents (anti-deposit compounds). It may also be advantageous to use a detergent gasoline as well.

DOUBLE BLAST VALVE ACTUATION

One way to eliminate the potential "fuel dribbling" caused by low differential pressure injection is to separate the "blast" phase of the injection from the "recharge" phase by having two separate valve actuation events. This is shown in figure 5.5. In the doubly actuated case, the blast valve is opened at the same time as usual, but is closed while the pressure differential is still positive.

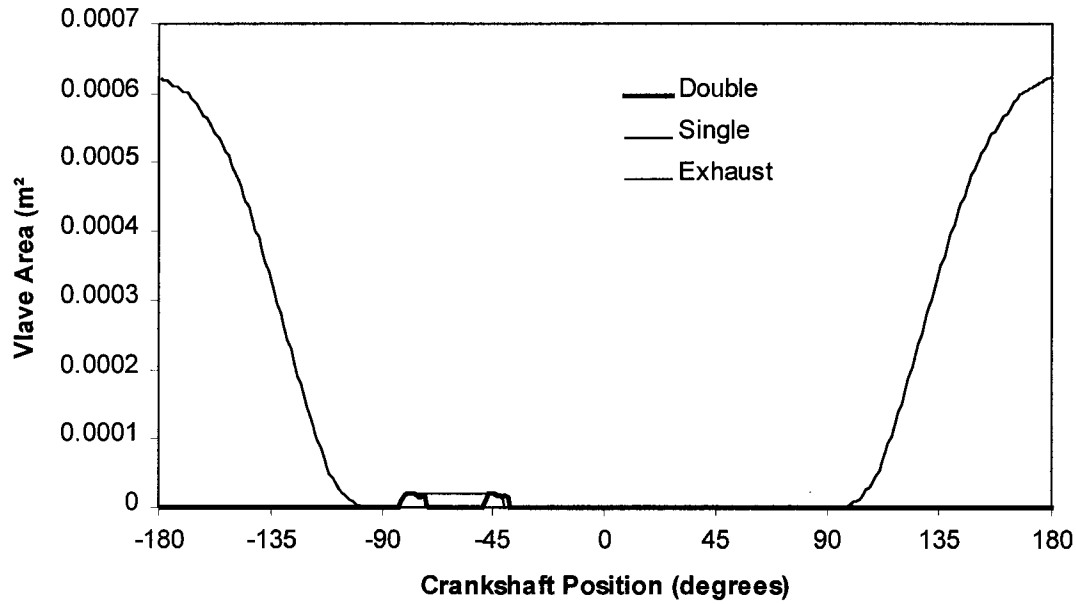

Figure 5.5 Exhaust port area, and blast valve area as a function of crank angle for single valve actuation and double valve actuation, 6000 rpm WOT.

During the blast phase mass is transferred from the mixing cavity into the combustion chamber until the blast valve is closed at the end of blast (EOB). After the

combustion chamber pressure has risen above that of the mixing cavity the blast valve is opened again, however, now the flow passes from the combustion chamber into the mixing cavity, thereby recharging it, as in figure 5.6.

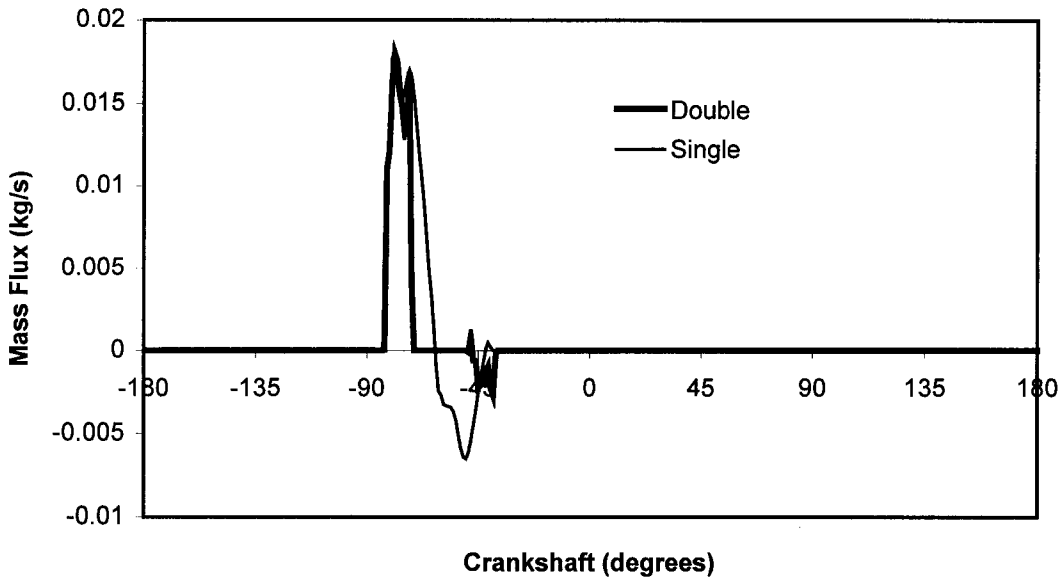

Figure 5.6 Mass flow through the blast valve for single and double actuation (separate blast and recharge phases) valve actuations. Positive mass flows represent flow from the mixing cavity into the combustion chamber. Modeled results for 6000 rpm, WOT.

Notice that more mass is transferred into the combustion chamber than is returned to the mixing cavity during the recharge. From figure 5.6 we measure this discrepancy to be approximately 0.0125 kg/s for 10 degrees CA, which is 278 μsec at 6000 rpm. This gives us a mass discrepancy of approximately 3.4 mg. The solution to this mystery is to recognize that we will later be adding fuel to the mixing cavity. At 6000 rpm and WOT we will be injecting 3.3 mg of fuel. This mass is blast into the combustion chamber

together with a smaller mass of air, and only a small amount of gas will be required to re-pressurize the mixing cavity later.

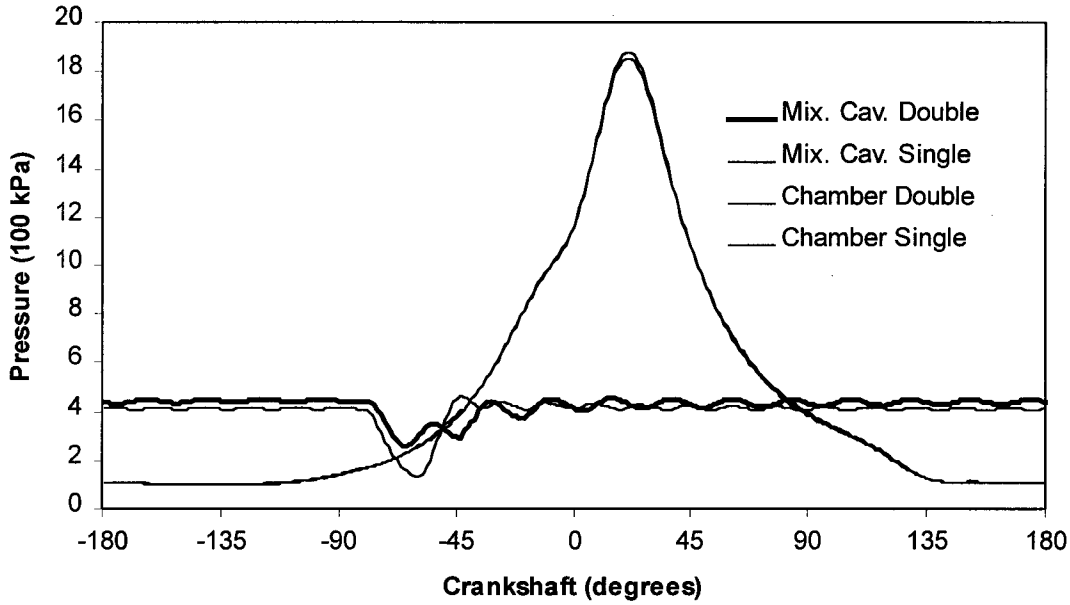

Figure 5.7 Modeled pressure of the combustion chamber, and mixing cavity as a function of crank angle for single and double blast valve actuation, 6000 rpm WOT.

We can clearly see the drop in pressure of the mixing cavity during blast injection in figure 5.7. In the case of the single-actuation of the blast valve the pressure differential actually goes negative from approximately 68 degrees BTDC to 50 degrees BTDC. Due to frictional losses a negative pressure differential will be required to recharge the mixing cavity; however, we can see that the pressure of the mixing cavity continues to drop to about 57 degrees BTDC, long after the cavity pressure has surpassed that of the mixing cavity. This is due to the inertial "ram effect" of the momentum of the gases leaving the blast valve at high velocity which essentially delays the onset of recharging by about 15°

in the single actuation case. This "ram effect" is not an issue for the doubly actuated scenario, as the flow has no outward momentum to overcome when the blast valve is opened for the recharge phase.

Note also that in both cases there is significant Helmholtz "ringing" of the pressure in the mixing cavity. This is due to resonant oscillations of the fluid in the neck connected to the mixing cavity. In a Helmholtz resonator a compressible fluid occupies a cavity and adjoining column, as shown in Figure 5.8 for our mixing cavity.

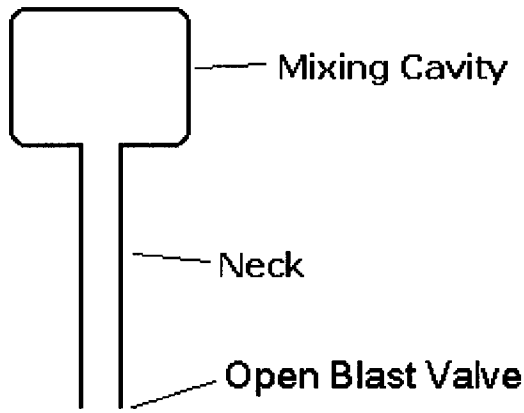

Figure 5.8 Schematic diagram of the mixing cavity as a Helmholtz resonator

When it is excited the fluid in the column will tend to oscillate in the direction of the column, alternately compressing or expanding the volume of gas in the cavity. This forms a simple single degree of freedom oscillator, where the gas in the column forms the mass, and the gas in the cavity forms the spring. The equation for the frequency of a Helmholtz resonator is:

$$\omega = \mathbf{a}\sqrt{A/VL} \qquad (5.1)$$

where ω is the natural frequency of the oscillation in rad/sec, **a** is the speed of sound appropriate for the temperature of the cavity, A is the cross-sectional area of the column in m^2, L is the length of the column in meters, and V is the volume of the cavity in m^3. For our model we have used a cavity volumes of V = 0.5 cc, the length of the column (actually broken into two sections for the model, the neck and collar) is L = 3.0 cm, and the diameter is 0.4 cm. If we use temperature of 320 K (the average temperature in the cavity according to the model), we calculate a speed of sound of **a** = 352 m/s (details are explained in chapter 6). Converting the linear dimensions to meters equation 5.1 gives us ω = 10,215 rad/sec. Converting this to cycles per second we have a natural frequency of 1626 cycles per second.

From figure 5.7 we estimate the period of the ringing to be approximately 22.5 degrees of a rotation in duration, or roughly $1/16^{th}$ of a revolution. At 6000 rpm each revolution takes $1/100^{th}$ of a second, yielding a "ringing" frequency of approximately 16 × 100 or 1600 Hz. This agrees well with the value of 1626 Hz based on the Helmholtz resonator equation.

Once the blast valve is closed, axial oscillations of the fluid in the neck continue, however the frequency is now characteristic of the acoustic resonance of the neck itself.

MIXING CAVITY DESIGN

The primary variable associated with the mixing cavity is its volume. As seen in figure 5.9, the original Aprilia fuel rail has a small volume already present between the

fuel injector and the blast valve. The liquid fuel injector is located at the top. Fuel enters the plastic fuel rail from the side and circulates around the injector. "O" ring gaskets at the top and bottom of the fuel injector prevent leakage of fuel past the injector.

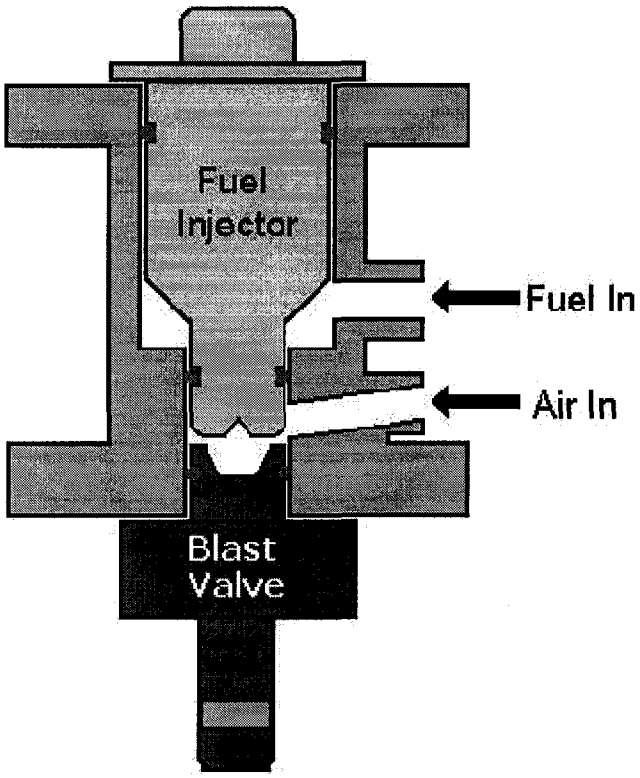

Figure 5.9 The Aprilia fuel rail and injectors

Fuel enters the injector via a fine screen just below the tapered section of the injector, and is ejected from the center of the inverted V at the bottom. The fuel sprays directly into the blast valve's collection area. Pressurized air is admitted to the top of the blast valve via a bore in the side of the fuel rail. Again, an "O" ring gasket prevents leakage of the pressure around the blast valve. When the blast valve is actuated the pressurized air

pushes the fuel through passages in the center of the blast valve into the combustion chamber below (not shown for clarity).

Several different CPDI mixing cavity designs are shown in figure 5.10, each representing the same overall mixing cavity volume. The liquid fuel injector can be seen centrally located at the top of each diagram.

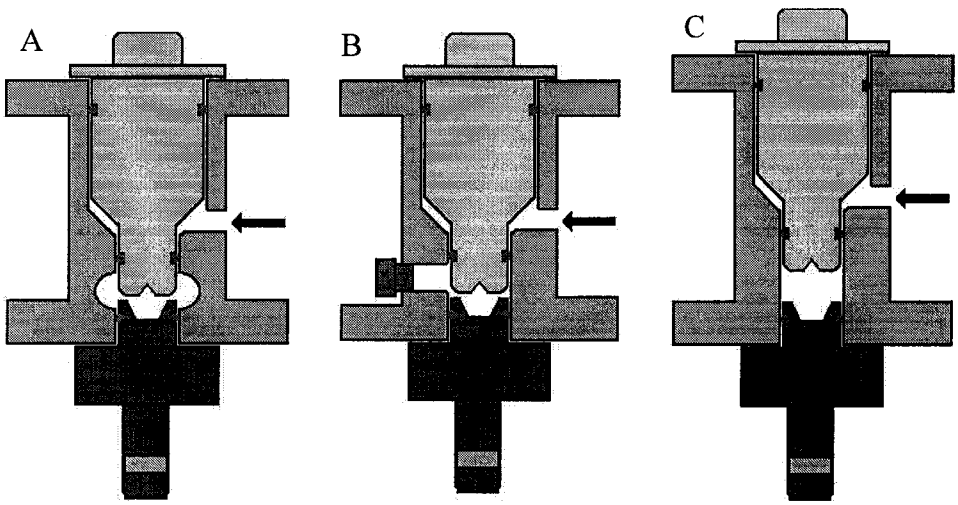

Figure 5.10 Various potential mixing cavity designs

In the design A, the mixing cavity is composed of an annular volume surrounding the injector interface area. While this design is appealing for its symmetry, it is also more difficult to manufacture. Design B has the volume located in a radial bore, blocked by an adjustable plug. This design would allow for easy changing of the overall mixing cavity volume, however, there is a greater possibility of fuel "hang up" in the recesses of the bore close to the plug. Design C on the right is perhaps the simplest design where the appropriate mixing cavity volume is attained by displacing the liquid fuel injector upwards. The major drawback of this design is that the fuel spray from the liquid fuel

injector will diverge more before arriving at the top of the blast valve. Given that during recharging of the mixing cavity air flow will be completely reversed, i.e. air will blow from the combustion chamber below the blast valve into the mixing cavity, the issue of fuel spray divergence in the mixing cavity area is assumed to be relatively less important, i.e. there are more traumatic disruptions to the fuel spray flow in the cavity. We have, therefore decided on the third design, i.e. design C, for our mixing cavity. This is shown in more detail in figure 5.11.

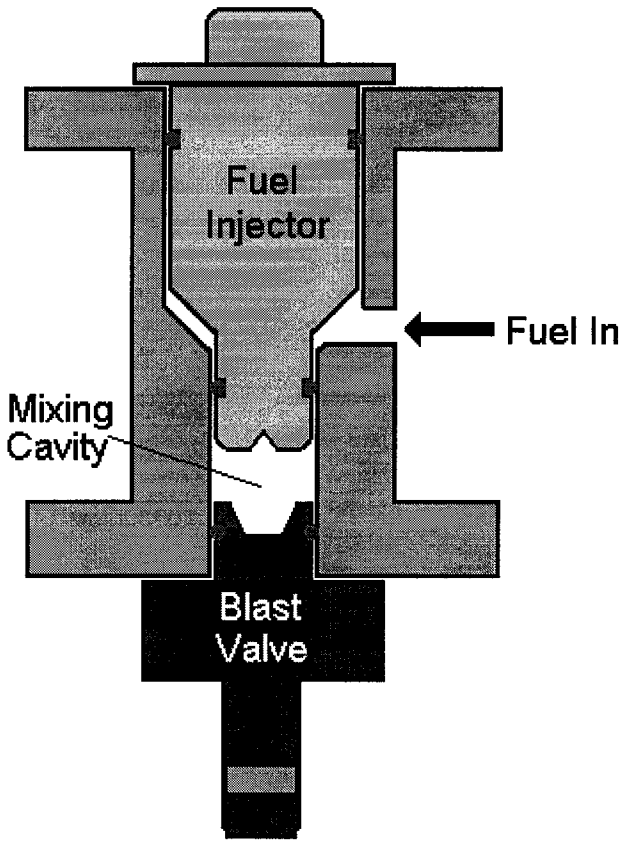

Figure 5.11 Schematic of the CPDI Mixing Cavity Design

MATERIALS CONCERNS

Several materials issues were considered in the design of the CPDI mixing cavity. The material will be exposed to moderately high temperatures, exceeding 200°C, and pressures in excess of 500 kPa in the mixing cavity. Additionally, it must withstand corrosion by gasoline, and preferably be capable of being tapped for threaded fasteners, and easily machinable. The original Aprilia fuel rail was injection molded from a high strength plastic for cost reasons. Cost is less of a factor in our prototype CPDI mixing cavity, and, as this will be subject to testing, which often involves "non-nominal" operating conditions, we would like greater thermal margin and strength than plastic. Based on these constraints a high yield strength aluminum (T7070) was selected.

The mixing cavity was formally drawn up using PRO-E solid modeling software. Figure 5.12 is an oblique view drawing generated in PRO-E.

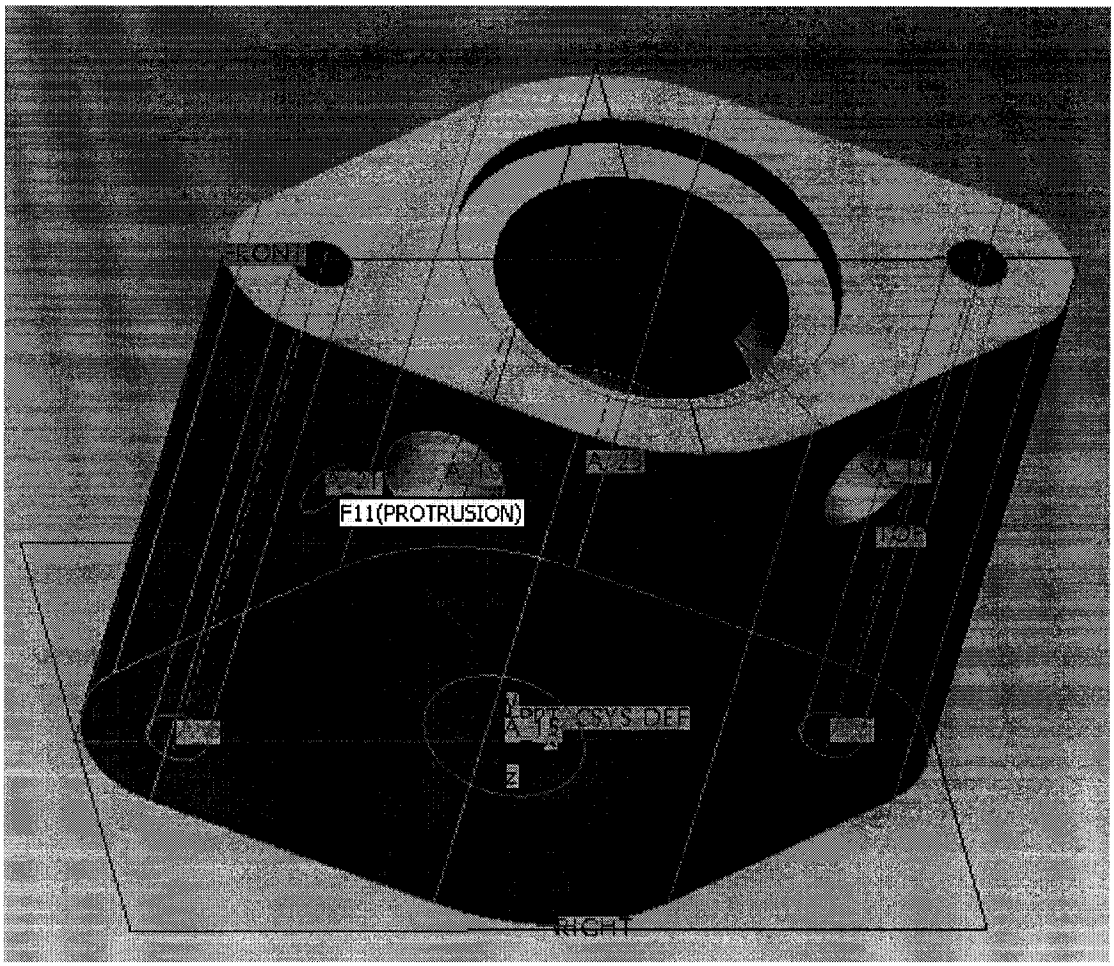

Figure 5.12 Drawing of the mixing cavity generated in PRO-E

The ultimate design varied from the PRO-E model in that the upper injector retainer clip mounting holes were skewed to allow easier access to the head mounting bolts. Additionally a recess was added to each side of the mixing cavity creating a shorter flange and allowing use of shorter head bolts.

Manufacturing of the CPDI mixing cavity was performed by the author at CSU's Mechanical Engineering machine shop in December of 2003. Pressure and mechanical fit testing were completed in January of 2004. The CPDI mixing cavity was tested

repeatedly to pressures of 1 MPa without leaks. Figure 5.13 is a photograph of the finished mixing cavity.

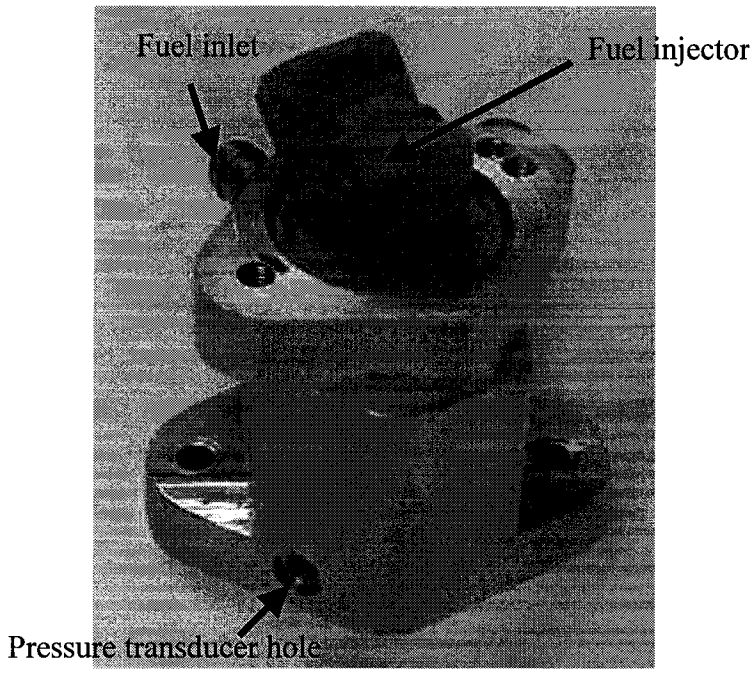

Figure 5.13 The CPDI mixing cavity.

The air blast valve fits into the bottom side, and 2 holes are visible where the mixing cavity bolts to the head. The large hole at the top is where the liquid fuel injector is inserted. Two holes can be seen penetrating the back wall of the hole where the fuel injector sits. These are the fuel entry port and fuel pressure indicator gauge port. Two additional holes can be seen in the top surface parallel to the bore, which are for fastening the fuel injector retainer. Finally there is a hole in the lower left, perpendicular to the bore. This is a pressure probe access port for measuring the internal pressure of the mixing cavity. This pressure transducer is only required during engine testing.

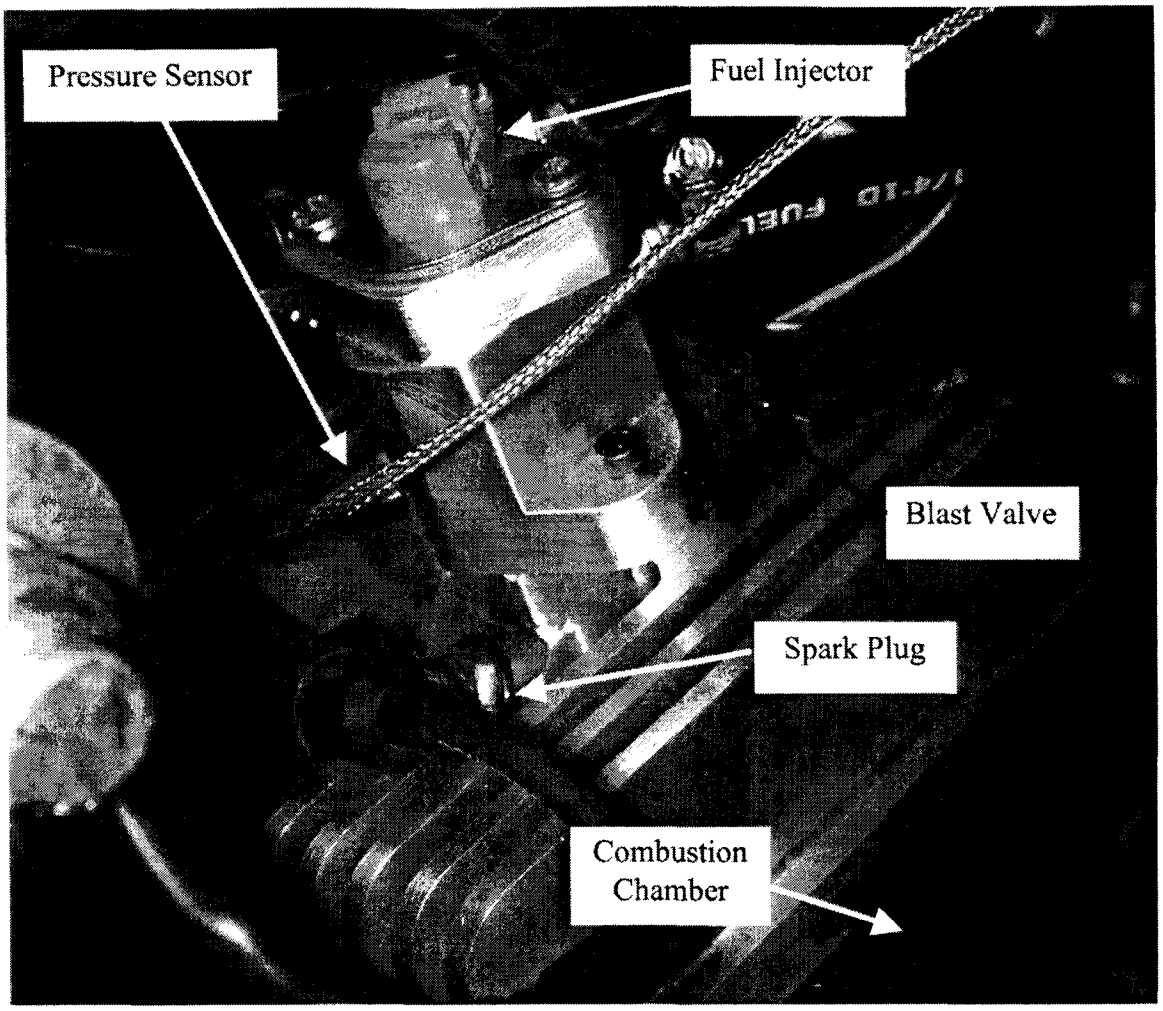

Figure 5.14 CPDI mixing cavity assembled to the ABDI head with injectors mounted.

The mixing cavity is shown assembled to the ABDI head in figure 5.14. The fuel injector is seen protruding from the top of the mixing cavity. Only the electrical connector of the air blast valve can be seen protruding from the bottom of the mixing cavity to the right. A pressure sensor is also seen protruding from the mixing cavity to the lower left. The large wire on the lower left is the spark plug wire. Below the head on the right, the black fins of the combustion chamber can be seen.

DOUBLE BLAST VALVE ACTUATION CIRCUIT

In recent years the "double injection" concept, sometimes called "pilot injection", has become more popular on both Diesel DI systems and automotive Port Fuel Injection (PFI) systems. Air blast DI fuel injection controllers, however, are only capable of operating each injector at most once per cycle. We were able to modify the injector timing maps of the Orbital fuel injection system and run the engine in single actuation mode. However, in order to have a double actuation of the blast valve we had to create a custom circuit to drive the blast valve. Two different techniques were used. Both of these techniques rely on an optical indexer (an inferred photoemitter-detector pair reading an index mark on the crankshaft) to synchronize with the engine as it rotates.

First an optically triggered circuit with variable duration was constructed. This allowed the timing of the start of the valve actuation to be triggered by the optical sensor. The end of the actuation, i.e. valve closure, was determined by the duration of the monostable multivibrator injector driver circuit, seen in figure 5.15, allowing for easy adjustment of the pulse duration via the 10k potentiometer. In this configuration, two index pulses were marked on the crankshaft and sent into the CNTRL line of the circuit. These were placed at start of blast (SOB) and start of recharge (SOR). The end of blast (EOB) and end of recharge (EOR) would then follow behind their respective starts by the time determined by the timer circuit.

In the second configuration a computer was used to control the timing of the actuation pulses. A single index pulse was fed into the computer via the parallel port. Based on the time from index to index, i.e. the period of the signal, the computer

determined the speed of the engine. Phase of the engine was estimated from the relative amount of time elapsed since the last index pulse. The engine's rotational speed is not constant as it slows during compression and speeds up during expansion. To minimize the effect of this speed variation the index pulse was placed as close as possible, nominally at 100° BTDC, to the SOB timing point. The computer then sent out a valve actuation signal to the CNTRL line of the injector driver circuit via the parallel port. To eliminate the monostable delay, the switch SW1 was placed in the "Raw" position allowing the actuation signal from the computer to directly activate the injector driver circuit. Timings were based on a program and could be varied online while the engine was running.

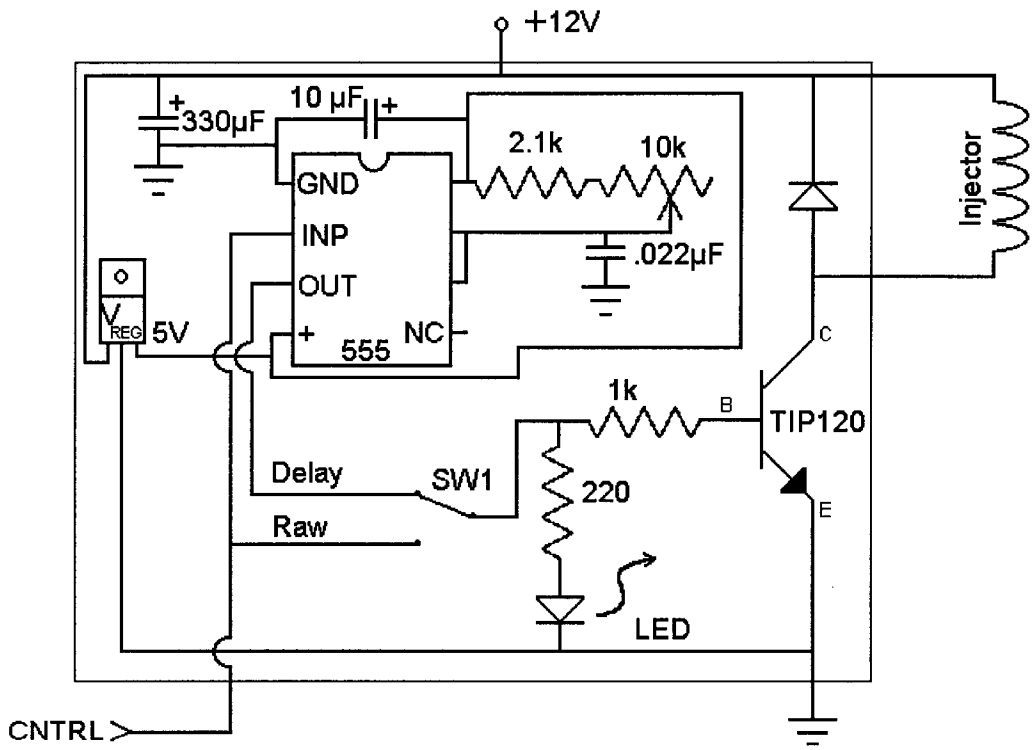

Figure 5.15 Optically triggered injector driver circuit. This circuit is capable of driving the air blast injector based on an optical trigger signal or directly from a computer control signal (CNTRL).

CHAPTER 6 EXHAUST TUNING OF TWO-STROKE ENGINES

EXHAUST TUNING FUNDAMENTALS

The performance of two-stroke engines is strongly influenced by exhaust tuning. There are two fundamental parts to exhaust tuning of two-stroke engines. First, the exhaust system may be shaped in such a way that aids the scavenging of the cylinder by presenting low backpressures when the engine is near BDC, thereby encouraging the contents of the cylinder to empty into the exhaust system. Second, the exhaust system should present a relatively high backpressure to the cylinder beginning around XPC and extending to approximately EPC, thereby "plugging" the exhaust port, and preventing spillage of the new charge in the cylinder into the exhaust system. This is accomplished in different ways for single and multi-cylinder engines.

SINGLE-CYLINDER ENGINES

The exhaust tuning of single cylinder engine is accomplished almost completely by shaping the exhaust pipe to reflect either a high or low-pressure wave to the exhaust port at the appropriate time. When a gaseous flow in a pipe encounters a reduction in the cross-sectional area of the pipe, a high-pressure wave is reflected back in the direction

from which the flow came. If instead, the gaseous flow in the pipe passes through an expansion of the cross-sectional area of the pipe, a low-pressure wave is reflected back in the direction the flow came from.

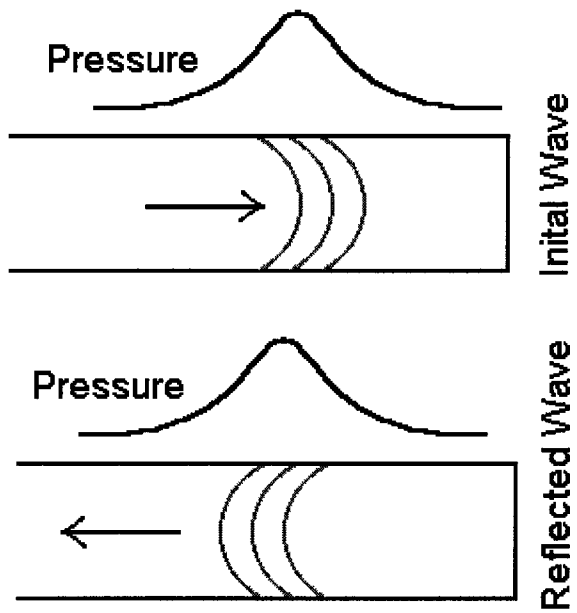

Figure 6.1 Schematic diagram of a pressure pulse is reflected from the closed end of a pipe as a high-pressure wave

Extreme cases of these situations are depicted in figure 6.1 where a pressure pulse is reflected from a closed end of a pipe, and figure 6.2 where a pressure pulse encounters the open end of a pipe.

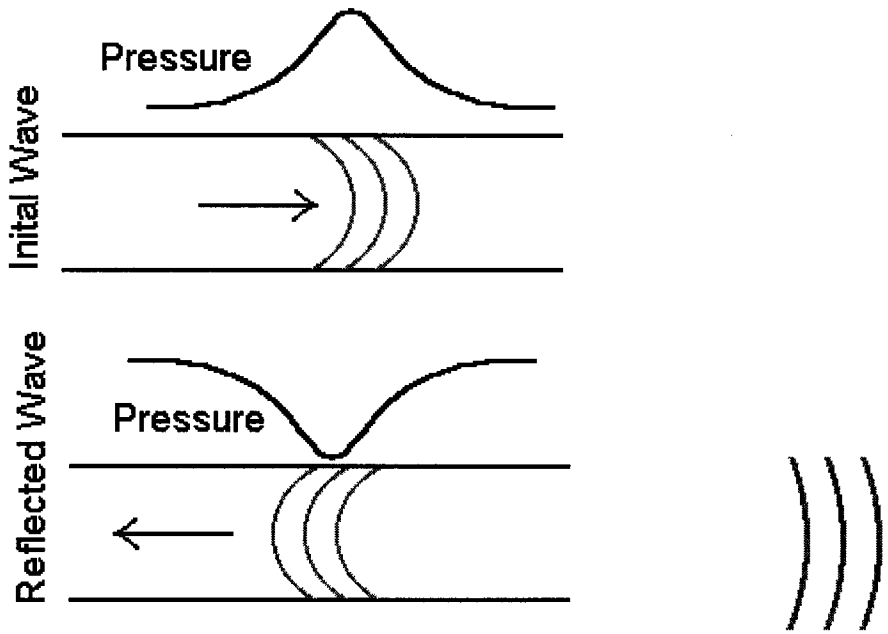

Figure 6.2 Schematic diagram of a pressure pulse reflecting a low-pressure wave from the open end of a pipe. Some of the pressure exits the pipe to the right.

When the exhaust port opens, the hot combustion gases rapidly expand out of the cylinder and enter the exhaust system. This high-pressure exhaust pulse has a duration of perhaps 40 degrees CA and travels into the exhaust system at the speed of sound, which we calculate based on the gas temperature of the exhaust according to:

$$a_0 = \sqrt{\gamma RT} \qquad (6.1)$$

where γ is the ratio of specific heat at constant pressure to specific heat at constant volume, R is the gas constant 287 m^2/s^2K and T is the temperature of the gas in Kelvin. For an exhaust temperature of 580 K, we calculate a speed of sound of a_0 = 475 m/s. In

order to have the exhaust pulse reflect back a low-pressure wave to the exhaust port near BDC, there must be an expansion in the exhaust system at a distance one half as far as the exhaust pulse will travel in the time between EPO and BDC. For example the Kawasaki HD-III engine has an exhaust port opening timing of 97° ATDC, and BDC is, of course, at 180° ATDC, so at 6000 rpm it takes 2.3 ms for the engine to rotate from EPO to BDC. In this time the exhaust pulse will have traveled 475 m/s × .0023 sec or 1.1 meters. To have a low-pressure wave reflected back at this time, we would need an expansion placed 1.1/2 or 0.55 meters into the exhaust stream. To reduce flow resistance and tune the exhaust system to a wider range of speeds this expansion may actually take place over a significant distance, rather than having a single expansion at exactly 0.55 meters into the exhaust system.

For the exhaust pulse to reflect back a high-pressure "plugging" pulse around EPC, we would need a constriction of the exhaust system placed such that the exhaust pulse coming out at 97 DCA reflects back shortly before EPC at 263° ATDC. At 6000 rpm it takes 4.6 ms for the engine to rotate from EPO to EPC. With a sonic speed of 475 m/s the pressure wave travels about 2.2 meters, so the restriction should be located approximately 1.1 meters into the exhaust system. Again, for broader tuning, this restriction is spread over a larger length of the exhaust system.

Blair presents a comprehensive analysis of exhaust system tuning for two-stroke engines using the above concepts (Blair 1996). Applying this to our engine at 6000 rpm we arrive at a tuned exhaust system presented in figure 6.3. As can be seen from the diagram, the distance to the expansion and contraction is very close to that which we have calculated above.

Distance (cm)	Diameter (cm)
12.8	3.6
35.2	4.4
23.4	5.8
11.8	6.8
14.1	6.8
30.7	2.1
30.7	2.1

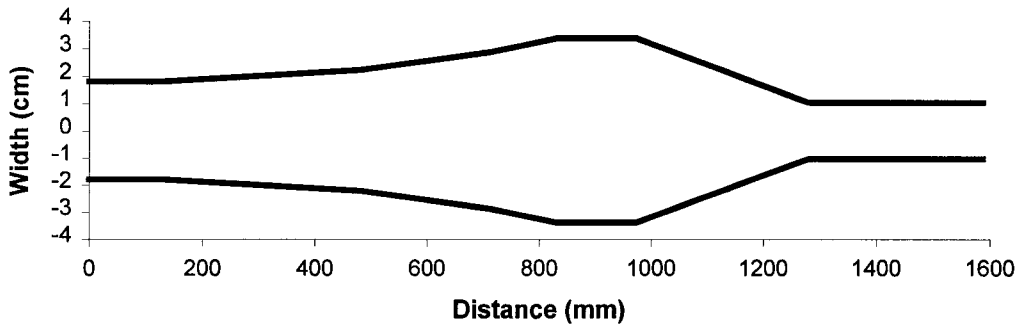

Figure 6.3 Tuned exhaust system for the HD-III two-stroke engine according to Blair's calculations

Applying this exhaust system to the carbureted model of the HD-III engine and comparing it to the stock exhaust system, we can see in figure 6.4 a clear improvement in power at the higher speeds with the tuned exhaust system. The stock exhaust system's power drops off sharply after 6000 rpm, effectively limiting the maximum useful speed of the engine to just over 6000 rpm. With the tuned exhaust system, however, the useful range is extended to over 7000 rpm. At medium speeds, however, the tuned exhaust system yields less power than the stock system, due to inappropriate timing of the reflected waves.

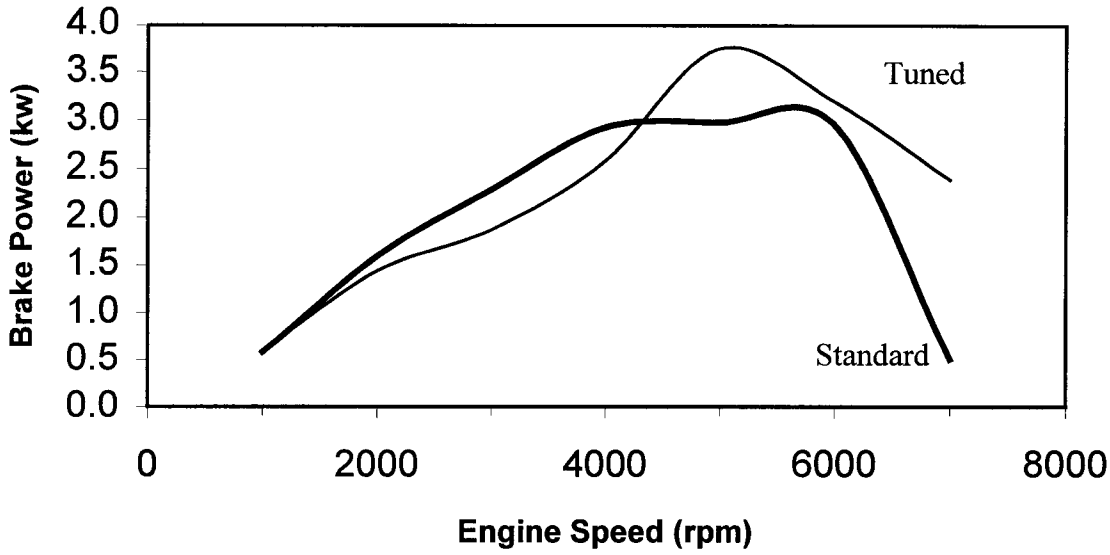

Figure 6.4 Simulated engine power (CARB) versus engine speed for the stock and the tuned exhaust system.

Fuel consumption for the two exhaust systems, shown in figure 6.5, is similar except at extremely high speeds, where the stock exhaust system has a sharp increase in BSFC as the power output of the engine is dropping. Because the tuned exhaust system still has a reasonably large power output, its BSFC remains relatively stable.

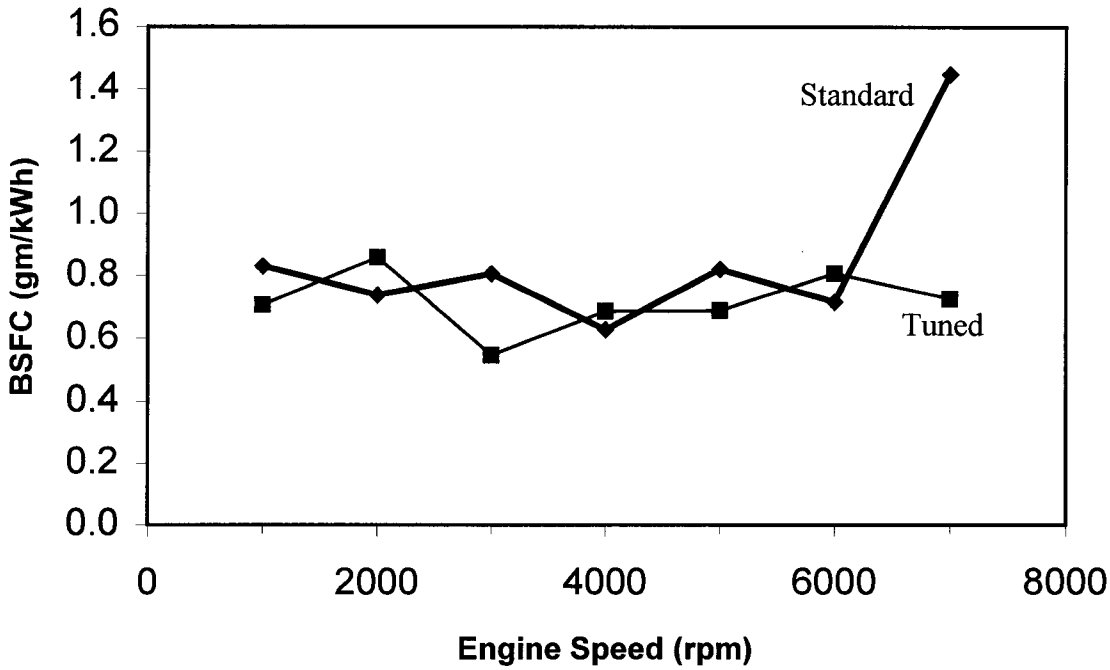

Figure 6.5 Simulated fuel consumption versus engine speed for the carbureted engine with the stock and tuned exhaust systems.

In figure 6.6, the ABDI system shows a similar increase in power at higher engine speeds, again at the expense of mid-speed power loss. This would result in a more "peaky" engine (i.e. one that has little power until higher speeds are reached, and then takes off), which might adversely affect the perceived drivability of the machine.

In general, tuned exhaust systems are only used in performance applications for two reasons. First, a tuned exhaust system is typically more expensive owing to the long length and complicated geometry of the pipe. Second, the sharp "peak" in the power curve adversely affects perceived drivability for non-performance applications.

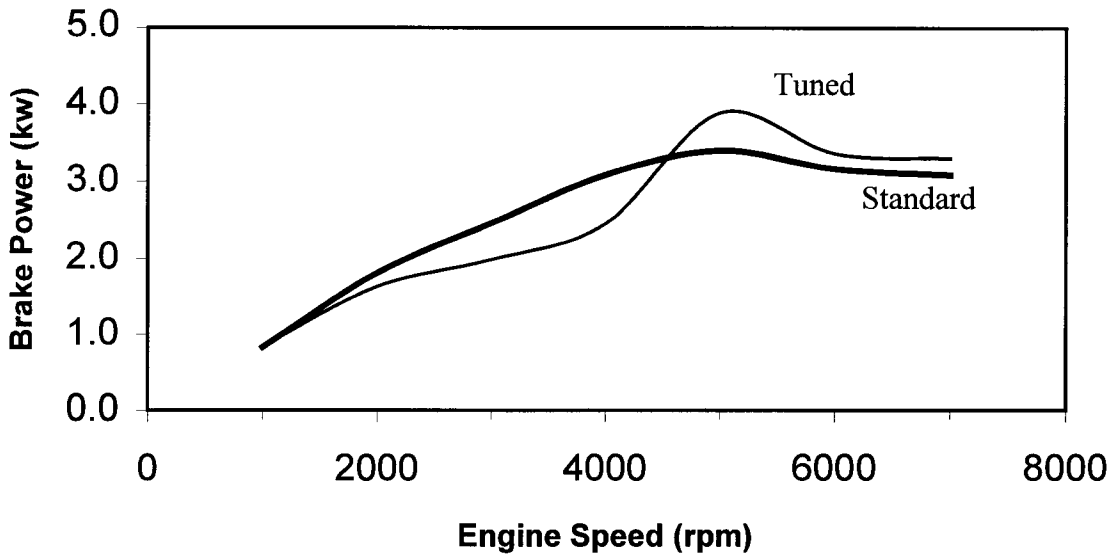

Figure 6.6 Simulated engine power (ABDI) versus engine speed for the stock and tuned exhaust system

MULTI-CYLINDER ENGINES

The single-cylinder tuning technique still plays a role in the tuning of multi-cylinder two-stroke engines. The expansion portion may be roughly similar to the single cylinder case but the dominant effect is now that of cross-cylinder charging. In effective cross-cylinder charging, the exhaust pulse from one cylinder should travel through the exhaust system and arrive at another cylinder shortly before it reaches EPC, thereby forcing as much of the charge to remain trapped in the cylinder as possible. In theory this may be accomplished by adjusting the exhaust manifold path length between cylinders, however, in practice it may be difficult to achieve a highly tuned exhaust manifold in a reasonably small package.

One exception to this is the small three-cylinder two-stroke engines common on some vehicular sporting equipment such as motorcycles, snow machines and watercraft. If the cylinder's ignitions are evenly spaced at 120°and the intake and exhaust ports are closed at approximately 120 and 95° BTDC respectively then each cylinder will experience a plugging pulse at approximately 120 + 95 or 215° ATDC (i.e. 145° BTDC). With a few degrees of travel time between the cylinders and a pulse duration of 40 degrees, the exhaust pulses should effectively plug the adjacent cylinders from approximately 140° BTDC to around 100° BTDC. This is exactly the right timing for effective charge retention, resulting in much better charge trapping for a three cylinder engine then an equivalent single cylinder engine.

The author has shown exhaust tuning to have a major effect on cylinder-to-cylinder variation in asymmetrically timed two-stroke engines (Adair et al. 2003).

CHAPTER 7 EXPERIMENTAL RESULTS

INITIAL TESTING

Initially, the mixing cavity pressurization concept needed to be confirmed. To do this, the engine was "motored" or spun by means of an external, in this case electric, motor while measuring pressures and actuating the blast valve accordingly. Pressures were measured inside the mixing cavity and in the combustion chamber using Kistler type 6052B1 high temperature pressure sensors designed specifically for use in internal combustion engines. These pressure transducers are very convenient for engine applications due to their small size, quick response and ruggedness; however, they measure relative pressure, and are prone to drift. To combat this drift, the signal occasionally needs to be "pegged" to a known absolute pressure. In some of the measurements, such as kick-starts, it was possible to "zero" the pressures to a known pressure, i.e. atmospheric pressure, either before or after the measurement. At other times, pressures had to be determined from a known pressure during part of the cycle, e.g. at relatively low speeds the pressure in the cylinder drops to near atmospheric pressure around BDC, or from relative pressures based on mass transfer characteristics, e.g. gases generally travel from high pressure regions to lower pressure regions.

To facilitate interpretation of the pressure signals, an index pulse with known timing, and valve actuation signals were also recorded. Figure 7.1 is a typical pressure plot obtained in such a manner for a single valve actuation event extending from approximately 80° BTDC to 40° BTDC.

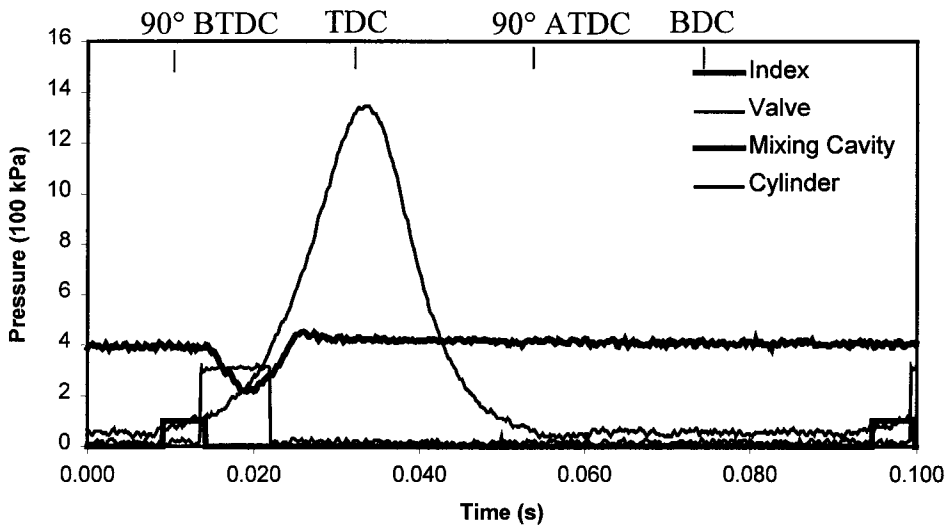

Figure 7.1 Measure pressure in the 1.44cc mixing cavity and combustion chamber versus time during motoring for single valve actuation. Index and valve actuation signals (square waves at bottom of plot) are shown (dimensionless) for reference.

The mixing cavity initially has a pressure of approximately 400 kPa from pressurization of previous cycles. The index pulse shown as the bold square wave has its rising edge at approximately 0.010 seconds corresponding to 100° BTDC. The valve is then opened at 80° BTDC when the combustion chamber has less than 200 kPa, and the contents of the mixing cavity are blast into the combustion chamber, reducing the pressure of the mixing cavity. Notice that the pressure does not begin to drop instantaneously. There are two reasons for this. First the valve requires a finite amount of time to open. This so-called "mechanical delay" has been measured by Orbital to be approximately 800μsec.

Secondly, the gas in the mixing cavity initially has no bulk motion, and therefore requires some time to overcome inertia and get in motion.

Near 20 milliseconds the pressures have equalized, and as compression continues the combustion chamber pressure rises above the mixing cavity pressure and gas is transferred back into the mixing cavity, raising its pressure. The flow reversal requires approximately 2 ms to begin raising the pressure. As noted previously in the modeled case, this is due to the "ram effect" or inertia of the flow exiting the mixing cavity, which must be overcome, before the flow can be reversed. The blast valve is closed at 40° BTDC. Notice again that the valve does not close instantly, as mass is still transferred into the mixing cavity for another 3 to 4 milliseconds, i.e. the valve actually takes longer to close than it does to open. This dynamic effect is due to the fact that the electro-magnetic force which forces the valve open (approximately 20N) is more than twice that of the spring which closes the valve. Only slight ringing is observed in the mixing cavity as the pressure settles down to approximately 400 kPa once again. Helmholtz ringing and acoustic resonances are less likely to be an issue with the actual mechanics than predicted by the model as the geometries are much more complex and less regular than the model. Finally the subsequent index pulse arrives at approximately 95 ms, for a cycle period of 85 ms, which corresponds to a speed of approximately 700 rpm.

It should be noted that the engine's rotational velocity is not constant over the course of a revolution. The engine will slow somewhat during compression as it performs work against the gases in the combustion chamber, and it accelerates during the power and expansion stroke. This will result in a phasing error of the timings. Due to this phasing error, our timings may deviate from the actual engine position, however, we still

have the ability to adjust the timings to within 1° precision. For example, what we are calling 40° BTDC may not actually be exactly 40° BTDC on the engine, however, we are still able to tune the valve timings in to within about 1° of the optimal time. To minimize phase error on our prototype, the index pulse has been placed as close as possible to the desired injection timings. This phase error is not generally a problem when operating under ECU control as the ECU uses a higher resolution position encoder for its timings.

Double actuation of the blast valve was accomplished using an external computer measuring the index pulses and calculating appropriate timings for valve actuation. Figure 7.2 shows a doubly actuated blast valve, separating the blast and recharge phases.

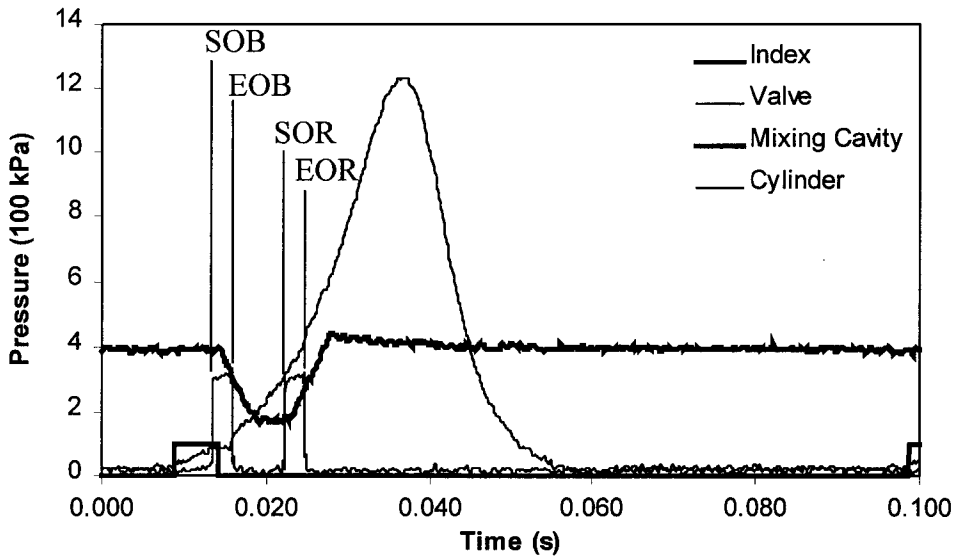

Figure 7.2 Measured pressure in 1.44cc mixing cavity and combustion chamber for double valve actuation during motoring. Notice the separate blast and recharge actuations of the valve.

The valve timings in figure 7.2 are SOB = 80°, EOB = 70°, SOR = 45° and EOR = 35° BTDC. Again the valve closure mechanical delay can easily be measured to be approximately 4 ms between EOR and when the pressure in the mixing cavity stabilizes. The mixing cavity initially holds approximately 400 kPa of pressure, and is drained down to around 200 kPa before the blast valve is closed. The valve remains closed and the pressure in it holds steady until it opens again slightly after SOR. In the separate recharge case the mixing cavity is recharged in approximately 5 ms as compared with 7 ms for the single actuation case in figure 7.1. This is due to the fact that the double actuation recharge begins as soon as the valve has been opened, where as the recharge of the singly actuated system does not begin until the flow has been reversed. Additionally, in the case of the data shown here, the blast valve is reopened for recharge after the pressure in the combustion chamber has significantly exceeded the pressure of the mixing cavity, creating a more advantageous pressure differential.

MIXING CAVITY VOLUME

The pressure drop in the mixing cavity during injection should be inversely proportional to the mixing cavity volume, i.e. the larger the mixing cavity volume, the less the pressure will drop for a given blast duration. To test this, mixing cavity pressure drops were measured for consistent blast valve timings of SOB = 90°, EOB = 80°, SOR = 35°, and EOR = 25° BTDC while spinning the motor at approximately 1000 rpm for mixing cavity volumes of 0.71, 0.99, 1.16 and 1.44cc. The various volumes were accomplished by shimming out either the fuel injector or the blast valve, or both. The

results, seen in figure 7.3, clearly show this inverse relationship, with the 1.44cc mixing cavity having the smallest pressure drop of approximately 210 kPa. Greater pressure drops will result in lower pressure differentials between the mixing cavity and the combustion chamber at the end of injection, degrading atomization of the fuel droplets. Larger mixing cavity volumes will require more time to charge, however, as seen below, this will not be a significant problem. For this reason a cavity volume of 1.44cc was chosen for the rest of the tests of the CPDI systems. Notice that this is significantly larger than the modeled case.

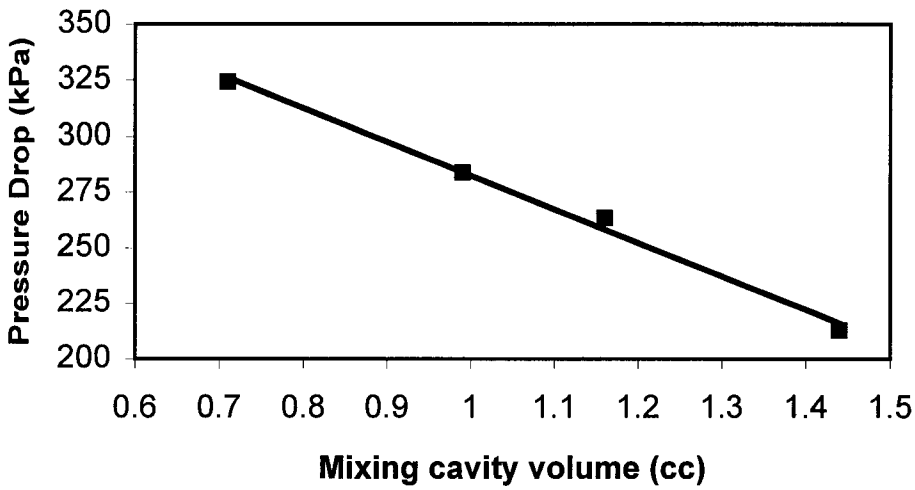

Figure 7.3 Mixing cavity pressure drop as a function of mixing cavity volume for constant blast valve timings at approximately 1000 rpm.

The data of figures 7.1 and 7.2 are from steady state motoring. During start up of the engine the mixing cavity will not initially be pressurized. The initial pressurization process can be seen in the data of figure 7.4 taken during "kick starting" of the CPDI engine with double valve actuation (CPDI-2), with ignition and fuel injection disabled.

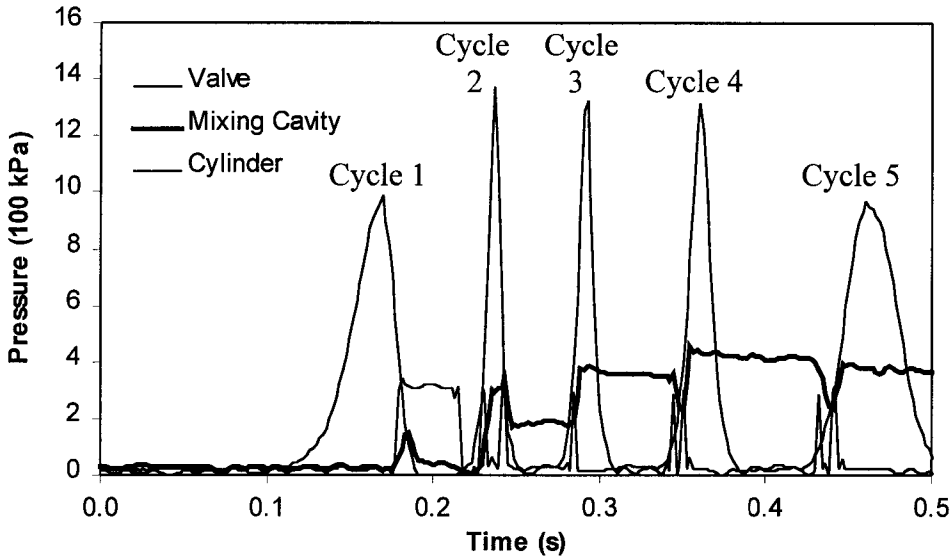

Figure 7.4 Pressure in mixing cavity and combustion chamber during the first cycles of a kick-start (non-firing) using double valve actuation. Timings same as Figure 7.2.

Initially both the mixing cavity and the combustion chamber are at ambient pressure. As the engine is accelerated by the kick, the index pulse passes the sensor for the first time at approximately 100 ms. The computer has not yet synchronized with the engine, and fires the blast valve inappropriately (based on a software default) at approximately 175 ms when the engine is already in the expansion stroke. On the second cycle the blast valve timings are somewhat more accurate and the mixing cavity pressurizes to approximately 200 kPa. By the third cycle the engine is no longer accelerating as rapidly, so the blast valve timings are approximately correct and the mixing cavity pressure continues to increase during the recharge phase. On the fourth cycle the mixing cavity pressure is correct, but the engine is now beginning to slow down, as the ignition was disconnected for this run.

As with the "phasing error" this initial pump-up problem would be greatly improved by the use of a specifically build CPDI-2 ECU.

FIRED TESTING

Having confirmed the mixing cavity pressurization concept, we commenced testing of the system with the ignition enabled. Figure 7.5 shows the resulting data from a kick-start of the "cold" CPDI-2 system with the ignition and fuel injection on.

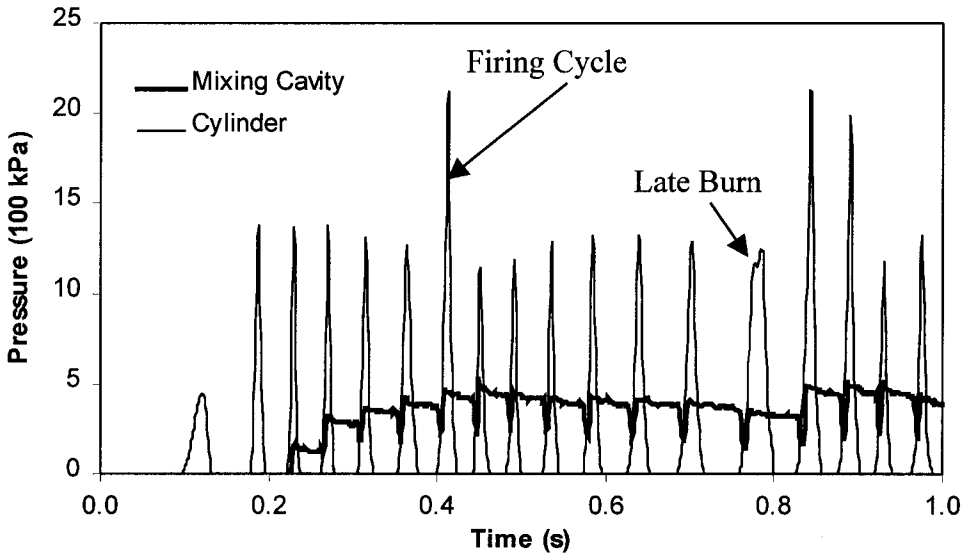

Figure 7.5 Pressure in the mixing cavity and cylinder versus time during a kick-start. Timings are again the same as figure 7.2.

Again it takes several cycles of the engine to build the mixing cavity pressure up to an acceptable level. The cylinder pressure on the 7th compression cycle (at approximately 400 ms) is seen to jump abruptly to over 2000 kPa (2 MPa). This is the result of successful combustion of fuel blast into the combustion chamber from the

mixing cavity. Combustion does not occur on the next several cycles until a late cycle burn occurs at approximately 800 ms. The next two cycles fire, and the engine is running at approximately 1400 rpm albeit roughly, with significant cycle to cycle variation. From the data, a pressure drop in the mixing cavity can be observed during the time when the blast valve is closed, i.e. the majority of the time between cycles. There are two reasons for this. First, when the engine is initially cold, the compressed gases entering the mixing cavity will be hotter than the temperature of the walls of the mixing cavity which are initially at room temperature. Heat is transferred from the warm gases in the mixing cavity to the walls of the mixing cavity, cooling the gases and reducing their pressure. Additional cooling will be provided by the evaporation of fuel which is introduced directly into the mixing cavity. A second possible factor is blast valve leakage. Good blast valves have been tested to over 800 kPa before they leak in the forward direction. As they are an outwardly opening poppet valve, reverse leakage should only be an issue if the valve seats are severely damaged.

MIXING CAVITY PRESSURE REGULATION

A series of tests were performed varying the EOR and measuring the ultimate mixing cavity pressure as the engine was motored at 700 rpm. To reduce the effect of SOR the valve was held open for a relatively long duration of 20°. The ultimate mixing cavity pressure varies strongly with EOR timing as is shown in figure 7.6.

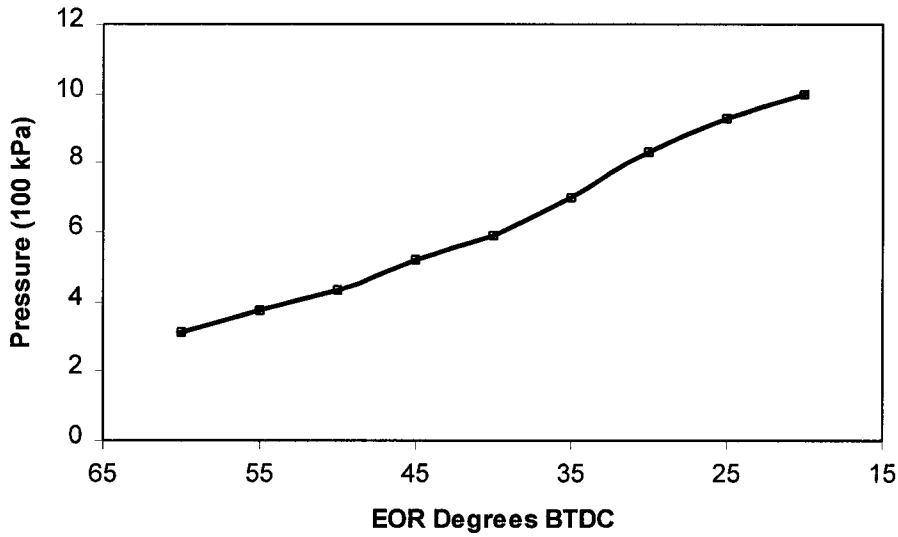

Figure 7.6 Ultimate mixing cavity pressure as a function of EOR for the CPDI-2 system during motoring.

This mixing cavity pressure dependence on EOR is one of the main controls in tuning the CPDI-2 system. Tuning of the blast valve timing was performed "on the fly" as the engine was running at an idle speed of approximately 1300 rpm. Combustion stability was monitored both audibly and via a multi-cycle combustion pressure plot while timings were adjusted. Both SOR and EOR were adjusted to achieve smooth idling.

The resulting optimized timings were SOB = 90°, EOB = 70°, SOR = 52° and EOR = 46° BTDC. Pressure traces from this condition can be seen in figure 7.7 for a single cycle of the engine.

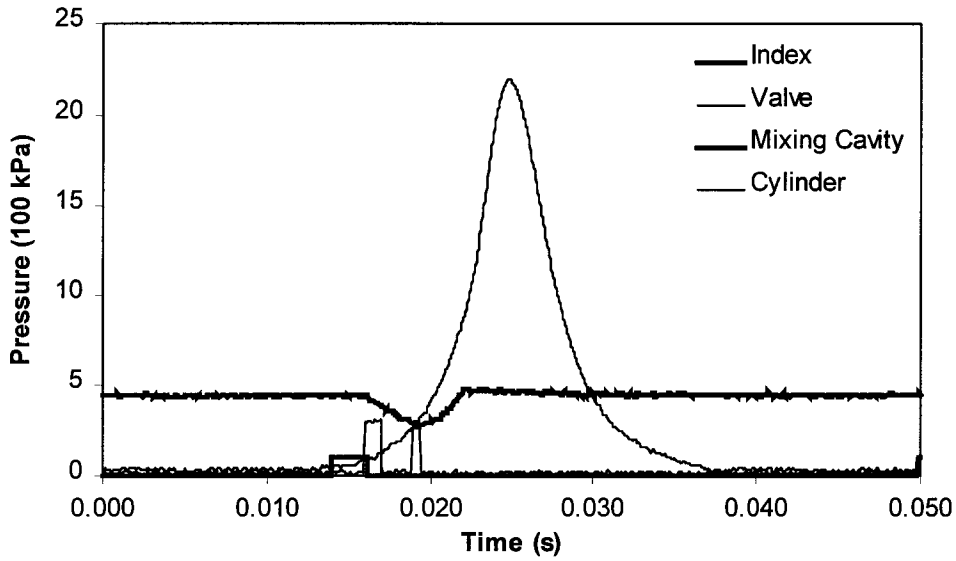

Figure 7.7 Typical pressure in the mixing cavity and combustion chamber for the CPDI-2 engine running optimized timings of the doubly actuated blast valve at 1250 rpm.

Cycle to cycle variation of the combustion pressure was greatly reduced with the appropriate tuning. Figure 7.8 shows the variation of combustion pressure over several cycles when run on the optimized timings where peak combustion chamber pressures are seen to vary between 2.1 and 2.5 MPa. A certain amount of cycle-to-cycle variation is inevitable as ignition depends strongly on the actual fuel/air ratio at the spark plug tips, which is affected by non-repeatable flow patterns inside the cylinder.

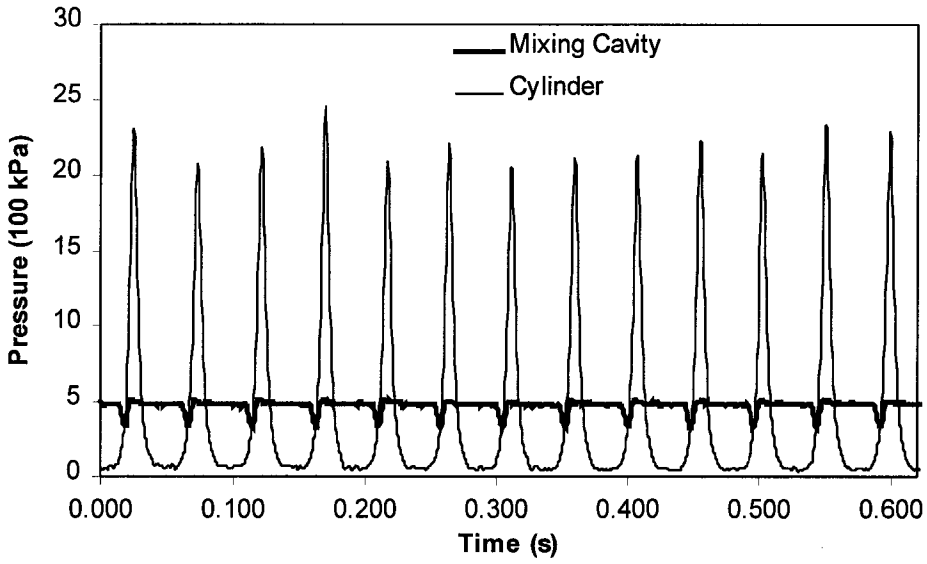

Figure 7.8 Multiple cycles of mixing cavity and combustion chamber pressure for the CPDI-2 engine idling with optimized blast valve timings, 1250 rpm.

ORBITAL ECU CONTROL

The blast valve timing maps of the Orbital Electronic Control Unit (ECU) were modified to reflect timings as close to those determined by the model (see figures 3.13) as possible. The major problem with using the Orbital ECU for operating the engine in the CPDI single blast mode (or CPDI-1) was that the maximum blast valve duration allowed by the ECU is 4.8 ms. This is a hardware limitation based on the architecture of the system, and would require a modification of the ECU to correct. This effectively limited the advance of the start of blast, which became a problem when operating at WOT conditions. With the updated timings, the ECU could directly control the blast valve, albeit with only a single actuation per revolution. Figure 7.9 shows the pressures and

valve timings of the CPDI-1 system under ECU control at idle. Notice that the valve actuation signal appears to be rather "erratic" during the valve actuation. This is a result of the use of a special pulse width modulation type injector drive circuit. It has the advantage of requiring less electrical power than a normal on-off type injector driver. During opening a full 12 Volts is applied to the injector, but once it is opened the 12V signal is "chopped" or modulated so that it is on just often enough to hold the valve open. This modulation will also affect the apparent mechanical closing delay, which from figure 7.9, is approximately 2 ms.

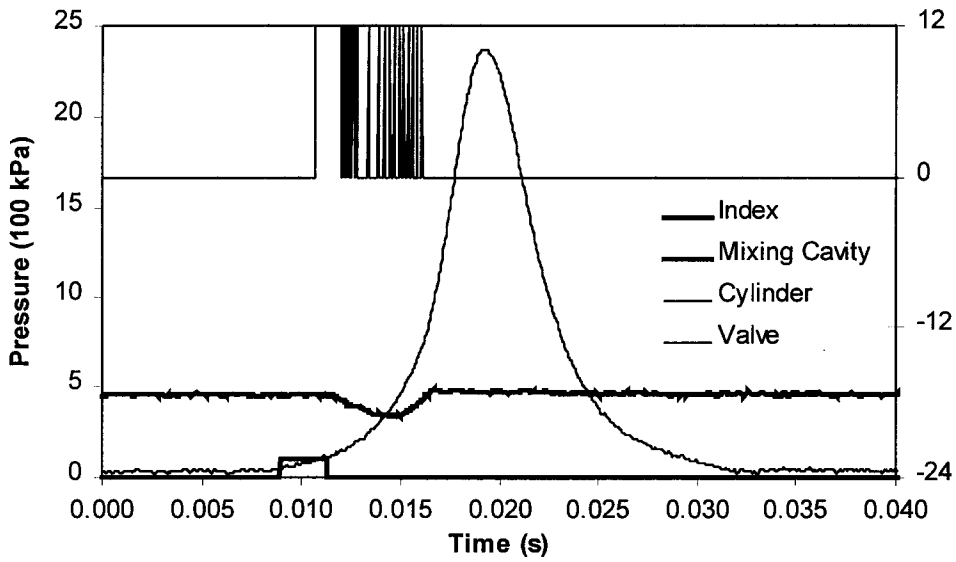

Figure 7.9 Pressure of the CPDI-1 system using single actuation of the blast valve under ECU control running at 1600 rpm

Again the mixing cavity is able to maintain a pressure of approximately 500 kPa. The valve is opened at approximately 11 ms, and held open until about 17 ms. The blast

portion, where fuel is transferred from the mixing cavity to the combustion chamber, lasts for about 3 ms and recharge takes approximately 3ms.

In some advanced ABDI systems special "pump up" codes are used for the first few revolutions to help pressurize the air rail. This code is available on the Orbital ECU. Figure 7.10 shows the system pressures during kick starting of the CPDI-1 engine under ECU control. Notice that on the first two cycles the blast valve is held open until past TDC, effectively charging the mixing cavity in the first revolution.

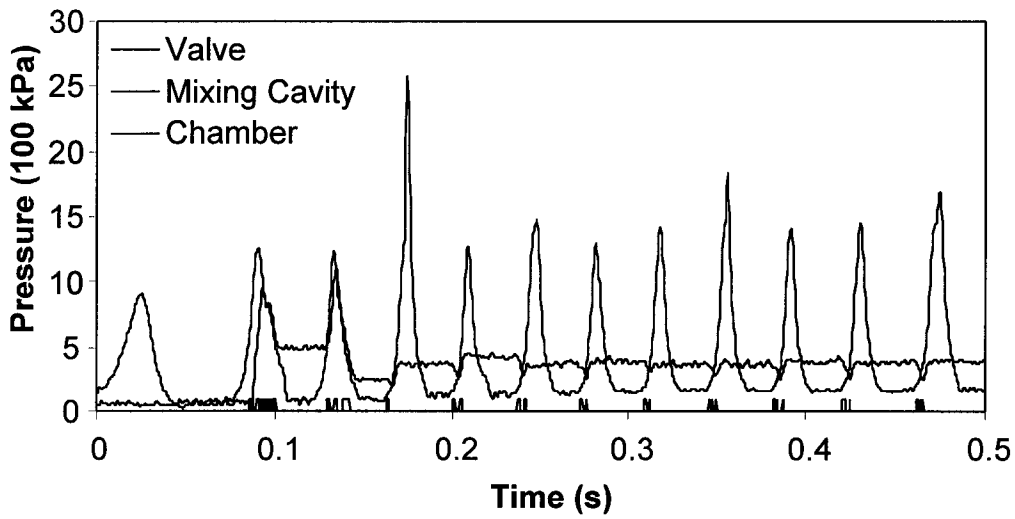

Figure 7.10 Kick-start of CPDI-1 system using full ECU control.

Initial combustion stability of the CPDI-1 system under ECU control was judged to be excellent based on audible feedback, and multi-cycle pressure traces. Figure 7.11 shows the combustion chamber and mixing cavity pressures for several cycles while the engine was running at idle. Peak combustion chamber pressures are seen to vary between 2.2 and 2.4 MPa.

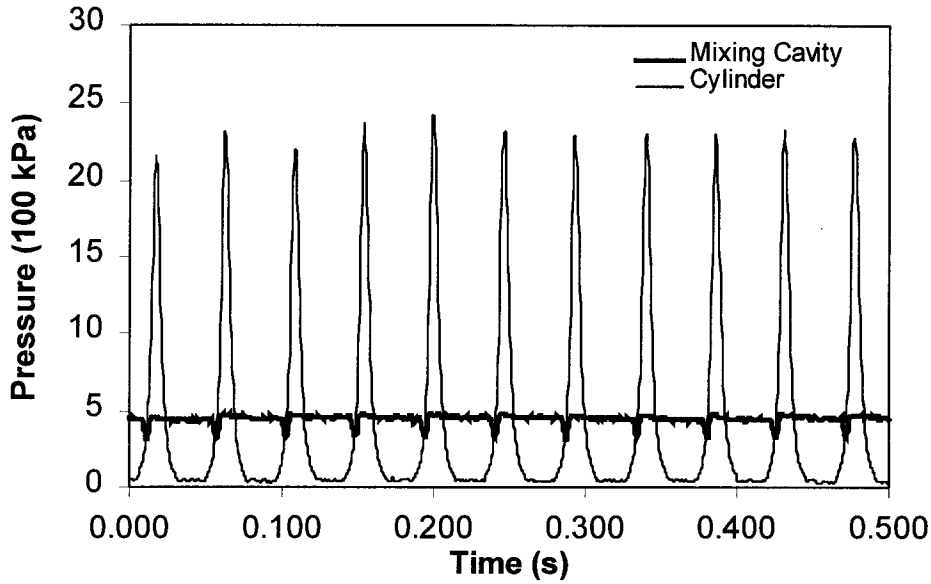

Figure 7.11 Multi-cycle plot of CPDI-1 system pressures during idle at 1300 rpm.

ABDI AND CARBURETED COMBUSTION STABILITY

For comparison purposes the ABDI and the original carbureted system combustion chamber pressures were measured during idle conditions. Figure 7.12 shows the results for the ABDI system, and figure 7.13 shows the results for the carbureted system. The ABDI system is well controlled by the ECU which has a closed loop PID (Proportional, Integral and Differential) control of engine speed. Peak pressures are seen to vary from 2.4 to 2.6 MPa and combustion is very consistent.

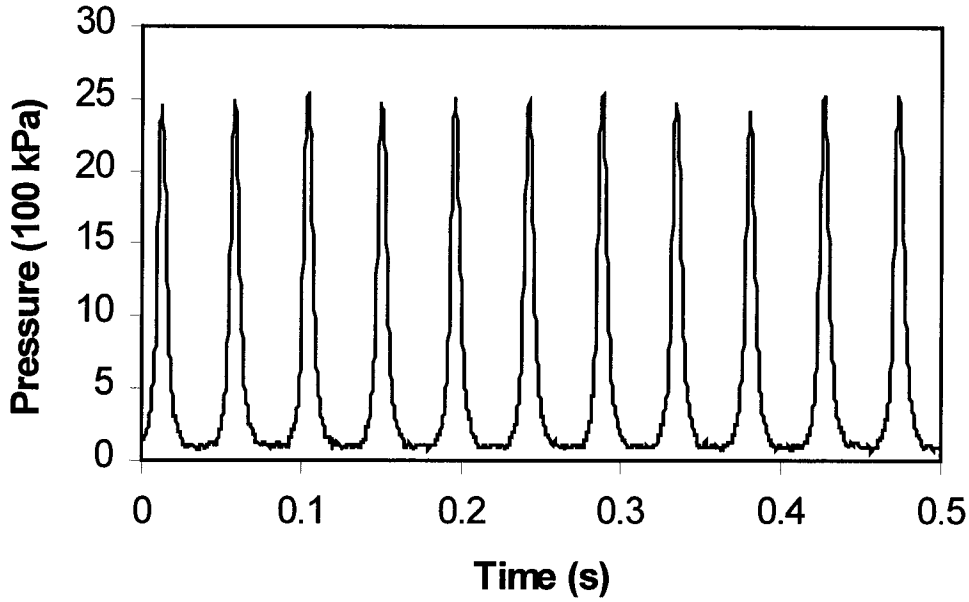

Figure 7.12 Multi-cycle plot of ABDI engine combustion chamber pressure during idle at 1300 rpm.

The carbureted engine idles "smoothly" to the ear, however, it was obvious that the engine was not firing on every cycle. Combustion tended to occur late in the cycle on every fourth cycle, giving very low peak pressures, and abnormally high emissions of un-burnt hydrocarbons. From figure 7.13 we can see that peak pressures range from about 1.5 MPa on the "missing" cycles to 1.9 MPa on the late burn cycles. The engine speeds up appreciably after the late burn cycles, then slows down continually until the next late burn occurs four cycles later. This inconsistency is due to variations in the air fuel mixture in the combustion chamber, especially near the spark plug, due to inconsistent scavenging.

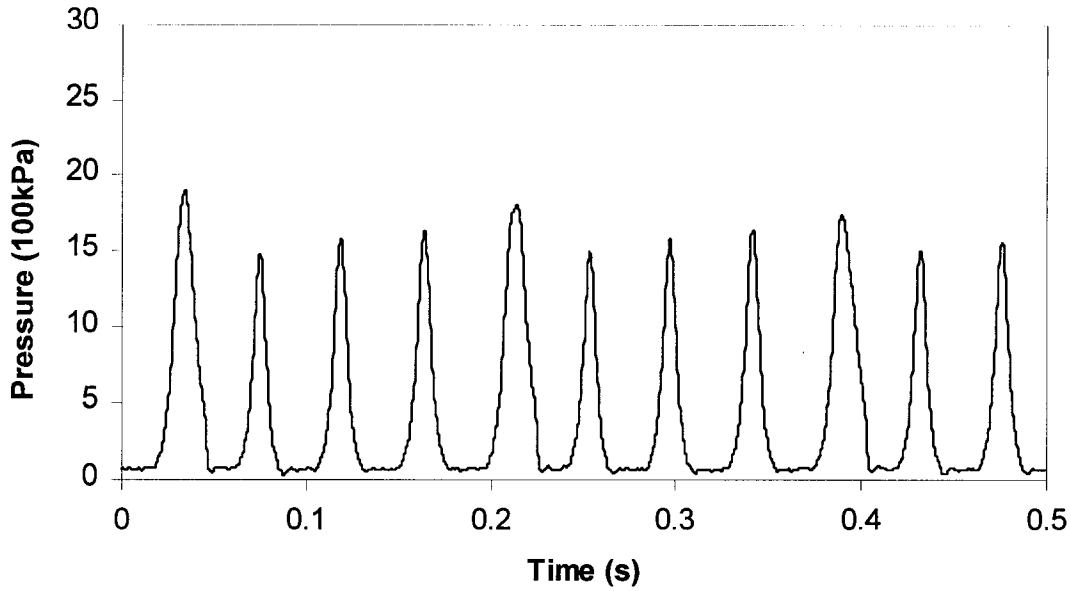

Figure 7.13 Multi-cycle plot of carbureted engine combustion chamber pressure during idle at 1300 rpm.

In the DI techniques, fuel is introduced directly into the combustion chamber very close to the spark plug, making the ignition less dependent on scavenging and engine speed variations. The carbureted version introduces fuel before the crankcase making the mixture in the combustion chamber more dependent on scavenging and speed variations.

POWER TESTING: DYNAMOMETRIC MEASURMENTS

The ultimate goal of this work is to demonstrate a compression pressurized direct fuel injection modification to the existing engine which will improve emissions and fuel consumption, while maintaining power. To test the engine under load and measure its power output it was connected to a dynamometer via the drive shaft sprocket. An eddy

current type dynamometer was used for control and measurement of engine power. The dynamometer consists of a drive shaft rotating a 60 tooth speed wheel and an induction disk as seen schematically in figure 7.14. The induction disk rotates inside a housing which contains electromagnetic coils. The housing pivots freely about the shaft. Rotation of the housing is resisted by a strain gauge connected to the frame of the motorcycle.

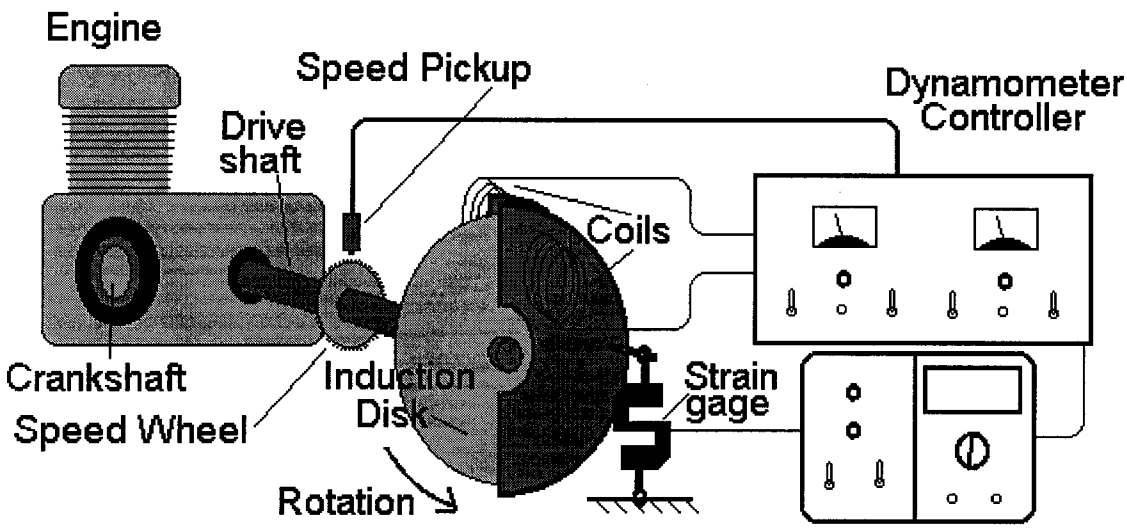

Figure 7.14 Schematic of the eddy current dynamometer used for engine power measurements.

Current running in the coils induces drag in the induction disk, resisting rotation of the drive shaft. The torque produced in the housing is measured by the strain gauge and may be recorded. The dynamometer controller measures the speed of the engine, and compares it to a speed set point which is either adjusted via the front panel, or an external voltage. If the speed of the shaft is greater than the speed set point the current in the coils is increased thereby increasing the drag on the drive shaft and slowing the engine. If the speed is below that of the set point the current in the coils is reduced. Very near the set point the controller outputs a Pulse Width Modulated (PWM) control signal to the coils.

This allows the controller to vary the load on the engine in order to maintain a given shaft speed.

The RAJ eddy-current type dynamometer, shown in figure 7.15 is rated at 30 kW and controlled by a modified Digalog dynamometer controller. Modifications of the controller consisted of rewiring it to operate the lower voltage coils (30V each) of the RAJ dynamometer, rather than the 130V it was initially supplying.

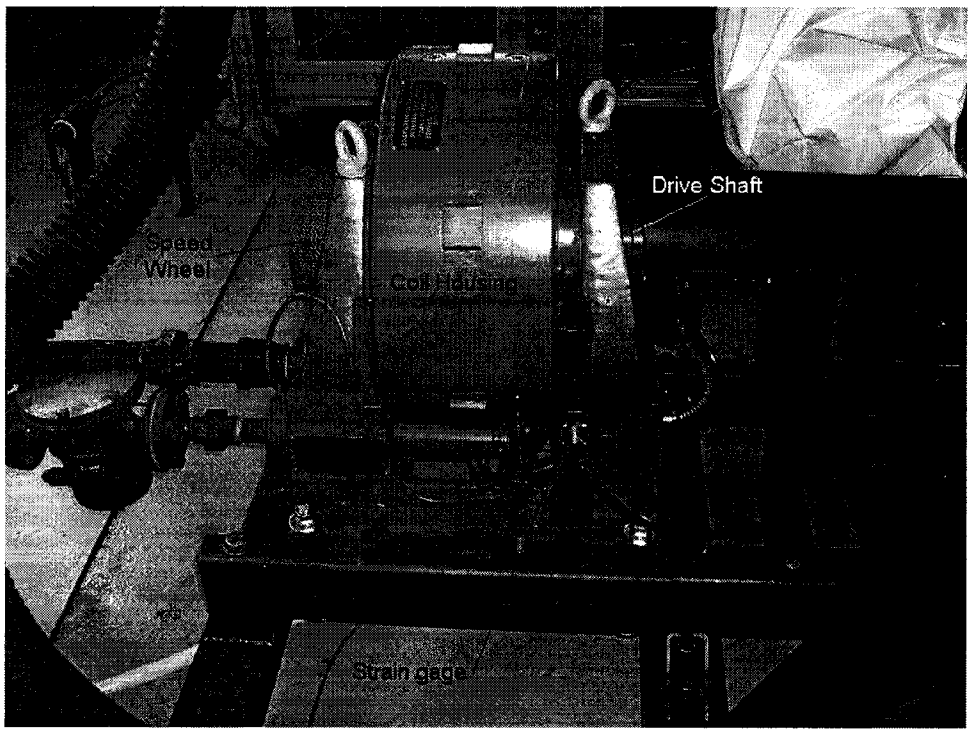

Figure 7.15 The RAJ eddy current dynamometer used for engine testing.

During power measurements it was necessary to provide sufficient cooling air to the engine to avoid overheating. This was supplied by a large fan and cowling which provided airflow over the engine at approximately 40 km/h. The temperature of the head was monitored continuously via a head mounted thermocouple throughout testing to

ensure it was not overheated. The dynamometer also required cooling to dissipate the heat generated by the induction wheel and coils. This was provided by circulating water through the dynamometer housing via the pipes seen in the left of figure 7.15.

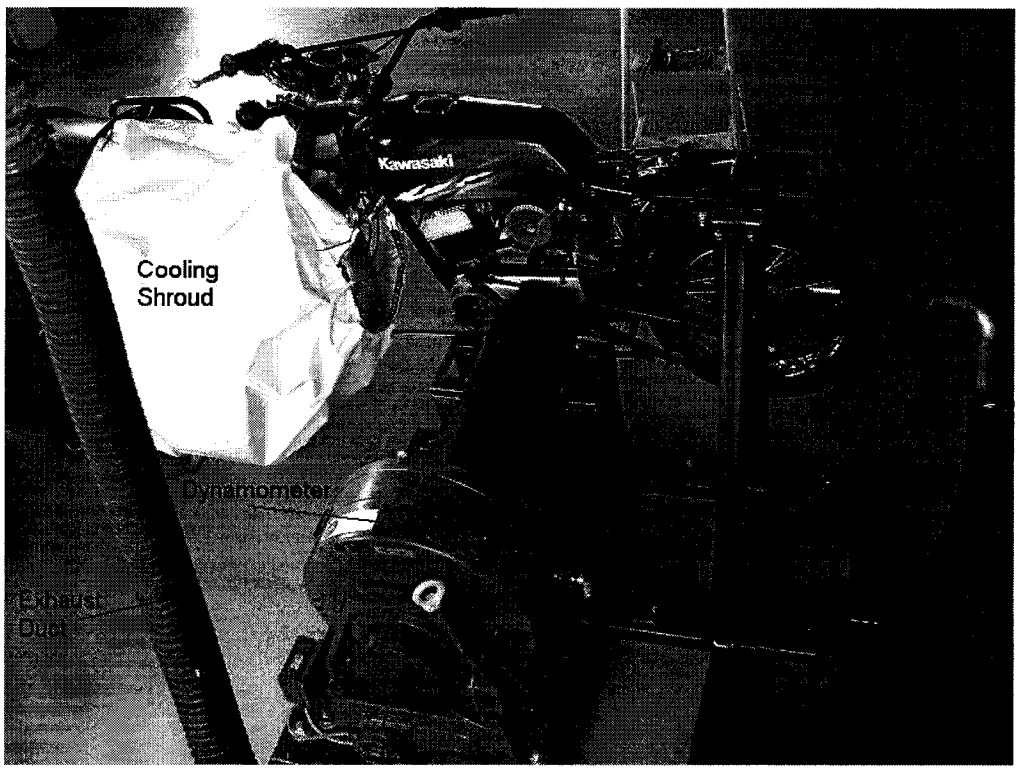

Figure 7.16 The Kawasaki HD-III with the ABDI system mounted to the RAJ dynamometer.

The dynamometer controller could vary the load on the engine and measure the drive shaft's speed, and torque. Typically the engine was operated at a given throttle setting, and the dynamometer was controlled to maintain a constant shaft speed. Shaft output power is calculated from the equation:

$$P = T\omega \qquad (7.1)$$

where P is power in Watts, T is the torque on the dynamometer in Nm, and ω is the rotational speed of the shaft in radians per second. These numbers could be converted back to actual engine numbers by dividing the torque by the gearing ratio, and multiplying the speed by the gearing ratio. Note, however, that this does not account for efficiency of the transmission, which for a typical motorcycle can be expected to be on the order of 90%. All of the power and torque numbers presented in this paper are the raw numbers, uncorrected for transmission losses.

A plot of the power and torque produced by the ABDI engine is shown in figure 7.17. This plot shows the results of several different runs performed in second, third, and fourth gears. The peak power is just over 5kW at 6000 rpm, and the peak torque is approximately 9 Nm at about 4200 rpm. Variation of the results taken at different times is on the order of +/- 5% for both power and torque for all of the systems tested.

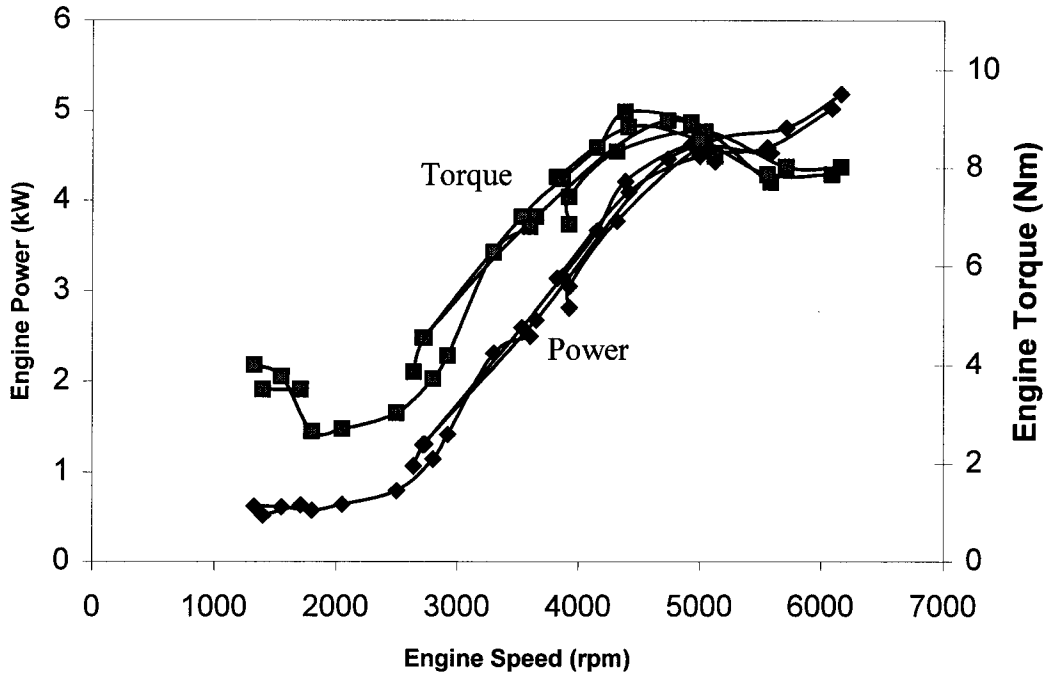

Figure 7.17 ABDI engine power and Torque as a function of engine speed, WOT.

For comparison purposes the original carbureted systems power and torque can be seen in figure 7.18. The carbureted engine produced a peak power of almost 5 kW at 6500 rpm, and a peak torque of 7.5 Nm at 6000 rpm. Note that the power output of the ABDI system is similar in magnitude to the power of the carbureted system, though slightly more "peaky", providing significantly more torque in the 4000 to 5000 rpm range.

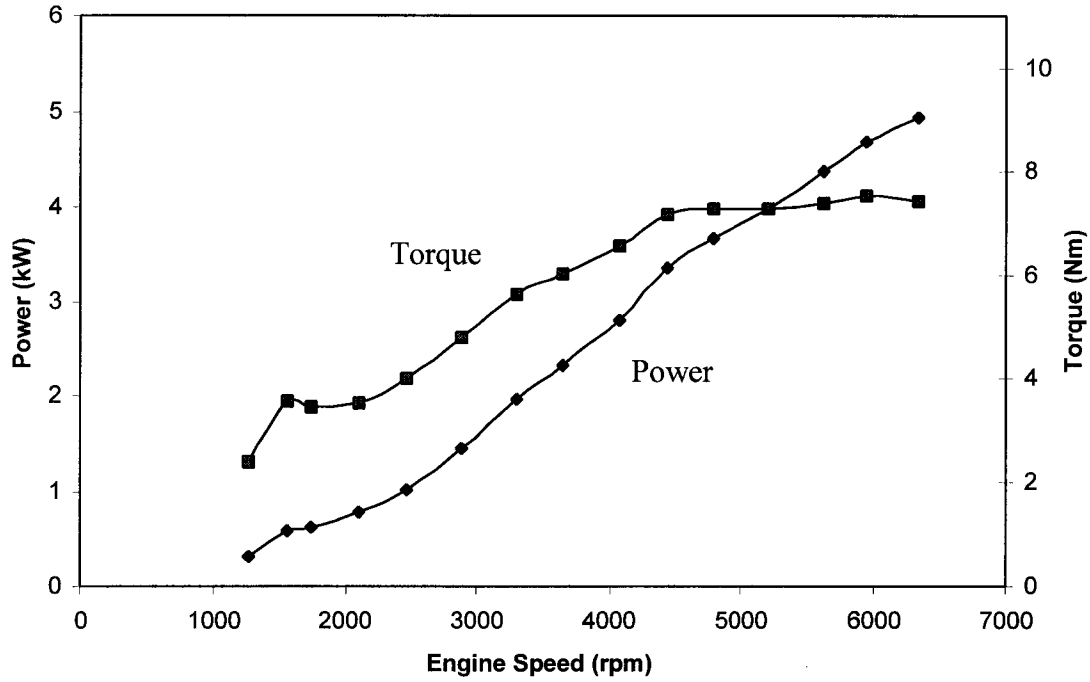

Figure 7.18 Carbureted engine power and torque as a function of engine speed, WOT.

CPDI-1 SYSTEM TUNING

As the ABDI system had undergone initial tuning, the repeatability and overall power output of the system in general was excellent. The CPDI system in both the single blast valve actuation (CPDI-1) and doubly actuated blast valve (CPDI-2) still required significant tuning before acceptable levels of power and repeatability were achievable. Throughout the course of the engine tuning it was noticed that the CPDI-1 system was very sensitive to spark plug fouling. If the engine was operated in a mode where the valve timings caused poor atomization, the resulting soot buildup on the plug would cause misfiring within a few hundred revolutions. Once the misfiring began, it often created an avalanche effect, resulting in more soot buildup, greater probability of misfiring, and

occasionally engine stalling. Once the spark plug was cleaned, the engine would run just as it had previously with valid valve timings. Figure 7.18 shows the plug taken from the CPDI-1 system after running the power curve presented in figure 7.19. The black tips and insulator are caused by soot due to insufficient atomization. This tended to be the case, except for high-speed operation (over 5000 rpm) and idle. When heavily loaded at lower speeds, a more advanced timing of the blast was required to get the fuel sufficiently mixed in the combustion chamber and vaporized before ignition, however, as the maximum duration of the blast valve open period was limited to 4.8 ms, it was not possible to attain the optimum start of blast and maintain the appropriate recharge. During testing "smoky" exhaust was noted from the CPDI-1 system under load at lower speeds, again indicative of insufficient atomization.

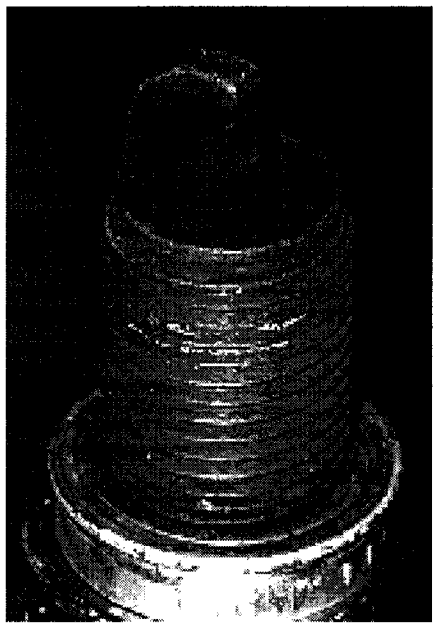

Figure 7.18 Sparkplug from the CPDI-1 system after heavy testing. Note the blackened tips.

At high speeds the maximum blast valve duration was sufficient to allow more advanced blast timings resulting in a more homogenous charge and better tuning of the CPDI-1 system. Another factor contributing to the sooting of the plug was the possibility of "fuel dribbling" as previously hypothesized with the CPDI-1 system.

Tuned

Once the valve timings had been tuned it was possible to operate the engine under load up to full speed. Figure 7.19 shows the power and torque created by the CPDI-1 engine. The CPDI-1 system's maximum power is 4.5 kW at 6200 rpm and maximum torque is approximately 7.8 Nm at 4500 rpm. Additional gains in power would be possible if the ECU allowed a wider range of blast valve timings.

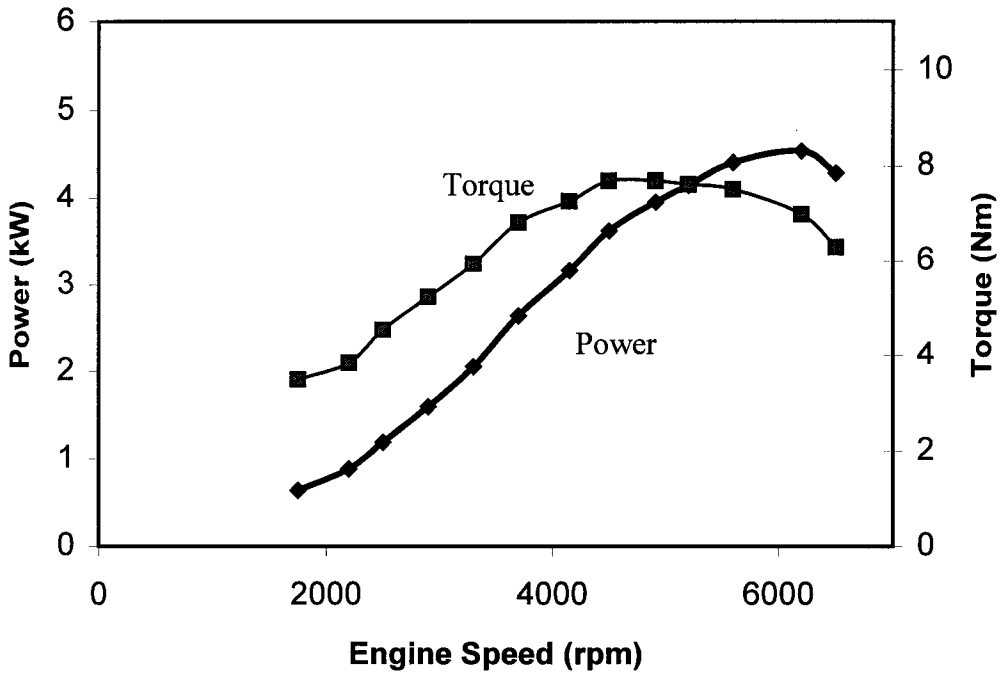

Figure 7.19 CPDI-1 power and torque as a function of engine speed.

Through engine tuning it was noticed that to produce maximum power at higher speeds it was necessary to advance the SOB timings significantly earlier than EPC. These advanced timings promote a more homogenous mixture in the combustion chamber and provide more time for the vaporization of the fuel droplets. By comparison, the relatively retarded timings used near idle will tend to result in a more stratified mixture, where fuel is only propagated a short distance into the combustion chamber making the area around the spark plug and blast valve fuel rich compared to the rest of the combustion chamber. As the spark plug is located quite near the blast valve, the technique of charge stratification is exploited to give good ignition stability near idle. As the ECU limited the maximum advance of the blast, it was not possible to fully tune the CPDI-1 engine to run reliably at WOT for speeds less than approximately 5000 rpm. The data of figure 7.19 were acquired by running the engine loaded at approximately 6750 rpm until the spark plug, piston and head were all hot, then rapidly reducing the dynamometer set speed and measuring the engine torque until the spark plug finally sooted up and stalled near 1800 rpm.

Although operating the engine with advanced blast timings promotes more homogenous mixing and increases power, it may also lead to an increase in HC emissions via short-circuiting if the injected fuel is able to reach the exhaust port before exhaust port closure.

CPDI-2 SYSTEM TUNING

As the Orbital ECU was not capable of operating the blast valve twice per revolution, in order to test the CPDI-2 system the valve had to be controlled by an external computer. At low speeds and throttle settings distinct blast and recharge phases could be observed, this is referred to as the "normal" mode of operation. At higher speeds the engine could be made to operate in a different mode characterized by smaller mixing cavity pressure changes, and recharge timing insensitivity. This mode was dubbed the "flat line" mode, in recognition of the relatively flat pressure trace from the mixing cavity. Figures 7.20 and 7.21 show pressure traces from each mode. At intermediate speeds and throttle settings, it was possible to switch between the two modes of operation by varying the blast valve timings. Short valve durations tended to result in "flat line" mode operation while more open timings resulted in normal mode operation.

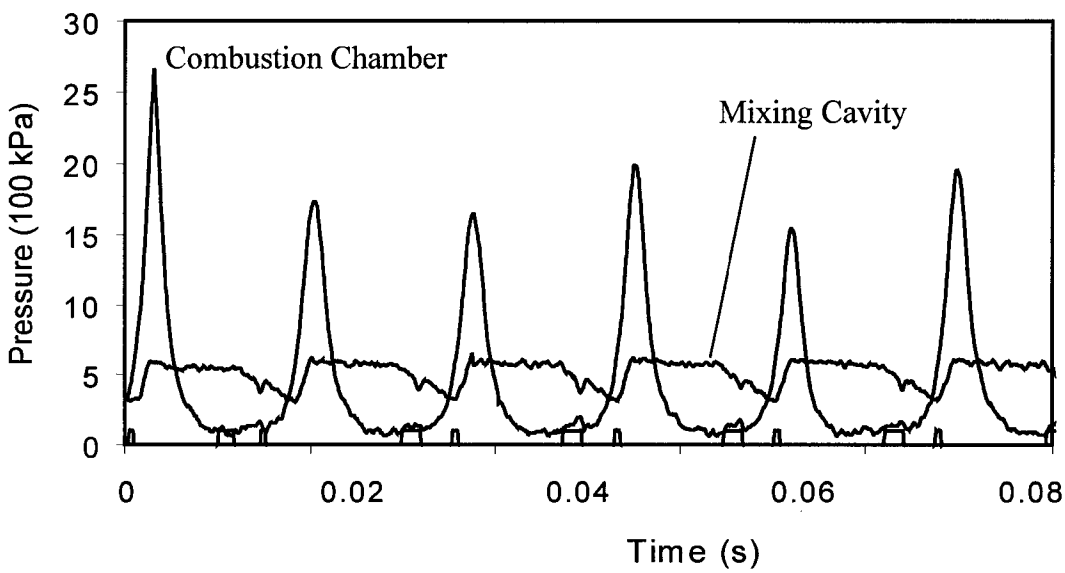

Figure 7.20 Pressure in the mixing cavity and the combustion during CPDI-2 operation in the normal mode 25% throttle, 4500 rpm.

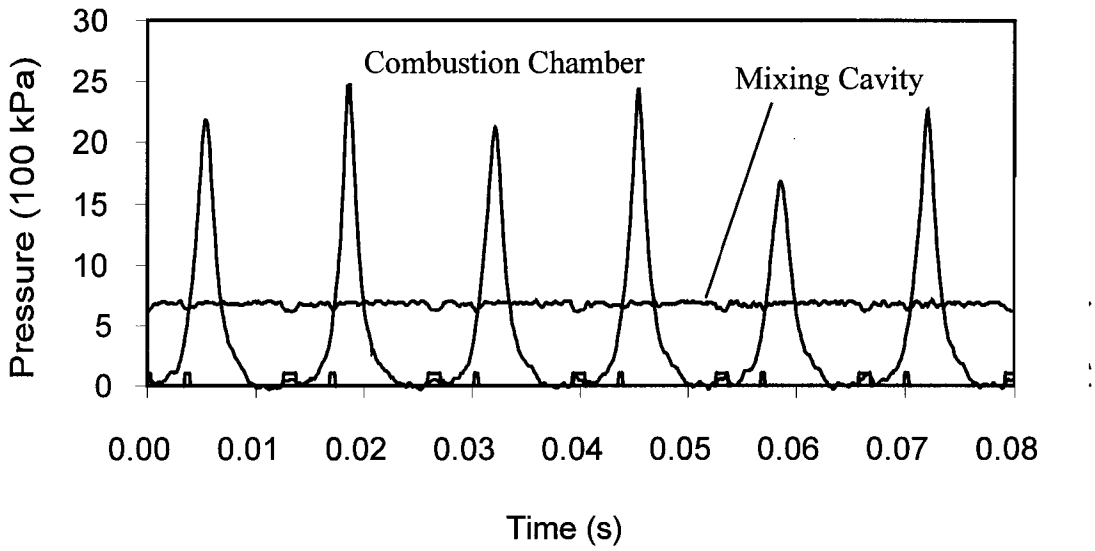

Figure 7.21 Pressure in the mixing cavity and the combustion chamber during CPDI-2 operation in the "flat line" mode, 25% throttle 4500 rpm.

The data of figure 7.20 were taken with valve timings of SOB = 160, EOB = 116, SOR = 44, and EOR = 32°BTDC, while the "flat line" mode of operation, figure 7.21, was achieved by advancing EOB to 127° BTDC under otherwise identical operating conditions. The change between the two modes is accompanied by an audible change in engine noise, and typically a slight change in the power output of the engine.

It is hypothesized that the lack of pressure variations in the "flat line" mode indicates less fluid transfer to and from the mixing cavity. Fuel is still being transferred from the mixing cavity to the combustion chamber, as evidenced by the engine's continued operation. However, it is believed that the mixing cavity may contain a larger amount of "hung-up" fuel. Any gas in the mixing cavity may be acting as a spring, partially compressing and aiding in the ejection of the fuel from the mixing cavity to the

combustion chamber. Upon halting the engine from the "flat line" mode of operation and removing the pressure transducer from the mixing cavity, significant amounts of fuel are observed to drain from the cavity. Relatively less fuel is observed when halting the engine from a "normal" mode of operation.

Both modes produced significant amounts of power. Under load at high speed the pressure drop in the mixing cavity was so small that it was difficult to tell exactly what mode the engine was operating in. Figure 7.22 shows a trace from the engine operating at 5330 rpm, WOT while operating in the flat line mode and producing 7.3 Nm or torque and 3.6 kW of power. Blast valve timings are SOB = 170°, EOB = 110°, SOR = 52°, EOR = 48° BTDC.

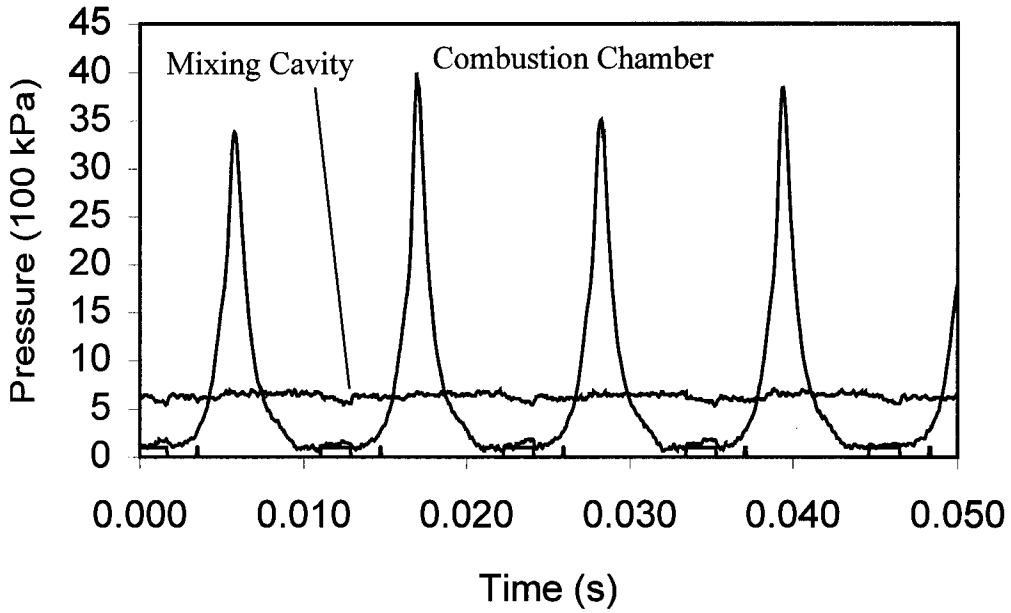

Figure 7.22 Pressure traces from the mixing cavity and combustion chamber for CPDI-2 operation in flat-line mode at 5330 rpm, WOT.

Higher speeds required significantly more advanced timings of the blast phase than at idle. Figure 7.23 shows pressure traces from a run at 4700 rpm. The blast valve timings are SOB = 210°, EOB = 113°, SOR = 45°, and EOR = 39° BTDC. In this configuration at WOT the engine produced 7.7 Nm of torque and 3.6 kW of power, and is clearly operating in the normal mode.

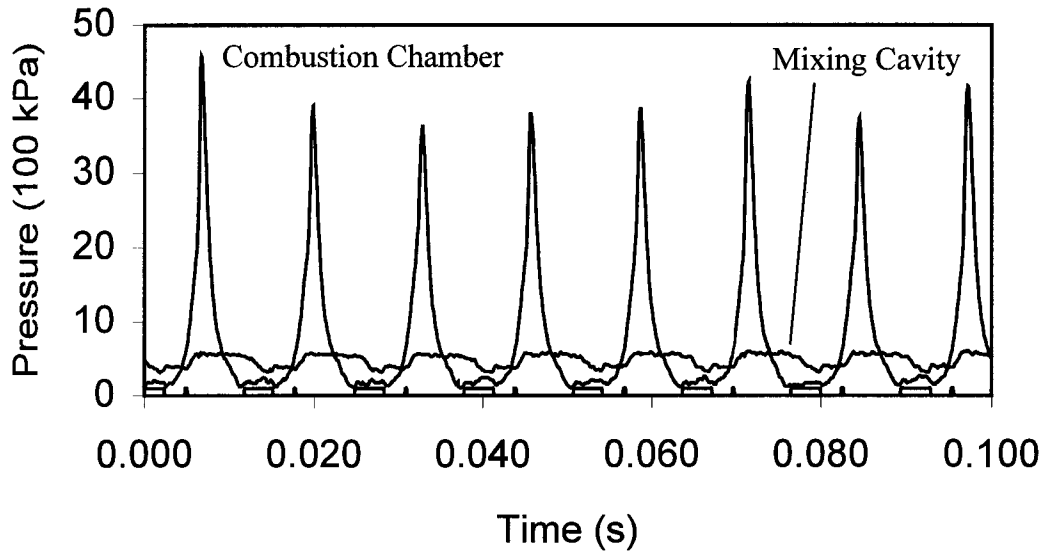

Figure 7.23 CPDI-2 normal mode Pressure traces at 4700 rpm, WOT.

Eventually it was possible tune the CPDI-2 engine sufficiently to measure power and torque over a wide range of operating speeds. Figure 7.24 shows the power and torque measured from the CPDI engine in the doubly actuated mode overlaid on the CPDI-1 curves previously presented.

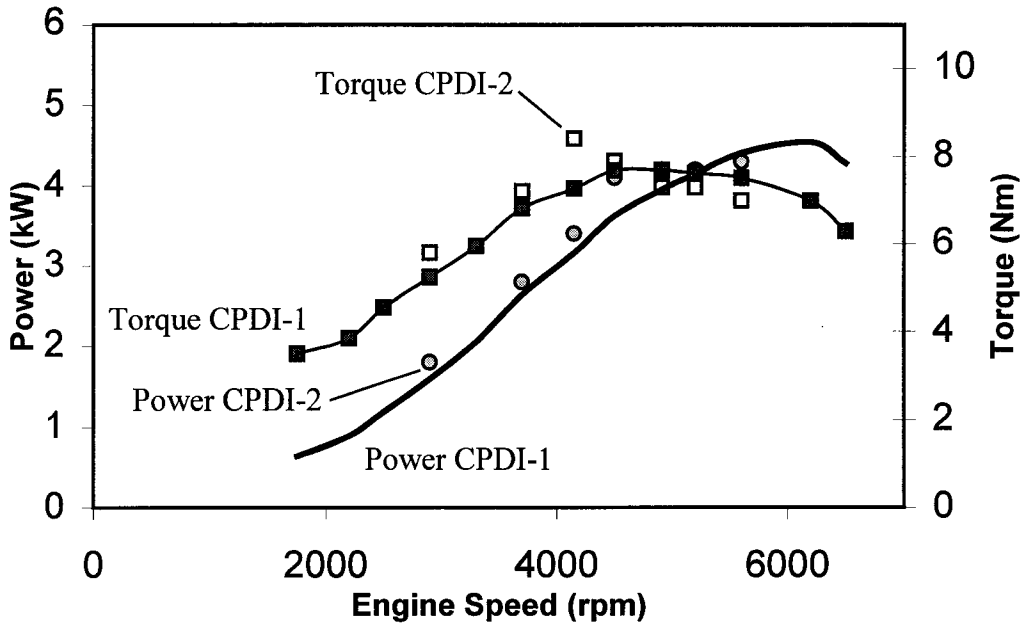

Figure 7.24 CPDI-2 power and torque points overlaid on the CPDI-1 curves

The power of the CPDI-2 system is superior to the CPDI-1 system in the 3000 to 4500 rpm region, largely due to superior vaporization and homogenization possible with the more advanced timings of the double blast technique. Figure 7.25 shows further evidence of the improved atomization of the dual blast technique. The spark plug taken from the CPDI-2 engine after testing is clearly much cleaner than the spark plug taken from the CPDI-1 system from a similar test shown earlier. Power of the CPDI-2 system appears to drop off at higher speeds, mostly due to the fact that we were limiting the maximum advance of SOB to 220° BTDC. This maximum advance was chosen in order to have reasonable timing control at lower speeds and reasonable power at intermediate speeds.

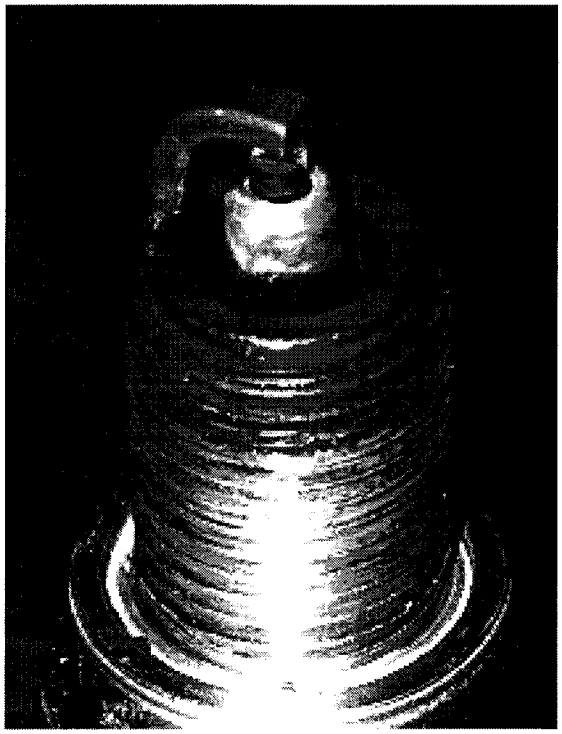

Figure 7.25 Spark plug taken from the CPDI-2 system immediately after testing. Note the light colored tips.

EMISSIONS TESTING

To quantify the improvements in emissions the CPDI-1 and CPDI-2 systems were tested for emissions and compared to the original carbureted engine, and the ABDI system. Emissions were measured using a Vetronix PXA-1100 Gas Analyzer pulling gas continuously from the exhaust duct. This gas analyzer is commonly used for measuring vehicular emissions of hydrocarbons, carbon dioxide, carbon monoxide and oxides of nitrogen. Hydrocarbons and NO_x are reported in parts per million (ppm) of the sampled air, the other gases are reported in % of sampled air. HC concentrations numbers for this analyzer were calibrated to hexane, i.e. the analyzer reports all HCs as though they were

hexane. Additionally the air to fuel ratio was calculated and reported by the gas analyzer. Figure 7.26 shows the emissions of the various systems at various engine speeds and throttle settings.

	RPM	Idle	2500	3500	3500	4000	4500	4500	4500	5500
	Throttle	0	40	40	80	40	60	80	100	100
HC (ppm)	CARB	5250	4050	3080	4400	2960	3330	3970	4480	4340
	ABDI	251	180	275	1080	275	325	703	530	613
	CPDI-1	200	NA	600	656	470	597	661	1334	390
	CPDI-2	NA	453	393	430	NA	NA	740	NA	NA
CO (%)	CARB	2.76	5.17	7.2	5.4	9.81	6.67	6.6	6.87	6.14
	ABDI	0.08	1.62	0.59	6.63	0.2	0.12	8	6.4	5.4
	CPDI-1	0.05	NA	1.5	2.28	0.63	0.17	1.33	4.07	1.88
	CPDI-2	NA	0.94	0.04	0.27	NA	NA	1.35	NA	NA
NOx (ppm)	CARB	57	143	106	328	79	264	328	301	355
	ABDI	261	227	700	468	570	612	490	560	350
	CPDI-1	289	NA	500	755	540	477	1086	888	823
	CPDI-2	NA	1227	740	1170	NA	NA	1700	NA	NA
Kw	CARB	0.0	1.4	1.2	2.7	1.1	2.0	2.8	3.2	3.2
	ABDI	0.0	1.8	1.5	2.9	1.1	1.7	3.1	3.7	3.3
	CPDI-1	0.0	NA	1.4	2.7	1.4	1.4	2.7	3.4	3.0
	CPDI-2	0.0	1.7	1.3	2.5	NA	NA	3.0	NA	NA

Figure 7.26 Emissions and power of the Carbureted, Air Blast DI, CPDI-1, and CPDI-2 systems at various engine speeds and throttle settings. Between the CARB version and the DI versions there are slight differences in the actual throttle setting at intermediate (i.e. 40, 60 and 80%) settings due to throttle design.

The carburetor was re-jetted and tuned for the 5000-foot altitude of the lab. Obviously the carbureted system suffers from high HC emissions across the board as it is tuned rich overall, and suffers from short-circuiting. The ABDI and CPDI engines can be tuned to any air to fuel ratio desired. Typically the DI systems were not run at stoichiometric, as this would result in heavy knocking (pre-ignition) which would

damage the engine. At throttle settings below 80% the DI systems were run in lean mode, injecting less fuel than stoichiometric, and at 80% and above the engine was operated on the rich side of stoichiometric for best power. Typically the engine power was approximately 20% greater on the rich side of stoichiometric. This results in relatively higher HC and CO emissions from the DI techniques at large throttle settings.

CO emissions were low for the DI techniques as long as they were running in lean mode, but increased notably when run on the rich side. Additionally the doubly actuated compression pressurized technique tended to have the lowest CO emissions. This is likely a result of operating leaner than the other techniques. Although the fuel map (fuel injector timings) was kept the same for all the DI techniques, the actual amount of fuel could vary. In the ABDI fuel pressure is regulated by a mechanical regulator maintaining it at approximately 70 kPa (10 psi) above the air pressure, which is regulated to approximately 480 kPa (70 psi). In the CPDI techniques the fuel pressure was fixed at 550 kPa (80 psi), however, the mixing cavity pressure was unregulated, and varied as a function of blast valve timings. Optimization of power via blast valve tuning tended to result in slightly higher mixing cavity pressures, thereby reducing the fuel flow from the fuel injector. When operating in the rich mode, this pressure related leaning would cause the CPDI systems to operate closer to stoichiometric, thereby increasing NO_x and decreasing CO emissions.

Finally the carbureted engine had the lowest NO_x emissions, and the CPDI-2 technique gave the highest NO_x emissions, again associated with the relatively rich tuning of the carbureted engine, and the leanness of the CPDI-2 technique.

To more easily compare the various techniques this data was averaged over the various speed and throttle setting points with equal weight, resulting in the average emissions of figure 7.27.

	Average Emissions			% Reduction		
	HC	NOx	CO	HC	NOx	CO
CARB	3984	218	6.3	0	0	0
ABDI	470	471	3.2	88	-116	49
CPDI-BST	548	804	1.0	86	-269	83
CPDI-1	614	670	1.5	85	-207	76
CPDI-2	504	1209	0.7	87	-455	90

Figure 7.27 Averaged emissions comparison of the Carbureted, ABDI, CPDI-1, and CPDI-2 engines. CPDI-BST corresponds to whichever CPDI technique giving the best emissions at each point.

The carbureted engine will inherently have high CO and HC emissions due to the short-circuiting of fuel. By contrast the ABDI system is a well-developed fuel delivery system which has exceptionally low HC and CO emissions. Based on the points sampled the ABDI system emits 88% less HC and 49% less CO than the carbureted engine. The CPDI-1 system under identical conditions (except for the 2500 rpm, 20% throttle point which was not measured with the CPDI-1 system) produced 85% less HC and 76% less CO than the carbureted engine. Only a few points were measured with the CPDI-2 system for reference. With an ECU capable of running the blast valve in the doubly actuated mode, apart from having significantly better control over the CPDI-2 system, it

would be capable of choosing to run in either the single blast, or dual blast mode whichever gave the best results. If we choose the CPDI technique having the best emissions at each point, we then have an overall HC reduction of 86% and a CO reduction of 83% when compared to the carbureted system.

While there are significant increases in NO_x emissions for the DI techniques, this is counterbalanced by a much greater reductions in HCs.

TEMPERATURES

Throughout the tests the temperature of the head was continuously monitored, and the temperature of the blast valve was measured for comparison. During the testing the head temperature never exceeded 210° C, well below the manufacturer's suggested limit of 250°C. The blast valve typically ran as much as 5° C hotter than the head during heavy loading. This is partly due to the increased heat load of the injector, which houses the solenoid coil and generates about 120W of heat whenever the valve is open. Additionally the blast valve is housed in a sealed chamber created between the head and the mixing cavity housing. This prevents air exchange with the outside air, which would otherwise help cool the valve. Based on this we concluded that the CPDI mode of operation was not likely to cause significant overheating of the blast valve.

MIXING CAVITY FLOODING AND PURGING

To assess the sensitivity of the CPDI system to mixing cavity fuel hang-up, two simple tests were performed. With the CPDI-2 engine running in normal mode under load at 4500 rpm the blast valve was disabled for approximately 20 cycles. As the engine inertia continued rotation the fuel injector continued to spray fuel into the mixing cavity, though the engine could no longer fire, as fuel was not present in the combustion chamber. This resulted in partial flooding of the mixing cavity with fuel. Once the blast valve was re-enabled, the engine would begin firing again, and within a few cycles reestablished its previous mode of operation exactly as before the blast valve was disabled.

To purge the mixing cavity of fuel, the blast valve was held open during approximately 20 cycles of engine operation. This caused large amounts of gas, including combustion gases, to be transferred to and from the mixing cavity. This promotes transportation and vaporization of fuel from the mixing cavity. Again as soon as the blast valve was returned to its proper operation the engine resumed its previous operation mode almost immediately. From this we concluded that the CPDI system is robust, being able to recover from mixing cavity purging and flooding relatively quickly.

SOURCES OF VARIABILITY

There are several possible contributors to variability of engine operation in the CPDI mode. As previously mentioned, operating the CPDI-2 system with a single index pulse for timing will result in phasing error. This error will not be perfectly repeatable, as the engine's angular velocity variations will depend on many factors including temperature, throttle setting, ignition delay and residual gas temperature and composition. These phase induced timing variations will result in pressure variations in the mixing cavity, and greater variability of the CPDI-2 technique. This would be remedied by an ECU capable of double actuation of the blast valve.

As fuel flow into the mixing cavity is inversely proportional to the pressure differential between the fuel rail and the mixing cavity, variations in mixing cavity pressure will result in fuel metering variations. This will cause variations in the equivalence ratio, and slightly lean or rich operation of the engine with the CPDI techniques. The ABDI technique has a fuel pressure regulator controlling the fuel pressure relative to the air pressure to eliminate this problem. The solution is, of course, to incorporate an air pressure regulator, or fuel pressure regulator which regulates relative to the air pressure.

Finally in two-stroke engines combustion instabilities may result in residual gas variations in composition and temperature, which will again affect the mixing cavity pressure. This should affect both ABDI and CPDI techniques similarly.

CHAPTER 8 ECONOMICS OF IMPLEMENTATION

As the CPDI technique has been demonstrated successfully, it may be possible to convert carbureted two-stroke engines to CPDI rather than ABDI. The savings in parts can be estimated from the approximate costs parts (taken from private conversations with an associate of Orbital), shown in figure 8.1.

Common Parts List:	ECU	
	Fuel Rail	
	Throttle Body	
	Air Injector	
	Fuel Injector	
	Fuel Pump	
	12V Generator	
	Head Temp Sensor	
	Heads	
	Index Wheel	
	Index Sensor	
	Wiring Harness	
	Mounting Index Sensor	
	Total Cost	$ 128.20
ABDI Specific Parts List:	Air Compressor	
	Mounting Air Pump	
	Case Casting	
	Total Cost	$ 37.00
	CPDI Parts Cost	$ 128.20
	ABDI Parts Cost	$ 165.20

Figure 8.1 Approximate high-volume manufacturing costs of components used in the ABDI and CPDI conversions. Common parts are those used in both systems.

While some of these numbers are only approximate, they serve as a starting point for a more thorough economic analysis. The CPDI technique eliminates the need for the air compressor and mounting and case casting, for a total savings of about $37.00. This represents approximately 22% of the total parts kit. Additionally, elimination of the air pump and housing bracket will allow use of the original engine side case, thereby eliminating a significant amount of work for kit installation. Reduction in down time for vehicle conversion represents an additional opportunity cost savings, but the savings is probably less significant than the simple convenience of getting the vehicle back sooner.

An additional savings may come in the form of improved reliability. As the CPDI techniques eliminate the need for the air pump, any potential failures of the air pump are thereby eliminated. This advantage was underscored by failures of the air pump/cam mechanism during testing of the prototype ABDI system, which provided additional time for CPDI system testing while the air pump was replaced.

Based on results obtained from engine testing and our best estimates of cost the final cost-benefit curve for the conversion of the Kawasaki HD-III engine to direct fuel injection is shown in figure 8.2. The relative "cost-to-benefit ratio" of the CPDI system is superior to the cost-to-benefit ratio of the ABDI system, indicating that the incremental advantage in emissions reduction for the CPDI technique is superior to that of the ABDI technique.

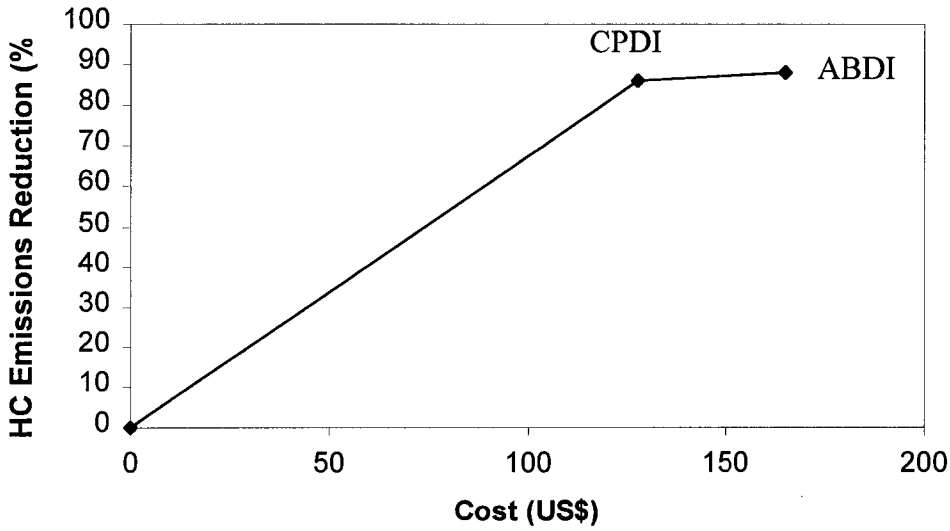

Figure 8.2 Cost-Benefit curve for the conversion of carbureted Kawasaki HD-III engine to compression pressurized DI and air blast DI.

Time to return on investment may be estimated based on the cost of the conversion project, and the projected savings. The goal of this work was to demonstrate an affordable engine conversion technique which significantly reduced emissions. Converting to a DI system will also result in a significant savings in fuel, due to the reduction of short-circuited fuel. As fuel consumption was not directly measured, these calculations will use the results from the model, which indicated an approximate 33% (figure 3.18) savings in fuel for the DI techniques. The cost of conversion to CPDI is estimated at approximately $128.00, so the time to investment payoff will depend on the average fuel consumption, which in turn depends on the vehicles fuel mileage and the number of kilometers driven.

Fuel mileage for a small, unladen, carbureted, two-stroke motorcycle is approximately 50 km/l (Leighton 2003). For a motorcycle bolted to a large sidecar loaded

with several passengers we may reasonably derate this to a vehicle fuel mileage of 30 km/liter for the carbureted vehicle. This of course depends strongly on the load which is likely to vary widely. Current fuel prices in the Philippines are approximately $0.45 per liter. Given a 33% reduction in fuel consumption with the CPDI system, the vehicle should now be able to save $0.15 in 30 km, or about $0.005/km. To pay for the $128 conversion in fuel savings the vehicle would have to be operated for 26,000 kilometers.

While 26,000 km/year may be excessive for a private motorcycle owner in the Philippines, it is not an unreasonable annual mileage for taxis, which are often operated continually by two shifts of drivers per day. We can therefore assume that a CPDI conversion should be able to pay for its self in fuel savings in about a year for tricycle taxi applications.

Additionally the DI techniques also greatly reduce the consumption of oil compared to the carbureted case due to elimination "fuel-washing" effect. Finally, savings will be incurred by the government and individuals in the form of reduced payments for health care, and lost time at work due to air pollution induced illnesses, which are more difficult to calculate.

CHAPTER 9 SUMMARY AND CONCLUSION

SUMMARY

A disproportionately large fraction of global air pollution is caused by two-stroke engines on small transports in developing countries. Regardless of improvements in future vehicles, the existing fleet of two-stroke vehicles will continue to be a polluting legacy for decades to come. We have analyzed several possible direct fuel injection techniques for improving the emissions of existing two-stroke engines. Based on our analysis, both the hydraulic ram injection system and compression pressurized direct injection (CPDI) hold promise as possible technologies for this purpose.

As the CPDI technique can leverage much from the proven air blast DI system, we concentrated on developing an economical CPDI system for retrofit application to two-stroke vehicles in developing countries. The main focus of our efforts was the elimination of the air pump necessary for the pressurization of the air rail in the ABDI systems in favor of a technique using compression pressure to blast the fuel into the combustion chamber. An appropriate engine was acquired and a fluid dynamic model based on careful physical measurement of the engine was created to aid in the design of our CPDI system. The model predicted similar power for the carbureted and CPDI

techniques, and approximately 90% lower HC emissions and approximately 33% better fuel consumption compared to the carbureted base engine. The model was successfully used as an aid in designing the actual CPDI engine. Specifically, blast valve timings were taken from the model's predictions of optimum valve timings.

The engine was tested under motoring conditions while monitoring the mixing cavity pressure and the combustion chamber pressure of the CPDI system for initial verification. The blast valve was actuated via two different methods. Initially the valve was controlled by a computer allowing for two actuations of the valve per revolution. Later the ECU of an ABDI system was used to control the blast valve using blast valve timings determined from the engine model's optimization. Both techniques were able to successfully pressurize the mixing cavity to the appropriate pressures.

Subsequent testing showed both techniques to be capable of running the engine in a stable manner, however, due to timing constraints, the ECU control used in the CPDI-1 technique was incapable of running the engine appropriately for full loads at lower speeds.

Idle valve timings agreed well with those predicted by the model. At higher speeds and power demands the actual timings were significantly more advanced than those predicted by the model. This is due to the fact that the model used had assumed instantaneous homogenous mixing of the fuel and air in the combustion chamber. A more elaborate model including predictions of the combustion chamber mixing would have been helpful in designing the valve timings for higher speeds.

CONCLUSIONS

Originally anticipated problems with air blast valve overheating were shown to not be an obstacle to CPDI implementation. Additionally, throughout the course of engine tuning it was learned that the CPDI engine prefers to operate in a stratified fuel distribution mode near idle, but requires a homogenous fuel distribution mode for full power generation. Finally, the CPDI system demonstrated the ability to recover quickly from both flooding and purging of the mixing cavity, indicating that the system is relatively robust in terms of recovering from fuel hang-up perturbations.

Power curves and emissions data were measured from the engine in the original carbureted configuration, ABDI and CPDI configurations. Results showed that for similar power produced, the ABDI reduced HC emissions by 88% and the CPDI reduced HC emissions by 86% compared to the carbureted engine. CO emissions were reduced by 49% with the ABDI system, and by 83% with the CPDI system compared to the carbureted case. Both of the DI systems significantly increased NO_x emissions compared to the carbureted engine, however, as someone once noted "In the fight to reduce emissions from small two-stroke engines, when our biggest battle becomes NO_x, the war has been won."

The lower CO emissions, and higher NO_x emissions of the CPDI technique compared to the ABDI technique were a result of the higher mixing cavity pressures of

the CPDI technique. Fuel flow was reduced by injecting into this higher pressure, resulting in a leaning of the charge.

Based on approximate parts costs, the CPDI technique appears to have a better cost/benefit factor (86% reduction in HCs for a cost of $128) than the ABDI technique (88% reduction for $165), indicating that the CPDI technique warrants further development.

FUTURE WORK

The initial results of the CPDI system are promising. However, much work remains to make it a market-ready option for the retrofitting of small two-stroke engines. It is therefore recommended that future work in this area focus on further understanding of the CPDI technique including analysis of the normal/flat-line mode differences, possibly including analysis of mixing cavity contents and visualization. Additional refinements to reduce air/fuel ratio variations should also include implementation of an air/fuel pressure regulator, which regulates the pressure of fuel to a constant pressure relative to the air pressure. Alternatively an air pressure regulator could be added to the mixing cavity to limit the maximum mixing cavity pressure. Additional tuning of the CPDI system is also required to further optimize the blast valve timings.

The next step in large-scale implementation of the compression pressurized direct injection technique is to develop a more robust engine controller capable of operating the engine in both the CPDI single blast and dual blast modes. This would allow further tuning and reliability testing of field models.

Finally, the technique needs to be proven in extensive field-testing of retrofitted vehicles under a variety of conditions and further refined before it can be accepted as an option for reducing the pollution from existing two-stroke engines.

REFERENCES

Adair J., Kirkpatrick A., Olsen D. B., Gitano-Briggs, H., 2003, "Simulation of the airflow Characteristics of a Two-Stroke Natural Gas Engine with an Articulated Crank" ASME ICES2003-552

Ahlvik P., et al, 1999, "Possible Abatement of Air Pollution from Urban Traffic in India" PoT-India, Ecotraffic R&D, Feb 1999

Ajootian, Carolina, 1999 "A Big Fix for OMC's Ficht" Boat/US Magazine, November 1999

Allen, J., et al., 1999 "Comparison of the spray characteristics of alternative GDI fuel injection systems under atmospheric and elevated pressure operation" JSAE Technical Paper No. 9935086

Ambler, M., et al., 2001, "Development of the Aprilia DITECH 50 engine" SAE Technical Paper No. 2001-01-1781/4204

Bartolini C. M., Caresana F., Vincenzi G., 2001, "Analysis of a New Water Hammer Gasoline Direct Injection System (WH-GDIS)" SAE Technical Paper 2001-01-1816/4236

Blair, Gordon, 1996, "*Design and Simulation of Two-Stroke Engines*"

Bortz, W., 1993, "*Engine Oils and Automotive Lubrication*"

Caines, A., et al, 1996, "*Automotive Lubricants Reference Book*"

Cobb, William T. Jr., 2001,"Compression Wave Injection: A Mixture Injection Method for Two-Stroke Engines Based on Unsteady Gas Dynamics" SAE Technical Paper 2001-01-1817/4237

Coultas D., et al., 2001, "The Development and Application of 2-Stroke Catalysts for 2-Wheelers in Europe and Asia" SAE Technical Paper No. 2001-01-1821/4242

Fraidl. G., et al., 1996, "Gasoline direct injection: actual trends and future strategies for injection and combustion systems", SAE Technical Paper 960465

Gambino M., Iannaccone S., 2001, "Two-stroke Direct Injection Spark Ignition Engine for Two Wheelers" Instituo Motori – CNR – Napoli

Gitano-Briggs H., Kirkpatrick A., Willson B., 2003, "Design of a Compression Pressurized Air-Blast Direct Injection System for Small Displacement Two-Stroke Engines" ASME ICEF2003-785

Gorham, Roger, 2002 "Air Pollution from Ground Transportation" UN Division for Sustainable Development, Dept. of Economic and Social Affairs

Heimberg W., 1993, "FICHT Pressure Surge Injection System", SAE paper 931502

Huston R., Cathcart G., 1998, "Combustion and Emission Characteristics of Orbital's Combustion Process Applied to Multi-Cylinder Automotive Direct Injected 4-Stroke Engines", SAE 980153

Iyer, N. V., 2000, "Technology and policy options to control emissions from in-use 2- and 3-wheelers" in "*Clearing the Air: Better Vehicles, Better Fuels*" TATA Energy Research Institute Page 141-145

Kataoka, R., et al., 1994, "Prospects for Two-Stroke Engine Development for Cars" JSAE No. 9431049

Leighton, Sam and Ahern, Steve, 2003, "Fuel Economy Advantages on Indian 2-Stroke and 4-Stroke Motorcycles Fitted with Direct Injection", SAE 2003-26-0019

Little, Aurther D., 2001, "Nonroad Recreational Vehicles Technologies and Costs" EPA420-R-01-044, 2001

Nuti, Marco, 1998, "*Emissions from Two-Stroke Engines*" SAE R223

Qin, W., et al., 2001, "Motorcycle Fleet Field Test Study of Two-Stroke Catalytic Converters in China" SAE Technical Paper No. 2001-01-1819/4240

Pundir, B.P., Amar K. Jan, Dinesh K Gogia, 1994, "Vehicle Emissions and Control Perspectives in India: A State of the Art Report" Indian Institute of Petroleum

Ricardo Inc., 2001, WAVE User's Manual: Basic Manual, Burr Ridge, Il, USA

Sogawa, M., et al., 2001, "Development of the high pressure direct injection (HPDI) system for two-stroke outboard motor" SAE Technical Paper No. 2001-01-1786/4209

Turns, Stephen R., 2000, "*An Introduction to Combustion: Concepts and Applications*" 2nd Edition, McGraw-Hill

Willson B., 2001, "Direct Injection as a Retrofit Strategy for Reducing Emissions from 2-Stroke Cycle Engines in Asia" International conference in Hong Kong

Willson B., et al., 2002, "Colorado State University Clean Snowmobile Challenge 2002" SAE Technical Paper 2002-01-2758

Wilson Bill, 1997, "Modern Two-Stroke Engine Lubrication" Industrial Lubrication and Tribology, Vol. 49, No. 1

Wilson Bill, 1997-2, "Conventional Two-Stroke Engine Lubrication" Industrial Lubrication and Tribology, Vol. 49, No. 1

World Bank 1997 as quoted in "The Changing Environment, Counting the Toll" Asian Environmental Outlook 2001

Zhao F., Harrington D., Lai M., 2002 "*Automotive Gasoline Direct Injection Engines*" SAE International

APPENDIX A FOUR-STROKE CYCLE ENGINES

All internal combustion engines (ICE) work on the principal of burning some form of fuel in an internal cavity where work can be extracted from the combustion products. In a typical four-stroke reciprocating piston engine the fuel is burned in a cylindrical chamber. The "top" end of the cylinder is covered by a head which generally houses intake and exhaust valves. In direct injection engines the injector is also usually located in the head. Spark ignited engines will also have one or more spark plugs located in the head. A piston rides in the lower part of the cylinder, and it typically has rings to help seal the pressure of the combustion chamber. The piston is connected to a rotating crankshaft via a connecting rod. As the crankshaft rotates the piston is driven up and down in the cylinder; this is referred to as the stroke of the piston. Work is extracted from the combustion products by the piston, which accelerates the crankshaft in its rotation. There is generally a large flywheel or inertial mass connected to the crankshaft to store energy and maintain rotation of the shaft during the power consuming parts of the engines cycle.

There are a number of ways to combine the fuel and oxidizer. The simplest systems use a carburetor in the air intake path before the head. This configuration is shown in figure A1. Air enters the engine through the pipe on the upper left, and passes through the carburetor where it is mixed with fuel. This mixture is admitted to the combustion chamber by the intake valve, and exhaust products are eliminated through the exhaust valve to the pipe at the upper right.

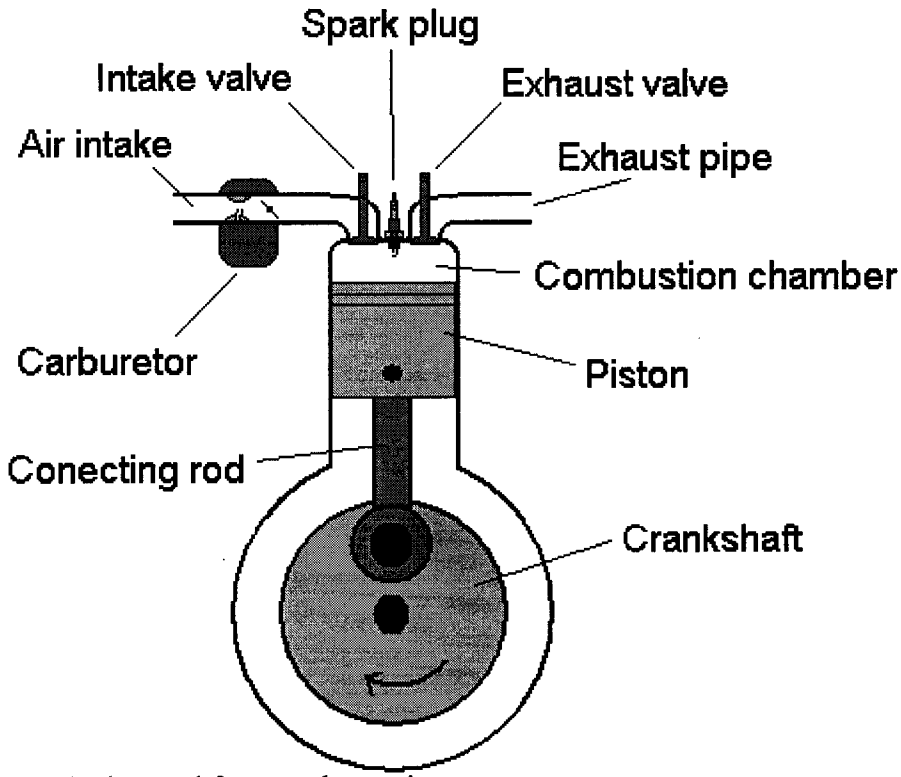

Figure A1 Carbureted four-stroke engine

The cycles of operation are shown in figure A2. In figure A2.a the piston is located at the top of its stroke. As the crankshaft is rotated the piston moves down in the chamber, increasing the chamber volume, and creating a pressure drop. During this "intake stroke" the intake valve is opened to allow the air/fuel mixture to enter the cylinder. When the piston gets to the bottom of the stroke the intake valve is closed. As the momentum of the flywheel continues the crankshaft rotation, the piston is pushed up into the chamber compressing the air fuel mixture (figure A2.d). This is the compression stroke.

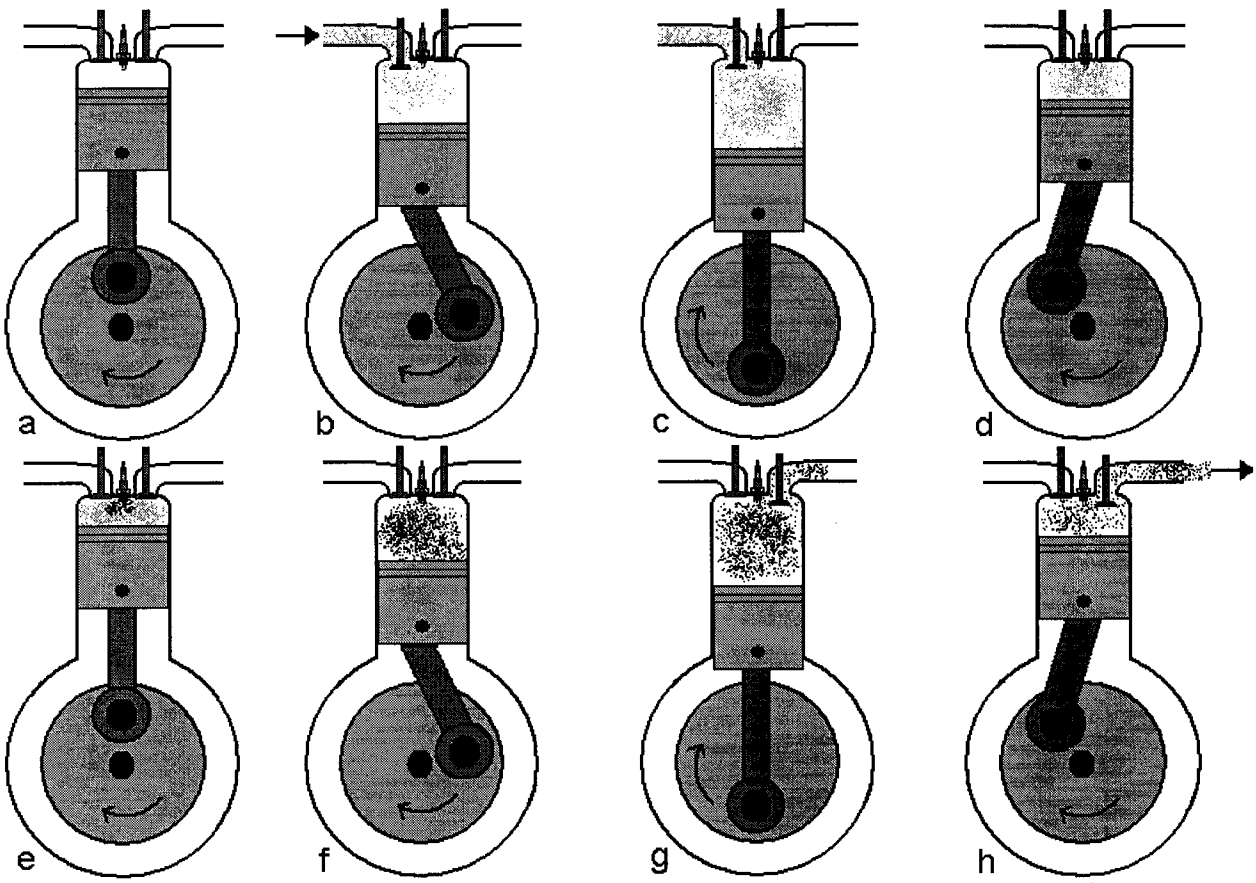

Figure A2 Four-stroke cycles. Light gray dots represent air/fuel mixture. Black dots represent exhaust products. Carburetor has been excluded for clarity.

When the piston is near the top of the stroke again (A2.e), the ignition system sends a high voltage to the spark plug, creating an ark in the spark plug gap, and igniting the compressed air/fuel mixture. The increase in temperature and quantity of gas exerts a high pressure on the piston, pushing it down in the cylinder (A2.f), and accelerating the crankshaft and flywheel. This is the power stroke.

Near the bottom of the stroke the exhaust valve is opened (A2.g), and the combustion products begin to escape to the exhaust system. As the piston rises in the cylinder, most of the gases are pushed out through the exhaust valve (A2.h). This is the exhaust stroke.

At the top of the stroke the exhaust valve is closed, and the intake valve begins to open for the subsequent cycle.

Notice there are two full revolutions of the crankshaft to complete one full cycle of the four-stroke engine. Also the crankcase is completely isolated from the combustion process, intake and exhaust gases. This allows for use of a recirculating, pump-pressurized, wet-sump type lubrication system.

APPENDIX B TWO-STROKE CYCLE ENGINES

Typical two-stroke cycle engines are similar to four-stroke cycle engines in that the combustion of the air fuel mixture takes place in a cylindrical chamber, with a head at the top, and a piston, crank and flywheel assembly at the bottom. In crankcase scavenged engines the valving and gas flow is, however, quite different.

There are a number of ways to combine the fuel and oxidizer. Figure B1 is a carbureted, piston-ported, crankcase-scavenged, spark-ignited two-stroke engine. Air enters the engine through the lower pipe on the right. It passes through the carburetor where fuel is entrained. Exhaust gases pass out of the engine through the pipe on the upper right.

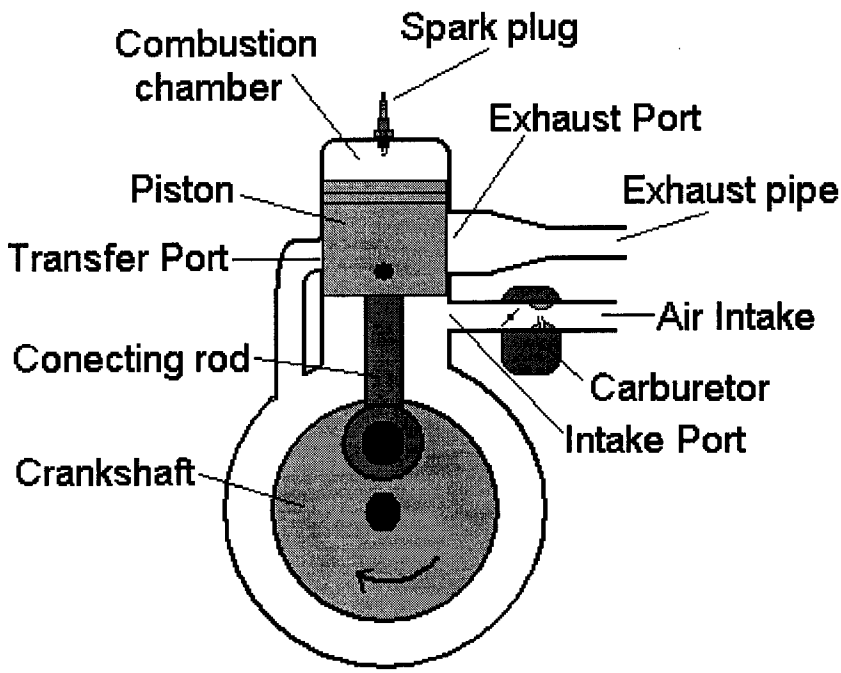

Figure B1 Carbureted, crankcase scavenged piston ported two-stroke engine

The cycles of operation are shown in figure B2. In figure B2.a the piston is at the top of the stroke. Assuming the engine is already in operation the combustion chamber will be filled with an appropriate air/fuel mixture and the crankshaft will be in motion.

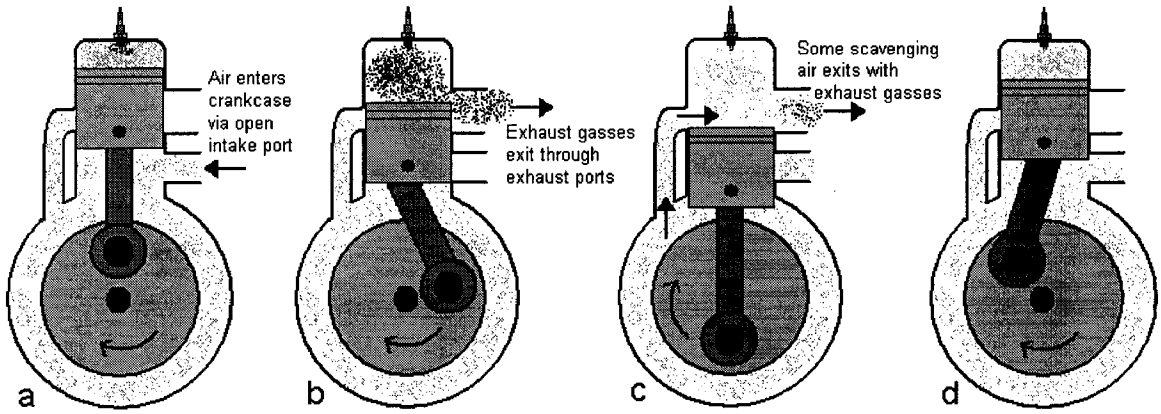

Figure B2 Two-stroke engine cycles. Light gray dots represent air/fuel mixture. Black dots represent exhaust products. Carburetor has been excluded for clarity.

The spark plug is given a voltage by the ignition system sufficient to create a spark at the gap, igniting the mixture. The combustion products push the piston down, accelerating the crank and flywheel. Once the piston has descended past the top of the exhaust port, exhaust gases begin to escape through the exhaust port to the exhaust system (figure B2.b). The air/fuel mixture in the crankcase, meanwhile, is being compressed as the piston descends.

As the piston continues downwards, the transfer port is uncovered, allowing the compressed crankcase gases to flow into the chamber through the transfer port. These gases help "push out" or scavenge the remaining exhaust products from the combustion chamber. Some of the scavenging gases (in this case air and fuel) will leak out the exhaust port as well. This is referred to as "short-circuiting" of the scavenging gases. Additionally there is the possibility of retaining significant amounts of exhaust products in the combustion chamber, as scavenging is less than perfect. This may adversely affect the subsequent cycle's ignition.

Rotation of the crankshaft pushes the piston towards the top of the stroke closing first the transfer port, and then the exhaust port. During this period the intake port is opened, allowing fresh air/fuel to enter the crankcase (figure B2.d). As the piston continues to rise, a low pressure is created behind it, pulling in air/fuel through the intake port.

Notice that one cycle is completed every revolution of the crankshaft. Additionally the crankcase is exposed to air/fuel mixture. This excludes the possibility of lubricating the crankshaft with a wet sump type system. Instead lubricating oil is generally mixed in with the air/fuel flow prior to admission to the crankcase. This inevitably results in the loss of the lubricating oil through the cylinder where it is either short circuited, or burned during combustion. A more complete discussion of this is located in Appendix C.

Three types of intake valves are common on crankcase scavenged two-stroke engines: piston porting (discussed above), reed valves or disk valves.

The reed valve, sometimes called an atmospheric valve, is essentially a check valve made of flexible petals covering flow passage (figure B3). In the absence of a pressure differential the petals act as springs, lying flat and covering the flow passage. If the pressure in the passage is sufficient compared to the pressure on the opposite side of

the petal, the petal opens and gases will flow around the petal. If, on the other hand, the pressure in the passage is lower then the pressure on the back of the petal, the pressure differential will force the petal to remain closed, negating any flow.

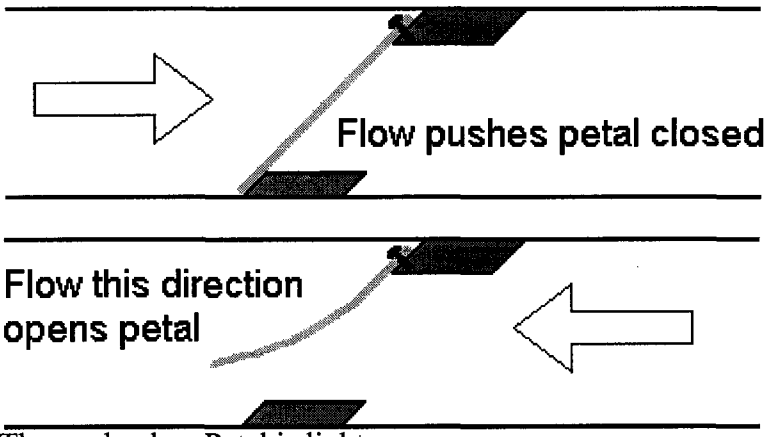

Figure B3 The reed valve. Petal is light gray.

The disk valve is similar to the piston port but with a rotational geometry. A disk is attached to the crankshaft as shown in figure B4. Whenever a hole or slot in the disk is aligned with the intake passage, flow may pass through (figure B5).

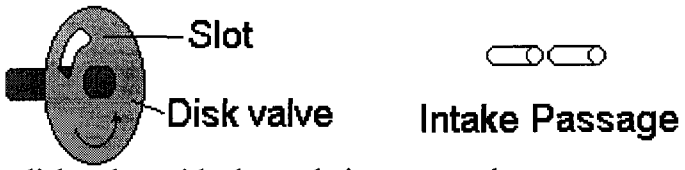

Figure B4 The disk valve with slot and air passage shown apart.

When the slot is not aligned with the intake passage, however, flow is blocked (figure B6). This type of valve has the advantage of being "asymmetric", i.e. the disk valve may be opened and closed at any crank angle desired. Piston porting requires that the port open and close at the same piston height, i.e. symmetrically.

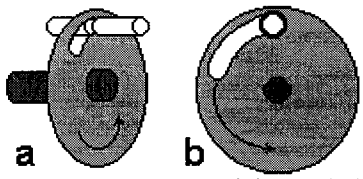

Figure B5 Open disk valve in oblique (a) and frontal (b) view.

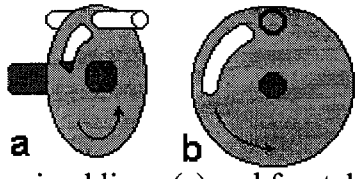

Figure B6 Closed disk valve in oblique (a) and frontal (b) view.

APPENDIX C TWO-STROKE ENGINE LUBRICATION

INTRODUCTION

One major classification of two-stroke engines can be made on the basis of how the scavenging pressure is supplied. In large engines this is predominantly supplied by a turbo or super charger. In most small gasoline engines, however, the crankcase is used as a low-pressure boost pump to provide scavenging air to the cylinder. The turbo and super charged two-stroke engines may be lubricated by the method commonly used on almost all four-stroke engines: i.e. oil is continuously circulated from a wet sump through a series of passageways to the bearings, and piston either by direct pressurization, spraying or splashing the oil on to the desired part. This is possible as the crankcase is, apart from slight venting, essentially a closed system. In crankcase-scavenged engines, however, the lubrication of the engine requires a different approach.

CRANKCASE SCAVENGED TWO-STROKE ENGINES

The total mass of air consumed by the engine passes through the crankcase in these small two-stroke engines. If they were to be lubricated via the "sump and pump" system an unacceptably high amount of oil would be lost to the air, resulting in rapid depletion of the oil supply.

Historically most small two-stroke engines have had a carburetor pre-mixing fuel with the air before entry into the crankcase. The most popular way of supplying lubricating oil was simply to mix it with the fuel prior to admission to the carburetor. The oil/fuel mixture would then pass through the crankcase where special bearing design (for example slots or holes through the connecting rod ends) allowed greater wetting of the bearing surfaces by the oil/fuel mixture. The gasoline and lighter components of the mixture tended to volatilize, and be removed, while the heavier lubricating oils tended to stay, and lubricate the surface. As there is no recirculation of the oil this type of system is referred to as a "total loss" lubrication system. The fuel to oil ratio was historically on the order of 20:1, occasionally going as low as 6:1 (Caines 1996), but in more recent years has been improved to between 50 to 100:1. This contrasts very poorly with typical four-stroke engine oil consumption rates of 10,000:1 (Bortz 1993).

There are two fundamental reasons why the two-stroke engines consume dramatically more lubricating oil than the four-stroke engines. First, as the oil in a two-stroke engine is transported in droplet form by the scavenging air a significant amount of the oil may remain suspended in the air, never becoming deposited on any surface of the engine. This oil reaches the combustion chamber and is either burnt, or exhausted in the

short-circuited air. Approximately 95% of the particulate emissions from two-stroke engines are raw, or partially combusted oil droplets (Kataoka, et al 1994).

Additionally once the oil has found a surface to lubricate, it must continually contend with being washed off by the fuel present in the circulating air. This makes it especially difficult to maintain an adequate oil film on parts of the piston and the rings.

Japanese motorcycle manufacturers pioneered the modern system two-stroke oil delivery separating the oil from the fuel supply. In this system lubricating oil is either gravity fed, or mechanically pumped to a metering valve controlled by the throttle. As the throttle is opened more oil is allowed to flow to the engine. Typically the oil is simply allowed to mix with the incoming air being transported in a manner similar to the fuel-oil premixed systems, but it may also be sprayed directly at critical components.

On vehicular sized engines the crankshaft is generally supported by roller bearings, and the connecting rod has needle bearings at both the crank and wrist pin ends. The transmission and clutch housings are generally lubricated in a normal wet-sump manner separated from the main crank chamber.

TWO-STROKE ENGINE LUBRICATION

Catastrophic wear problems such as piston scuffing, bearing wear and piston ring sticking had plagued initial two-stroke engine designs, resulting in the use of high oil to fuel ratios, until specific two-stroke oils were developed. Today use of spesific two-stroke oils in two-stroke engines may extend the life of the engine by a factor of four over the same engine run with four-stroke oil (Wilson 1992-2).

The unique circumstances of two-stroke lubrication place unique requirements on the oil. In a four stroke very little of the lubricating oil ideally makes its way into the combustion chamber as anything more than a surface film on the cylinder wall. In a two-stroke engine, however, all of the lubricating oil eventually passes through the combustion chamber. Approximately 66% of the oil is eventually present in the combustion chamber during a combustion event. As the oil is generally less combustible than the fuel, it tends to form significant deposits inside the combustion chamber and exhaust system. These deposits can create "hot spots" potentially causing premature ignition, they can cause plug fouling, and in the worst cases form deposits in the exhaust system thick enough to cause significant power loss.

To resist "fuel washing" two-stroke oils often contain "bright stock", a low volatility component which helps coat the piston skirt and the lower end of the connecting rod (Caines 1996). Additionally detergent components, often containing metals, are added to two-stroke oils to resist the tendency to form large deposits.

LOW EMISSION MODIFICATION CHALLENGES

Due to the high emissions of hydrocarbons (HC), carbon monoxide (CO) and particulate matter (PM) two-strokes have been the focus of emissions reduction research and legislation. Two of the most promising technologies for reducing the emissions from small crankcase scavenged two-strokes are direct fuel injection and the use of an

oxidizing catalyst. In several parts of the world laws have been passed requiring the use of catalysts on handheld and motorbike two-stroke engines (Caines 1996). Both of these techniques place new demands on the lubrication of the engine.

DIRECT FUEL INJECTION

Direct injection techniques (Sogawa, et al 2001 and Ambler, et al 2001) have been applied to a large number of different two-stroke engines with a great deal of success. In engines using direct fuel injection, the lubricant is still applied to the crankcase in the form of an air-borne oil mist. Typically the oil is injected up stream of the crankcase, and is metered to flow proportional to engine load, varying from 50:1 to 200:1 depending on load (Wilson 1997). Approximately 1/3 of this oil may be recovered from the bottom of the crankcase and recycled to the lubrication system.

Injecting the fuel directly into the combustion chamber after the exhaust port is closed completely eliminates the short-circuiting of fuel and may reduce HC emissions by 75%, reduce CO emissions by 37% and improve fuel economy by 36% (Willson 2001) on small transport engines. In addition the fuel-washing problem is eliminated, allowing lower lubricant flows, and possibly reformulation of the oil. Flows as low as 400:1 with oil consumption rates of 3 liters per 10,000 km have been achieved in direct injected two-stroke engines (Wilson 1997). Depending on the specifics of the injection technique there may be additional requirements placed on the lubricating oil, for example to reduce the tendency to form deposits in the neighborhood of the injector. An oil specifically for direct injection two-strokes has been formulated by several companies (Castrol, Shell, Lubrizol and Oronite) and is characterized by low combustion chamber deposits, good lubricity in boundary layer lubrication, low viscosity for good pumpability, low ash, no smell and no visible smoke (Wilson 1997).

OXIDATION CATALYSTS

Oxidation catalysts contain thin layers of precious metals which operate at high temperatures to oxidize HC and CO in emission gases to CO_2. These layers are subject to attack by a number of compounds including sulfur, phosphorus, metals and buildups of carbon-laden deposits. Most of the inexpensive two-stroke oils with detergents contain amounts of metals incompatible with the use of a catalyst. The petroleum oil base may also contain significant amounts of sulfur, which will degrade the catalyst effectiveness. In addition the overall HC loss from the engine is likely to overwhelm a reasonably sized catalyst, resulting in overheating and premature failure of the supporting matrix.

Careful lubricant formulation may help overcome these two issues. Polybutene + ester oils are more expensive then conventional two-stroke oils, but they tend to burn more completely, reducing the HC loading of the catalyst and deposit formation, and they do not contain metal or phosphorus laden detergents. For two-stroke engines using catalysts it may therefore be necessary to use a similar synthetic oil. Use of the incorrect oil was shown to cause catalyst failure in as little as 200 km of use on small motorbikes

equipped with oxidation catalysts, where as the appropriate oil gave catalyst lives of greater than 6000 km (Qin, et al 2001).

Temperature fluctuations on a two-stroke catalyst may be extremely taxing as well. Due to the large amount of recirculated exhaust gas, and the "short circuited" scavenging air, the catalyst temperature may be too low at idle conditions to appropriately function. On the other hand, if the engine is carbureted, the scavenging air will also contain large amounts of fuel, potentially overheating the catalyst at wide-open throttle conditions.

Two-stroke specific oxidation catalysts have been developed for small motorbike applications, and have shown HC conversion efficiencies of approximately 60%, which remained fairly stable over a 30,000 km test. CO conversion efficiencies as high as 50% have been achieved but tended to degrade more (to 28%) after 30,000 km of service (Coultas et al., 2001).

When an oxidation catalyst is used in combination with direct injection, HC reductions of over 98% have been achieved (Willson et al. 2002).

CONCLUSIONS

The most successful emissions reduction strategy for small two-stroke engines combines direct fuel injection and a catalytic oxidation exhaust after treatment. Direct injection of the fuel allows reduced lubricant flow rates, and reduces the HC loading of the catalyst. For such an application the appropriate changes to the lubrication system consist of using a synthetic, metal-free two-stroke oil, and recalibrating the oil delivery rate to obtain the minimum necessary for adequate system lubrication, and a two-stroke specific oxidation catalyst.